NASA CONTRACTOR REPORT

NASA CR-1771

SPACE QUALIFIED Nd:YAG LASER (PHASE I - DESIGN)

by J. D. Foster and R. F. Kirk

Prepared by
SYLVANIA ELECTRONIC SYSTEMS, WESTERN DIVISION
Mountain View, Calif. 94040
for Electronics Research Center

NATIONAL AERONAUTICS AND SPACE ADMINISTRATION • WASHINGTON, D. C. • OCTOBER 1971

1. Report No.	2. Government Accession No.	3. Recipient's Catalog No.
NASA CR-1771		

4. Title and Subtitle	5. Report Date
SPACE QUALIFIED Nd:YAG LASER (PHASE I - DESIGN)	October 1971
	6. Performing Organization Code
7. Author(s) J. D. Foster and R. F. Kirk	8. Performing Organization Report No.
	10. Work Unit No.
9. Performing Organization Name and Address Sylvania Electronic Systems (Western Division) P. O. Box 188 Mountain View, California 94040	11. Contract or Grant No. NAS12-2160
	13. Type of Report and Period Covered Contractor Report
12. Sponsoring Agency Name and Address National Aeronautics and Space Administration Washington, D.C. 20546	14. Sponsoring Agency Code

15. Supplementary Notes

16. Abstract

This report presents the results of a design study and preliminary design of a space qualified Nd:YAG laser. A theoretical model of the laser is developed to allow the evaluation of the effects of various parameters on its performance.

Various pump lamps are evaluated and sum pumping is considered.

Cooling requirements are examined and cooling methods such as radiation, cryogenic and conductive are analysed.

Power outputs and efficiences of various configurations and the pump and laser life-time are discussed.

This report also considers modulation and modulating methods.

17. Key Words (Suggested by Author(s))	18. Distribution Statement
Lasers, Space, Communications, Laser Modulation, Efficiency	Unclassified - Unlimited

19. Security Classif. (of this report)	20. Security Classif. (of this page)	21. No. of Pages	22. Price*
Unclassified	Unclassified	188	$3.00

*For sale by the National Technical Information Service, Springfield, Virginia 22151

FOREWORD

This report is the Final Engineering Report summarizing the work performed on Phase I (design Phase) of NASA Contract NAS12-2160 entitled "Space Qualified Nd:YAG Laser", covering the period 1 July 1969 to 1 June 1970. This report was prepared by the Electro-Optics Organization of Sylvania Electronic Systems - Western Division, Mountain View, California. The principal investigator on the program was Dr. J. D. Foster. Other contributors on the program were Mr. R. F. Kirk, Dr. L. M. Osterink, Mr. C. B. Hitz, Dr. G. A. Massey, Dr. P. J. Titterton and Mr. R. S. Reynolds.

All the work performed under this contract was administered by the Optics Branch, NASA-Electronics Research Center, Cambridge, Massachusetts. Mr. John F. Fantasia was the principal technical representative for the Optics Branch.

ABSTRACT

This report presents the results of a design study and preliminary design of a space qualified Nd:YAG laser. A theoretical model of the Nd:YAG laser is developed that allows evaluation of the effect of various parameters on laser performance.

Low power (1 watt) space qualified Nd:YAG lasers will be low gain devices. The efficiency of the laser will be much effected by internal dissipative loss in the laser cavity. Good performance can, therefore, not be expected if intracavity elements such as non-linear, second harmonic generation crystals or electro-optic modulator crystals have significant loss.

Various pump lamps are evaluated. Lamp heat loss is shown to greatly influence the laser pumping efficiency. Potassium lamps with sapphire jackets and operated in vacuum for minimum heat loss are found to be the best pump lamp for Nd:YAG. An output of 1 watt can be expected with 150 watts into these lamps. Lifetimes of 10,000 hours appear possible in the near or immediate future.

Radiation cooler weight requirements make cryogenic laser operation impractical. Incoherent semiconductor diodes appear to be possible with near room temperature operation. Such diode array laser pumps have not yet been made, but should produce very good laser performance when they are developed. An output of 1 watt can be expected with 100 watts into such a diode array. Lifetime of these devices may be extended to 100,000 hours with further development.

Sun pumping, especially in a dual pumping arrangement appears to be a feasible, very long-life approach for space qualified Nd:YAG.

Conductive cooling of the Nd:YAG laser rod and use of heat pipes to move the heat to a radiation cooler is the preferred design technique for the space qualified laser.

Mode locking by injection locking is shown to be possible with low loss at high c/2L frequencies (500 MHz). Low frequency modulation (50 MHz) requires an intracavity modulator. Fused quartz resonant acoustic modulators produce the lowest intracavity loss.

TABLE OF CONTENTS

Section	Title	Page
1	INTRODUCTION	1
	1.1 General	1
	1.2 Technical Discussion	3
2	THEORETICAL MODEL OF THE ND:YAG LASER	8
	2.1 Introduction	8
	2.2 Four-Level Rate Equation Analysis	8
	2.3 Model for Radiation Emission From Pump Source	21
	2.4 Theoretical Model for the Nd:YAG Laser	23
	2.4.1 Side Pumped Laser	23
	2.4.2 End Pumped Laser	27
	2.5 Discussion of the Theoretical Model	29
	2.5.1 Material Constants and Their Experimental Determination	29
	2.5.2 Optimum Output Coupling	32
3	LAMP PUMPED ND:YAG LASERS	34
	3.1 Lamps Available for Pumping	34
	3.1.1 Introduction	34
	3.1.2 Tungsten-Halogen Pump Lamps	35
	3.1.3 Krypton Arc Pump Lamps	40
	3.1.4 Potassium-Mercury Arc and Potassium Arc Pump Lamps	44
	3.1.5 Rubidium Iodide-Mercury Arc Pump Lamps	56
	3.2 Characteristics of an Optimum Lamp Pumped Nd:YAG Laser	60
4	INCOHERENT SEMICONDUCTOR DIODE PUMPED ND:YAG LASERS	70
	4.1 Effect of Temperature on Nd:YAG Laser Performance	70
	4.2 $GaAs_{1-x}P_x$ Diode Pumped Nd:YAG	74
	4.3 $GaAl_{1-x}As_x$ Diode Pumped Nd:YAG	84
	4.4 Characteristics of an Optimum Incoherent Diode Pumped Nd:YAG Laser	86
	4.5 Expected Life of Room Temperature GaAlAs Laser Pumping Diodes	91

TABLE OF CONTENTS (Continued)

Section	Title	Page
5	SUN PUMPED ND:YAG LASERS	93
	5.1 Consideration of Previous Sun Pumping Research	93
	5.2 Dual Pumped Laser Design Approach	96
6	HEAT REMOVAL FROM ND:YAG LASER IN SPACE	101
	6.1 Laser Rod Mounting	102
	6.2 Heat Pipe Considerations	106
	6.3 Thermal Resistance from Laser Rod to Radiation Cooler	112
	6.4 Dissipation of Energy by Radiation	116
	6.4.1 Laser Rod Heat Dissipation	119
	6.4.2 Potassium Arc Lamp Heat Dissipation	123
	6.4.3 Diode Array Heat Dissipation	124
7	MODE LOCKING OF THE SPACE QUALIFIED ND:YAG LASER	129
8	PRELIMINARY DESIGN OF THE SPACE QUALIFIED ND:YAG LASER	142
	8.1 Laser Design	143
	8.1.1 Design Requirements	143
	8.1.2 Pump Cavity Design	144
	8.1.3 Prototype Lamp Pumped Laser Design	146
	8.1.4 Power Supply Design	150
	8.2 Laser Conductive Cooling Experiments	158
9	CONCLUSIONS AND RECOMMENDATIONS	171
	9.1 Conclusions	171
	9.2 Recommendations	173
10	REFERENCES	175

LIST OF ILLUSTRATIONS

Figure	Title	Page
2-1	Energy Levels of Nd:YAG, a Four Level Laser Material	9
2-2	Narrow Band Radiation Output as a Function of Input for the Tungsten-Iodine Lamp	22
2-3	Optically Side Pumped Laser	24
3-1	Experimental Arrangement for Determining the Nd:YAG Pump Band Absorption for Various Pump Lamps	37
3-2	Nd:YAG Absorption of Tungsten Radiation	38
3-3	Narrow Band Radiation Output as a Function of Input for the Krypton Arc Lamp	41
3-4	Nd:YAG Absorption of Krypton Arc Radiation	42
3-5	Narrow Band Radiation Output as a Function of Input for the Potassium-Mercury Arc Lamp and the Rubidium Iodide Mercury Arc Lamp	47
3-6	Nd:YAG Absorption of Potassium-Mercury Arc Radiation	48
3-7	Potassium-Mercury Emission Spectrum for Varying Input Power	49
3-8	Theoretical Gain of 3mm x 75mm Nd:YAG for Various Pump Lamps	51
3-9	Nd:YAG Fluorescence as a Function of Input Power for a 1/4 Inch by 1 Inch Arc Length Potassium Arc Lamp (After Nobel[17])	53
3-10	Life Test on Na-Hg Lamps in Reflective Cavities	55
3-11	Nd:YAG Absorption of Rubidium Iodide-Mercury Radiation	57
3-12	Narrow Band Radiation Output as a Function of Input to the Rubidium Iodide-Mercury Lamp for Several Heat Insulation Conditions	59
3-13	Theoretical Most Optimistic Estimate of K-Hg Pumped Nd:YAG Laser Performance	63
3-14	Optimum Theoretical Efficiency for Various Dissipative Losses for Potassium Arc Pumped Nd:YAG	67
3-15	Efficiency of 2mm Nd:YAG Laser as a Function of Dissipative Loss, α_o, for Various Gains or Input Powers to a Potassium Arc Lamp.	68

LIST OF ILLUSTRATIONS (Continued)

Figure	Title	Page
4-1	Effect of Temperature on Nd:YAG Laser Threshold	72
4-2	Optimum Efficiency of Potassium Arc Pumped 77^{o} Nd:YAG Laser	75
4-3	Absorption Spectrum of 8800 A Pump Band for 0.203", 1% Nd:YAG	76
4-4	Absorption Spectrum of 8100A Pump Band for 0.203", 1% Nd:YAG	77
4-5	Absorption Spectrum of 7500A Pump Band for 0.203", 1% Nd:YAG	78
4-6	$GaAs_{1-x}P_x$ Emission and Computed Transmission Through 5mm of Nd:YAG	79
4-7	$Ga_{1-x}Al_xAs$ Emission and Computed Transmission Through 5mm of Nd:YAG	85
4-8	Theoretical Efficiency of 77^{o}K GaAsP Diodes and Potassium Arc Pumped 77^{o}K Nd:YAG Laser	87
4-9	Efficiency of 20^{o}C GaAlAs Diodes Pumped Nd:YAG Laser	89
4-10	Efficiency of 20^{o}C GaAlAs Diodes and Potassium Arc Lamp Pumped 20^{o}C Nd:YAG	90
4-11	Konnerth, Marinace and Topalian's[29] Data on Life of Liquid-Epitaxy and Zinc Diffused GaAs Incoherent Diodes	92
5-1	Sun-Pumped Laser Design	97
5-2	Sun-Pumped Laser Design	98
5-3	Sun-Pumped Laser Design	99
6-1	Conductively Cooled Nd:YAG Laser Rod Mounting Arrangement	103
6-2	Test Apparatus for Simulated Laser Rod Thermal Inputs to Heat Pipes.	109
6-3	Test Results for Anhydrous Ammonia Heat Pipe - 25" Dia. x 12" Long (Purchased from Energy Conv. Systems) Pipe-Horizontal	110
6-4	Test Results for Methanol Heat Pipe - .25" Dia. x 12" Long (Purchased From Energy Conv. Systems) Pipe-Horizontal	111
6-5	ΔT - Laser Rod to Radiator	113
6-6	Radiating Fin Configuration	118

LIST OF ILLUSTRATIONS (Continued)

Figure	Title	Page
6-7	Efficiency of Longitudinal Fin of Rectangular Profile	120
6-8	Radiating Surface Area Required to Dissipate 100 Watts as as Function of Temperature.	128
7-1	Acoustic Loss Modelocking	131
7-2	Injection Modelocking	133
7-3	Injection Locking	135
7-4	Effect of Modelocking Frequency and Detuning on Injection Modelocking	141
8-1	Space Qualified Nd:YAG Laser Layout Drawing	145
8-2	Assembly Drawing of Space Qualified Nd:YAG Laser	147
8-3	Pump Cavity Assembly Drawing of Space Qualified Nd:YAG Laser	148
8-4	Block Diagram Space Qualified Nd:YAG Laser Power Supply and Space Craft Interface	152
8-5	Power Supply System Block Diagram	154
8-6	Typical Simplified Circuit	155
8-7	Voltage Converter and Waveforms	156
8-8	Conductively Cooled Flash Pumped Nd:YAG Laser Experiment	159
8-9	Assembly Drawing of Krypton Arc Pumped Conductively Cooled Nd:YAG Laser	161
8-10	Krypton Arc Pumped Conductively Cooled Nd:YAG Laser	162
8-11	Krypton Arc Pumped Conductively Cooled Laser	163
8-12	Pump Cavity of Conductively Cooled Nd:YAG Laser	164
8-13	Conductively Cooled Nd:YAG Rod Mounting and Heat Pipe	165
8-14	Conductively Cooled Nd:YAG Laser Rod Mounting	166
8-15	Potassium-Mercury Arc Lamp and 2mm Nd:YAG Laser Rod	168
8-16	Assembly Drawing of Potassium Arc Pumped Conductively Cooled Nd:YAG Laser	169

LIST OF TABLES

Table No.	Title	Page
3-1	Na-Hg Life Test Data in Reflectors	54
5-1	Sun-Pumping Merit Factor, G(Degree Above Threshold), for a 24-Inch Solar Collector and Laser Material at Room Temperature	94
6-1	Internal Surface Reflectivity of Various High Adherence Gold Coatings on Fused Quartz Plates	105
8-1	Power Supply Specifications for Space Qualified Nd:YAG Laser	151

SECTION I

INTRODUCTION

1.1 General

The development of a space qualified Nd:YAG laser has been planned as a two phase sequential work program covering design (Phase I), and hardware development, construction, and test (Phase II). This report, which covers the results of the design phase, gives the details of the design study and preliminary laser design as well as the results of experimental studies performed during the first phase.

The object of the program is to provide NASA with several working models and a continuing source of supply for solid state cw mode-locked, doubled, space-qualified, lasers suitable for optical communications, laser ranging, navigation and meterological probing.

The object of this Phase I program was to perform an engineering design study in accordance with the design goals which will be outlined below. The study was to include:

(1) Calculation of the interaction of all critical parameters.

(2) Laboratory experiments intended to support calculations of critical parameters.

(3) Perform trade-off studies to optimize overall efficiency, minimize weight and size, maximize reliability and lifetime, and assure uniformity of performance.

(4) Literature review.

(5) Investigation of the state-of-the-art in commercial lasers, cooling technology and laser pumping techniques (including past work on solar-pumped Nd:YAG).

(6) Consultation with NASA centers for elucidation of the spacecraft systems configurations and environmental conditions.

(7) Visits to universities and non-NASA government laboratories for information exchange purposes.

Preliminary design configurations were to be developed at the culmination of the design study and its review with NASA technical personnel.

The design goals for the Space Qualified Nd:YAG Laser were:

(1) Laser to operate in cw mode-locked configuration.

(2) Laser to be Neodymium doped solid state rod, to operate at 1.06 μm wavelength. If material other than Nd:YAG is chosen, performance superior to Nd:YAG to be demonstrated.

(3) Provision in the engineering design should be made for inclusion of second harmonic generator as an adaptation of the system.

(4) To operate with an initial average output power of (5) watts (preferably at 5320Å).

(5) To demonstrate the capability of an operating/nonoperating life of three (3) years, the cumulative intermittent operating portion of which shall be not less than 2,000 hours. (An operational life of 10,000 hours shall be a goal.) The average output power shall not drop below one (1) watt at 2,000 hours intermittent operating time.

(6) To have operation with a polarized output.

(7) To operate in the TEM_{oon} mode with a beam divergence not to exceed three (3) milliradians. The beam should be circular in cross section within 50% of diffraction limit.

(8) To operate with a cooling system compatible with space environment.

(9) Cooling system to introduce negligible mechanical vibration and/or distortion into the optical performance of the laser undergoing operating conditions.

(10) System to operate with negligible interference from the pump light.

(11) To operate with negligible electromagnetic field leakage.

(12) To operate normally without readjustment following environmental tests.

1.2 Technical Discussion

In this section the "state of the art" in Nd:YAG lasers will be assessed and compared with the design goals of this program. From this comparison the primary technical obstacles to realizing a space qualified Nd:YAG laser will be defined.

The 1.06 micron Nd:YAG laser was discovered in 1964.[1] The rare earth Nd ion had been successfully incorporated into a number of crystalline and glass hosts and operated in both pulsed and continuous lasers prior to this. The exceptionally good thermal and mechanical properties of the Yttrium Aluminum Garnet (YAG) crystal resulted in its quickly becoming the primary continuous Nd laser material. It also found application in a number of pulsed lasers.

Laser thresholds as low as 400 watts were reported using tungsten-iodine pump lamps.[2] Laser output powers as high as 305 watts and efficiencies as high as 3.5 percent were reported using Kr arc pump lamps.[3] The laser has been mode locked[4,5] and frequency doubled.[6] The Nd:YAG laser was indeed one of the primary continuous lasers and its consideration for space qualification was well founded. A high efficiency continuous laser possibly mode locked and doubled seemed achievable at the 1 to 5 watt level desired for space application.

The space qualified Nd:YAG laser requires the combination of the good attributes of a number of different laser experiments. High efficiency has been achieved only at high output powers (hundreds of watts); however, the space application requires high efficiency at low power (watts). Good mode locking and high efficiency doubling of the attainable 1.06 micron laser power into 0.53 micron power have been obtained with inefficient 1.06 micron lasers. Low laser thresholds have been achieved with high reflectivity mirrors with very low laser output power. Operating life greater than 100 hours has been rare indeed for Nd:YAG laser pump lamps. Long operating life (> 2000 hours) Nd:YAG laser experiments have, however, been obtained at low (< 1 percent) laser efficiency. Polarized and single spatial TEM_{oo} mode output has been obtained at low efficiency.

We find then in reviewing the Nd:YAG laser "state of the art" that each of the space qualified laser design goals can be obtained individually. The question to be answered is whether they can be obtained collectively. In particular, can all of the design goals be obtained with a low threshold laser that operates at high efficiency? A primary part of the design study to be

reported here, involves development of a theory for the Nd:YAG laser that includes sufficient parameters that these questions can be answered.

The feasibility of a particular Nd:YAG laser meeting a particular set of design goals depends critically on the input power available from a space craft. We posed the question of how much spacecraft power could be made available for a laser to a number of NASA and Air Force people experienced in spacecraft design. The answer, in general, was as follows:

> Laser input power of 50 watts can usually be made available. As much power as 100 watts can be made available on some future spacecraft. Powers of 200 watts and more are only intermittently available and require shut-down of most other spacecraft functions.

We have, therefore, placed special emphasis on operation at input powers as much below 200 watts as possible. This is somewhat inconsistent with the design goal of 5 watts output at preferably 0.53 microns. However, we found a general disagreement between various potential space laser users, and the typical requirement appears to be more like 1 watt at 1.06 microns or 100 milliwatts at 0.53 microns. A goal of trying for as low of threshold as possible and efficient operation at the low available spacecraft powers appeared most prudent. It would of course be possible to modify such a laser for higher power operation.

Review of the technical literature has turned up two approaches to Nd:YAG laser design that shows promise for space application. The first of these uses arc pump lamps that efficiently pump Nd:YAG and the other uses incoherent semiconductor diodes. The arc lamp pumped Nd:YAG laser experiments most closely meeting the requirements for a space qualified Nd:YAG laser are

those utilizing the K-Hg arc lamp[7]. These experiments utilized a large heavy spherical pump cavity and water cooling which are not desirable in a space qualified laser but they did come close to meeting the desired threshold and efficiency. The results of these experiments have important bearing on the lamp pumping sections of this design study.

Incoherent $GaAs_{1-x}P_x$ electroluminescent diodes have been used[8] to operate a Nd:YAG laser continuously when both the diodes and the laser rod were maintained at $77^{o}K$. Operation at this low temperature greatly eases the problems of making the incoherent diodes and significantly lowers the laser rod threshold. Such low temperature operation significantly increases the space radiator size and weight required to dissipate waste heat into space, however. It is probably not practical to use temperatures much below $300^{o}K$ in space qualified lasers. The possibility of extending incoherent diode-pumped Nd:YAG lasers to higher operating temperatures is therefore explored in the design study. Incoherent semiconductor diodes exhibit very long lifetimes when operated at moderate output levels. This is a great advantage for a space qualified laser pump. The low pump power per diode, however, means that arrays of many diodes are required to obtain laser output powers of watts.

Nd:YAG is a four level laser material and has a low population of the lower laser level at the outset of optical pumping. An inversion is, therefore, easily attained and the laser threshold is low. The lower laser level is nevertheless slightly thermally connected with the ground state and empties quickly thereby not producing a bottleneck. The gain therefore saturates slowly and high circulating laser power levels may be maintained. The pump bands of Nd:YAG are rather thin, however, and only a small portion of a

broad band pump light is usefully absorbed. It is, therefore, difficult to obtain high inversion levels. The net result of these effects is that the gain in Nd:YAG lasers is never very high for output powers of a few watts as required for the space qualified laser. The technology of Nd:YAG lasers, of up to a few watts output power, is therefore that of low optical loss. We will show in the design study that follows that the optical loss introduced by a particular design item is the primary consideration for choosing between alternatives.

SECTION 2

THEORETICAL MODEL OF THE ND:YAG LASER

2.1 Introduction

In this section we will develop a theoretical model of the Nd:YAG laser that includes as many of the laser design parameters as possible. The analysis will start from a set of four-level rate equations. Using proper simplifying assumptions, these equations will be reduced to a set of two rate equations--one for the inversion density, and one for the laser photon density. The steady state solution of these equations gives the desired theoretical model. The optical pumping parameters in this model will then be expressed in terms of the laser rod size and the input power to the pump lamps. We will then have a theoretical model containing most of the parameters at our disposal in designing a laser.

We will then show the effects of various parameters in the theory on the laser output power.

2.2 Four-Level Rate Equation Analysis

Nd:YAG is an example of a 4-level laser material. Figure 2-1 depicts the various levels involved. The ground state has energy E_1, the lower laser level has energy E_2, and the pump bands have an energy distribution which we call E_4. In a good laser material such as Nd:YAG the following sequence is followed. The laser material is irradiated with pump light photons that result in a certain pumping rate W_{14} from level 1 to level 4. The laser ions in level 4

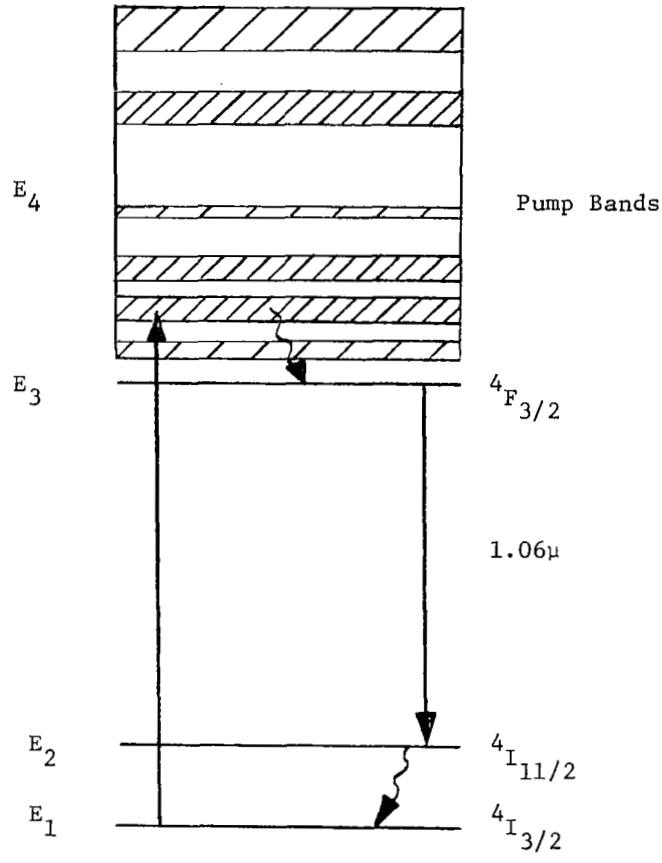

Figure 2-1 Energy Levels of Nd:YAG, a Four Level Laser Material

spontaneously decay with various lifetimes τ_{4A} into the lower lying levels. The lifetime τ_{43} for decay into the upper laser level is ideally much shorter than any of the other decay times from level 4.

The upper laser level, E_3, is usually metastable with a long lifetime for decay into all its lower lying levels. The spontaneous decay from level 3 to level 2 of course produces the photons that initiate laser oscillation. An important consideration for initiation of laser oscillation is the total number, p, of resonant modes possible in the laser resonator volume, V_R, since in general only one of these modes is initiated into oscillation. This number is given by the familiar expression

$$p = \frac{8\pi\nu^2\Delta\nu V_R}{c^2} \qquad (2\text{-}1)$$

where ν = the laser optical frequency

$\Delta\nu$ = the frequency width of the level 3 to level 2 spontaneous emission

V_R = the optical resonator volume

c = the speed of light

For successful laser operation the primary loss mechanism from level 3 is stimulated emission with a transition rate W_{32}.

The lower laser level, E_2, should ideally have low population at all times. The decay lifetime τ_{21} should therefore be very fast and the pumping rate from the ground state W_{12} should be low.

We also have to consider the photons stored in the laser resonator cavity. The number stored per unit volume of resonator will be designated by ρ. Photons are lost from the resonator by transmission of the laser mirrors to produce the laser output power and by dissipative scattering and absorption losses in the optical cavity. The photon cavity lifetime, τ_c, is then given by

$$\tau_c = \frac{1}{(\text{loss per round trip})(\text{round trips per second})}$$

$$= \frac{1}{(2\alpha)(c/2L_R)} = \frac{L_R}{\alpha c} \qquad (2\text{-}2)$$

where α = the average single pass loss

L_R = optical resonator length

c = speed of light

We may now write rate equations for the number of ions N_1, N_2, N_3, and N_4 per unit volume stored in the various laser ion levels.

$$\frac{dN_4}{dt} = W_{14}(N_1-N_4) - \frac{N_4}{\tau_{43}} - \frac{N_4}{\tau_{42}} - \frac{N_4}{\tau_{41}}$$

$$\frac{dN_3}{dt} = W_{13}(N_1-N_3) + \frac{N_4}{\tau_{43}} - \frac{N_3}{\tau_{32}} - \frac{N_3}{\tau_{31}} - W_{32}(N_3-N_2)$$

$$\frac{dN_2}{dt} = W_{12}(N_1-N_2) + W_{32}(N_3-N_2) + \frac{N_3}{\tau_{32}} + \frac{N_4}{\tau_{42}} - \frac{N_2}{\tau_{21}} \qquad (2\text{-}3)$$

$$\frac{dN_1}{dt} = W_{14}(N_4-N_1) + W_{13}(N_3-N_1) + W_{12}(N_2-N_1) + \frac{N_4}{\tau_{41}} + \frac{N_3}{\tau_{31}} + \frac{N_2}{\tau_{21}}$$

$$\frac{d\rho}{dt} = W_{32}(N_3-N_2) + \frac{N_3}{p\tau_{32}} - \frac{\rho}{\tau_c}$$

Let us now simplify these equations. In the rate equation for level 4 let us account for the τ_{42} and τ_{41} terms by a quantum efficiency factor η'. Assume that $N_1 >> N_4$ so that we can replace $N_1 - N_4$ by N_1. The simplified rate equation for level 4 becomes

$$\frac{dN_4}{dt} = W_{14}N_1 - \frac{N_4}{\tau_{43}\eta'} \tag{2-4}$$

The lifetime of level 4 is in general very short so we can assume steady state conditions and $\frac{dN_4}{dt} = 0$. This assumption is of course exactly true in the continuous case. The population density N_4 is then

$$N_4 = \eta' N_1 W_{14} \tau_{43} \tag{2-5}$$

We may now substitute for N_4 in the rate equation for level 3. Also assume $N_3 << N_1$ so that we can replace $N_1 - N_3$ by N_1. The simplified rate equation for level 3 becomes

$$\frac{dN_3}{dt} = W_{13}N_1 + \eta' W_{14}N_1 - W_{32}(N_3 - N_2) - \frac{N_3}{\tau_{32}} - \frac{N_3}{\tau_{31}} \tag{2-6}$$

Let us define the pumping rate W and the quantum efficiency η by

$$\eta W = W_{13} + \eta' W_{14}$$

Then,

$$\frac{dN_3}{dt} = \eta W N_1 - W_{32}(N_3 - N_2) - \frac{N_3}{\tau_{32}} - \frac{N_3}{\tau_{31}} \tag{2-7}$$

Assume that the terms in τ_{42} and W_{12} may be neglected in the rate equation for level 2. Then,

$$\frac{dN_2}{dt} = W_{32}(N_3-N_2) + \frac{N_3}{\tau_{32}} - \frac{N_2}{\tau_{21}} \tag{2-8}$$

Define the inversion density $N = N_3-N_2$. Subtracting equation (2-8) from equation (2-7).

$$\frac{dN}{dt} = \eta W N_1 - 2W_{32}N - 2\ \frac{N_3}{\tau_{32}} - \frac{N_3}{\tau_{31}} + \frac{N_2}{\tau_{21}} \tag{2-9}$$

Define,

$$\frac{2N}{\tau_T} = \frac{2N_3}{\tau_{32}} - \frac{N_3}{\tau_{31}} + \frac{N_2}{\tau_{21}}$$

$$= 2N\left[\frac{1}{\tau_{32}} + \frac{1}{2\tau_{31}} + \frac{N_2}{2N}\left(\frac{1}{\tau_{21}} + \frac{2}{\tau_{32}} - \frac{1}{\tau_{31}}\right)\right] \tag{2-10}$$

where τ_T will be called the total lifetime of the inversion. In general $N_2 << N_3$ so that $N_2/N << 1$ and we may assume

$$\frac{1}{\tau_T} = \frac{1}{\tau_{32}} + \frac{1}{2\tau_{31}} \tag{2-11}$$

This is slightly different than the total upper laser level lifetime which would be given by $\frac{1}{\tau_f} = \frac{1}{\tau_{32}} + \frac{1}{\tau_{31}}$. The upper laser level lifetime is easily measured by time observation of spontaneous fluorescence and is readily available in the literature. If the branching ratios r_{32} and r_{31} are known τ_T may be deter-

mined with the following equation

$$\frac{1}{\tau_T} = \frac{r_{32}}{\tau_f} + \frac{r_{31}}{2\tau_f} \tag{2-12}$$

Substituting τ_T into equation(2-9),we get our final rate equation for the inversion density

$$\frac{dN}{dt} = \eta W N_1 - 2W_{32}N - \frac{2N}{\tau_T} \tag{2-13}$$

The rate equation for the photon density in (2-3) is for the case where the laser material volume and the laser resonator volume are equal. We will generalize this to the external mirror case where the laser material volume, V_L, and the laser resonator volume, V_R, are different. Since in general $N_3 >> N_2$, we will assume that $N_3 = N$ in the spontaneous emission term. We will also generalize to the multimode case where n modes of the laser can be excited. The photon density rate equation is then

$$\frac{d\rho}{dt} = W_{32}N + \frac{nN}{p\tau_{32}} - \frac{\rho}{\tau_c} \tag{2-14}$$

The stimulated emission rate W_{32} must be expressed in terms of parameters. The number of stimulated emissions, N_s, per unit time per unit volume is

$$N_s = W_{32}N = I_L \sigma N \tag{2-15}$$

where I_L = the laser light irradiance or photons per unit area per unit time traversing the laser material.

σ = the stimulated emission cross section per inverted laser ion.

The photon intensity, I_L, considering those moving both directions in the laser resonator is

$$I_L = \rho c \tag{2-16}$$

where c is the speed of light.

The pumping rate W must also be expressed in terms of parameters. The number of pump photon absorptions, N_p, per unit time per unit volume is

$$N_p = WN_1 = I_p \sigma_p N_1 \tag{2-17}$$

where I_p = the pump light irradiance or photons per unit area per unit time traversing the laser material.

σ_p = the average pump light absorption cross section per laser ion.

The pump photon intensity, I_p, depends on the size of the laser material and the pump lamp and pump cavity configuration. Let us assume that we have a well designed laser such that the pump light is imaged on the laser rod for each rod size we consider. With this assumption, the irradiance, I_p, is just the total number of pump photons, ϕ_p, emitted per unit time divided by the cross section of the laser rod presented to the pump light. Considering cylindrical laser rods for side pumping

$$I_p = \frac{\phi_p}{Ld} \quad \text{(side pumping)} \tag{2-18}$$

where L = laser rod length

d = laser rod diameter

and we have assumed only one or two passes of the pump light through the laser rod.

For end pumping

$$I_p(\ell) = \frac{4\phi_p}{\pi d^2} e^{-\frac{\ell}{L_M}} \quad \text{(end pumping)} \tag{2-19}$$

where ℓ = the axial distance from the entrance end of the rod.

L_M = the axial distance at which the irradiance has decreased by e.

To simplify this case we will determine the average, $\bar{I}_p$, of $I_p(\ell)$ in an end pumped laser rod of length L.

$$\bar{I}_p = \frac{1}{L}\int_0^L I_p(\ell)\,dL$$

$$\bar{I}_p = \frac{4\phi_p}{\pi d^2}\,\frac{L_M}{L}\,\left(1-e^{-\frac{L}{L_M}}\right) \tag{2-20}$$

Utilizing (2-2), (2-13), (2-14), (2-15), (2-16), and (2-17), we can write the two coupled rate equations that govern operation of the Nd:YAG laser

$$\frac{dN}{dt} = \eta N_p - 2c\sigma\rho N - \frac{2N}{\tau_T} \tag{2-21}$$

$$\frac{d\rho}{dt} = \frac{V_L}{V_R}\,c\sigma\rho N + \frac{nN}{p\tau_{32}} - \frac{\rho\alpha c}{L_R}$$

Let us now consider the steady state solution of these coupled rate equations. $\frac{dN}{dt} = \frac{d\rho}{dt} = 0$

$$c\sigma \rho N + \frac{N}{\tau_T} = \frac{\eta N_p}{2} \tag{2-22}$$

$$c\sigma \rho N + \frac{V_R}{V_L} \frac{nN}{p\tau_{32}} - \frac{V_R}{V_L} \frac{\rho\alpha c}{L_R} = 0 \tag{2-23}$$

Solving (2-22) for N, substituting into (2-23) and solving for ρ and assuming we can neglect the term containing p we get

$$\rho = \frac{L_R}{\alpha c} \frac{nN_p}{2} \frac{V_L}{V_R} - \frac{1}{c\sigma\tau_T} \tag{2-24}$$

Using (2-16), the two way laser irradiance, I_L, is

$$I_L = \frac{L_R}{\alpha} \frac{\eta N_p}{2} \frac{V_L}{V_R} - \frac{1}{\sigma\tau_T} \tag{2-25}$$

The one way laser irradiance will be half of I_L. If the area of the laser beam is A, the laser mirrors have a total output transmission, T, and we multiply by $h\nu_L$, the photon energy, the laser output power in watts is given by

$$P_{out} = \frac{I_L}{2} TA\ h\nu_L$$

$$= \frac{TA\ h\nu_L}{2}\left(\frac{L_R}{\alpha}\frac{\eta N_p}{2}\frac{V_L}{V_R} - \frac{1}{\sigma\tau_T}\right)$$

$$P_{out} = \frac{T}{\frac{2\sigma\tau_T}{Ah\nu_L}}\left[\frac{\frac{\eta N_p \sigma\tau_T L_R V_L}{2V_R}}{\alpha} - 1\right] \qquad (2\text{-}26)$$

Let us define the following

$$g_o = \frac{\eta N_p \sigma\tau_T\ L_R\ V_L}{2V_R} \qquad (2\text{-}27)$$

$$\beta = \frac{2\sigma\tau_T}{A\ h\nu_L} \qquad (2\text{-}28)$$

Then, equation (2-25) becomes

$$P_{out} = \frac{T}{\beta}\left(\frac{g_o}{\alpha} - 1\right) \qquad (2\text{-}29)$$

Let us now determine the significance of each of the variables in equation (2-29). We have already defined the total mirror transmission, T, (the sum of T_1 and T_2), and the single pass loss, α. The transmission loss is of course included in α. Let's further define α as composed of half of the double pass transmission loss, T, and a single pass dissipative loss, α_o.

$$\alpha = \frac{T}{2} + \alpha_o \qquad (2\text{-}30)$$

Let us also define the one-way or circulating power P_c in the laser cavity.

$$P_c = \frac{I_L}{2} A \tag{2-31}$$

The laser output power is then just the product of the transmission T and P_c.

$$P_{out} = T P_c \tag{2-32}$$

Equating (2-29) and (2-32),

$$P_c = \frac{1}{\beta}\left(\frac{g_o}{\alpha} - 1\right)$$

$$\frac{g_o}{\alpha} = 1 + \beta P_c$$

$$\alpha = \frac{g_o}{1+\beta P_c} \tag{2-33}$$

Now, in the steady state condition gain, g, must equal the loss α. The gain must, therefore, be expressed by

$$g = \frac{g_o}{1+\beta P_c} \tag{2-34}$$

This is just the equation for saturated single pass gain in a homogeneous laser material.[9] Our formulation of the rate equations has assumed homogeneous broadening since we have assumed that any photon can stimulate any inverted ion. The homogeneous assumption is correct for Nd:YAG. It becomes somewhat incorrect for Nd:Glass.

The gain decreases or saturates with increasing circulating power, P_c. We see that g_o is the single pass gain at zero circulating power and β is the saturation parameter. Specifically, $1/\beta$ is the value of P_c at which the gain saturates to half of the initial value. It should be noted that this definition of β is for oscillators and assumes that P_c traverses the laser material in two directions. For amplifier calculations a different quantity $\beta_a = \beta/2$ must be used. This formulation can also be used for oscillators if the total power $2P_c$ traversing the laser material is used.

It is useful before we leave this subject to consider the relationship of g_o to the inversion density, N. Consider in (2-21) the rate equation for N for the steady state case, $dN/dt = 0$ and the unsaturated case $\rho=0$. Then

$$N = \frac{\eta N_p \tau_T}{2} \tag{2-35}$$

Using equation (2-27),

$$g_o = \frac{\eta N_p \tau_T \sigma L_R V_L}{2V_R} \tag{2-27}$$

Assuming the resonator and the laser material have the same diameter, $V_R = \frac{\pi}{4} d^2 L_R$ and $V_L = \frac{\pi}{4} d^2 L$, and substituting from equation (2-35),

$$g_o = \sigma L N \tag{2-36}$$

2.3 Model for Radiation Emission from Pump Source

In this section we will introduce a model for the pump radiation emission from a pump source. As an example, let us consider a tungsten-iodine lamp with which we ran the experiment shown in Fig. 2-2. The output from the lamp is filtered by a narrow band filter that transmits energy only in the primary Nd:YAG laser pump band spectral range. The radiation transmitted is detected and a record is made of detected radiation as a function of input power to the pump lamp.

A graph of the data from such an experiment performed with a tungsten-iodine pump lamp is shown in Fig. 2-2. The graph starts from the coordinate origin which at first has a curved characteristic and then becomes linear. The linear portion of this graph can be accurately represented by a linear intercept equation.

$$P_r = k_r (P_{in} - P_o) \tag{2-37}$$

where P_r = the power radiated into the desired spectral region

k_r = the slope representing the efficiency of converting input power into the desired radiation

P_{in} = the input power to the lamp

P_o = the intercept of the linear curve with the P_{in} axis.

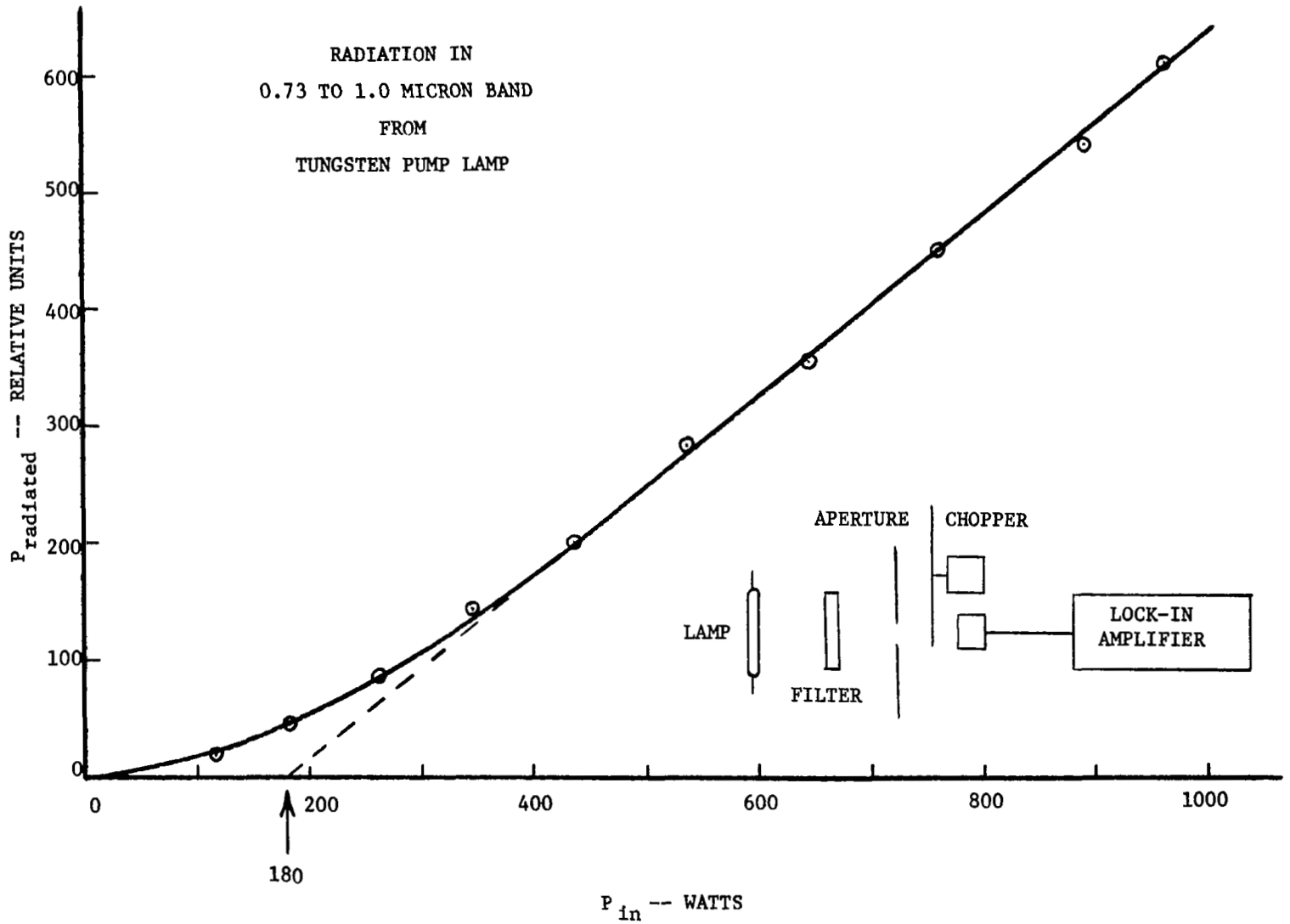

Figure 2-2 Narrow Band Radiation Output as a Function of Input for the Tungsten-Iodine Lamp

This model not only holds for the tungsten-iodine lamp shown in Fig. 2-2. It also applies to the Hg arc[10], and we have found it applies to the Kr arc, the K-Hg arc, and the RbI-Hg arc. With $P_o=0$ it also applies to the ideal linear input-output characteristic which is approached by incoherent semiconductor diodes.

2.4 Theoretical Model for the Nd:YAG Laser

We can now formulate our theoretical model of the Nd:YAG laser. Because of the difference in the average pump light irradiance for the side pumped and the end pumped laser cases, we will have to have a model for each. We will show all details for development of the side pumped theoretical model but will only give the final results for the end pumped case.

2.4.1 Side Pumped Laser

Consider that we have a side pumped Nd:YAG laser of the type shown in Fig. 2-3.

The power radiated into the laser pump bands is given by equation(2-37).

$$P_r = k_r (P_{in} - P_o) \tag{2-37}$$

The total number of pump photons, ϕ_p, reaching the laser rod is

$$\phi_p = k_p \frac{P_r}{h\nu_p} \tag{2-38}$$

where k_p = the pump cavity transfer efficiency. (This constant includes the effect of multiple reflections in the pump cavity.)

$h\nu_p$ = the average pump photon energy.

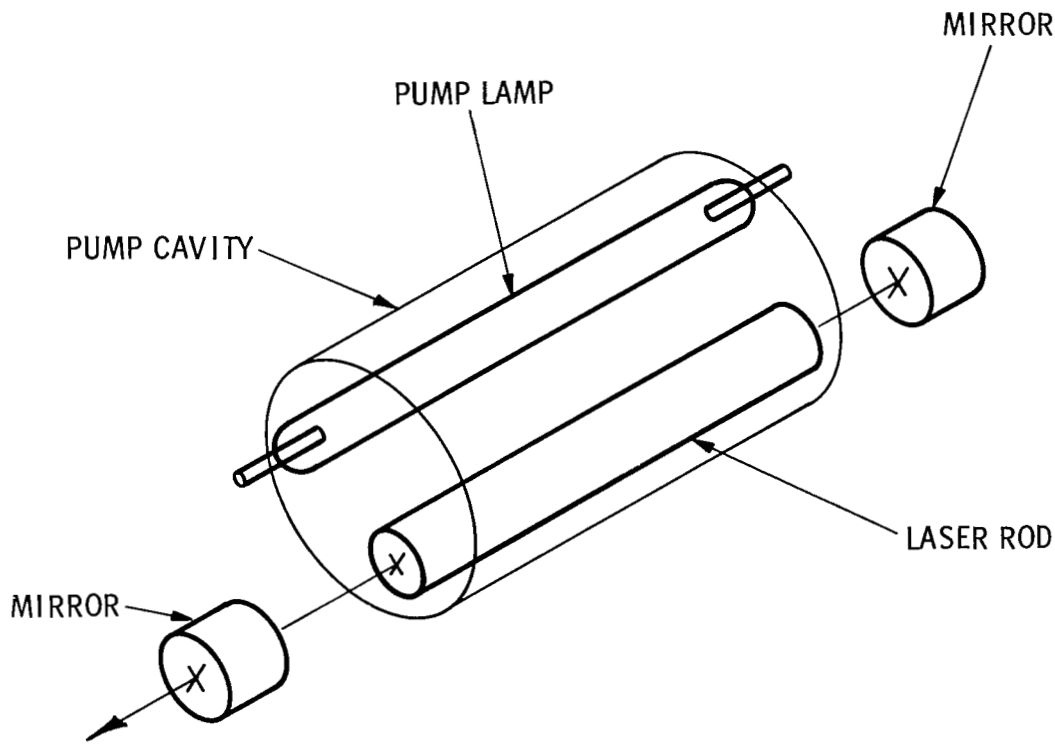

Figure 2-3 Optically Side Pumped Laser

The pump light irradiance in the laser rod is then from equation (2-18)

$$I_p = \frac{k_p k_r \left(P_{in} - P_o\right)}{h\nu_p Ld} \tag{2-39}$$

where L = the laser rod length

d = the laser rod diameter

The pump photon absorptions per unit time, per unit volume is then from equation 2-17.

$$N_p = \frac{\sigma_p k_p k_r N_1}{h\nu_p Ld} \left(P_{in} - P_o\right) \tag{2-40}$$

where again

σ_p = the average pump light absorption cross section per laser ion.

N_1 = the ground state laser ion density ions per unit volume.

Using equation (2-27), and assuming the diameter, d, of the laser rod and the laser resonator are the same, the single pass unsaturated gain, g_o, is

$$g_o = \frac{\sigma_p k_p k_r \eta N_1 \sigma \tau_T}{2h\nu_p d} \left(P_{in} - P_o\right) \tag{2-41}$$

where σ = the stimulated emission cross section per inverted laser ion.

τ_T = the total inversion lifetime.

Let define,

$$K = \frac{\sigma_p k_p k_r \eta N_1 \sigma \tau_T}{2hV_p d} (P_{in} - P_o) \qquad (2\text{-}42)$$

Then,

$$g_o = K (P_{in} - P_o) \qquad (2\text{-}43)$$

To complete our model of the side pumped Nd:YAG laser we need to repeat equations (2-28) and (2-29).

$$\beta = \frac{2\sigma\tau_T}{Ah\nu_L} \qquad (2\text{-}28)$$

where $A = \pi/4\ d^2$ the laser rod cross sectional area,

$h\nu_L$ = the laser photon energy,

and

$$P_{out} = \frac{T}{\beta} \left(\frac{g_o}{\alpha} - 1 \right) \qquad (2\text{-}29)$$

where again,

$T = T_1 + T_2$,the sum of the two laser mirror output transmissions

$\alpha = \frac{T}{2} + \alpha_o$, the total single pass loss

α_o = the single pass dissipative loss.

Substituting (2-43) into (2-29) and rearranging, we get

$$P_{out} = \frac{KT}{\alpha\beta}\left[P_{in} - \left(P_o + \frac{\alpha}{k}\right)\right] \tag{2-44}$$

Define,

$$\eta_d = \frac{KT}{\alpha\beta}, \tag{2-45}$$

and

$$P_{th} = P_o + \frac{\alpha}{K} \tag{2-46}$$

Then,

$$P_{out} = \eta_d\,(P_{in} - P_{th}) \tag{2-47}$$

This is the familiar linearized laser input-output equation with slope efficiency, η_d, and threshold, P_{th}. We have, therefore, developed a theoretical model for the parameters that affect the experimentally observable laser performance.

2.4.2 End Pumped Laser

Following the same procedure as for the side pumped case we develop the following equations for the end pumped case:

$$\bar{I}_p = \frac{4k_p k_r}{\pi h\nu_p d^2} \frac{L_M}{L} (1-e^{\frac{-L}{L_M}}) (P_{in} - P_o) \tag{2-48}$$

$$N_p = \sigma_p N_1 \bar{I}_p \tag{2-49}$$

$$g_o = K (P_{in}-P_o) \tag{2-43}$$

$$K = \frac{2\sigma_p k_p k_r \eta N_1 \sigma\tau_T}{\pi h\nu_p d^2} L_M \left(1-e^{\frac{-L}{L_M}}\right) \tag{2-50}$$

The following equations are the same for both cases

$$\beta = \frac{2\sigma\tau_T}{Ah\nu_L} \tag{2-28}$$

$$P_{out} = \frac{T}{\beta} \left(\frac{g_o}{\alpha} -1\right) \tag{2-29}$$

$$\eta_d = \frac{KT}{\alpha\beta}$$

$$P_{th} = P_o + \frac{\alpha}{K} \tag{2-46}$$

$$P_{out} = \eta_d (P_{in} - P_{th}) \tag{2-47}$$

These equations for the end pumped case have been included for completeness. In the remainder of this report, we will consider only the side pumped case unless a specific statement of a different consideration is made.

2.5 Discussion of the Theoretical Model

2.5.1 Material Constants and Their Experimental Determination

Material parameters can be lumped into a single constant for a given material in a given experimental configuration. We can determine the value of this lumped material constant experimentally. We will restrict ourselves to consideration of the side pumped case.

Rearranging equation (2-42)

$$dK = \frac{\sigma_p k_p k_r \eta N_1 \sigma \tau_T}{2h\nu_p} = \left(\frac{\beta A}{2}\right)\left(\frac{N_1 \sigma_p \eta}{2}\right)\left(\frac{\lambda_p}{\lambda_L}\right) \quad k_p k_r \tag{2-51}$$

All parameters on the right are dependent upon the laser material or the pump lamp with the exception of k_p, the pump cavity efficiency. We can assume that in all cases we will maximize k_p such that it will always have very close to the same value. We, therefore, conclude that for a particular laser material and pump lamp in a good pump cavity the quantity dK is a constant.

$$dK = \text{constant} \tag{2-52}$$

Rearranging equation (2-28)

$$\frac{2}{\beta A} = \frac{h\nu_L}{\sigma \tau_T} \tag{2-53}$$

All parameters on the right are dependent only upon the laser material. We can

assume they are constant for a given laser material.

$$\frac{2}{\beta A} = \text{constant} \tag{2-54}$$

This quantity is the total laser power density at which the laser gain is reduced by a factor of 2.

Equation (2-52) represents gain characteristics of a given laser material-pump lamp combination. Equation (2-54) represents the saturation characteristics of a given laser material. These two characteristics will have important bearing on design of a space qualified Nd:YAG laser.

Let us now consider how we determine these constants. Consider that we have a laser and that we have a set of mirrors with several different transmissions, T, but with constant total single pass dissipative loss, α_o. Let us plot laser output power versus input power for each total mirror transmission combination. From these plots we determine the threshold, P_{th}, and the slope efficiency, η_d, for each mirror transmission, T.

Consider equations (2-46) and (2-30)

$$P_{th} = P_o + \frac{\alpha}{K} \tag{2-46}$$

$$\alpha = \frac{T}{2} + \alpha_o \tag{2-30}$$

Combining these,

$$P_{th} = \left(P_o + \frac{\alpha_o}{K}\right) + \frac{1}{2K}(T) \tag{2-55}$$

We have several experimental values of P_{th} as a function of T. If we draw a graph of P_{th} versus T, the ordinate intercept is $\left(P_o + \frac{\alpha_o}{K}\right)$ and the slope is $(1/2K)$.

Consider equations (2-45) and (2-30)

$$\eta_d = \frac{KT}{\alpha\beta} \tag{2-45}$$

Combining,

$$\frac{1}{\eta_d} = \frac{\beta}{2K} + \frac{\beta\alpha_o}{K}\left(\frac{1}{T}\right) \tag{2-56}$$

Again, we have several experimental values of η_d versus T. If we draw a graph of $1/\eta_d$ versus $1/T$, the ordinate intercept is $\frac{\beta}{2K}$ and the slope is $\frac{\beta\alpha_o}{K}$. The two intercepts and the two slopes from equations (2-55) and (2-56) allow determination of K, α_o, β and P_o. From these and the known laser rod diameter, we can determine dK and $2/\beta A$.

We should emphasize that a number of different mirror transmissions must be used for this experiment and that the plots of P_{th} versus T, and $1/\eta_d$ versus $1/T$ must form straight lines. If α_o is different for the various mirrors or if α_o is a function of circulating laser power, the data will not form straight lines and this method cannot be used. Intracavity nonlinear crystals will

sometimes produce such effects even when the nonlinear process is not phase-matched.

2.5.2 Optimum Output Coupling

Consider that we have a laser with a pump lamp having a certain operating point that produces an unsaturated single pass laser gain, g_o. We will now determine the laser mirror transmission, T, that produces the optimum amount of laser output power. Consider equations (2-29) and (2-30).

$$P_{out} = \frac{T}{\beta} \left(\frac{g_o}{\alpha} - 1 \right) \tag{2-29}$$

$$\alpha = \alpha_o + \frac{T}{2} \tag{2-30}$$

Combining,

$$P_{out} = \frac{T}{\beta} \left[\frac{g_o}{\alpha_o + T/2} - 1 \right]$$

Differentiating twice with respect to T,

$$\frac{dP_{out}}{dT} = \frac{g_o T}{2\beta(\alpha_o + T/2)^2} + \frac{g_o}{\beta(\alpha_o + T/2)} - \frac{1}{\beta}$$

$$\frac{d^2P_{out}}{dT^2} = \frac{-g_o}{2\beta(\alpha_o + T/2)^2}$$

Setting the first derivative equal to zero to find extremum and solving for the second derivative of this extremum.

$$\frac{dP_{out}}{dT} = 0 = g_o\alpha_o - (\alpha_o+T/2)^2$$

$$T = 2\left(\sqrt{g_o\alpha_o} - \alpha_o\right)$$

$$\frac{d^2P_{out}}{dT^2} < 0$$

The extremum is, therefore, a maximum and the optimum laser output transmission, T_{op}, is

$$T_{op} = 2\left(\sqrt{g_o\alpha_o} - \alpha_o\right) \qquad (2\text{-}57)$$

SECTION 3

LAMP PUMPED Nd:YAG LASERS

In this section we will consider lamp pumping of the space qualified Nd:YAG laser. We will assume side pumping in an efficient optical pump cavity as is shown in Fig. 2-3. We will first consider the various possible pump lamps and lamp design characterisitcs of interest for space qualified lasers. The best possible lamp will then be considered with the theoretical model developed in Section 2. Curves that show the effect of various parameters on laser gain, threshold and output power will be developed. These curves will be used in designing the space qualified lamp pumped Nd:YAG laser in a later section of this report.

3.1 Lamps Available for Pumping

3.1.1 Introduction

Nd:YAG is a four level laser material with which it is relatively easy to obtain an inversion. As a result, Nd:YAG lasers have been operated continuously with many different types of lamps. In this section we will consider a few of these. The lamps we will consider include those of most interest for space qualified Nd:YAG, plus enough others to show the important characteristics of pump lamps in general. We will consider the tungsten filament lamp[1], especially the halogen cycle type and several jacketed arc lamps. These include the krypton arcs[11,12], the doped mercury arcs[7], rubidium iodide-mercury and potassium mercury, and the pure potassium arc. Incoherent semiconductor diode pump lamps for Nd:YAG will be considered in Section 4.

3.1.2 Tungsten-Halogen Pump Lamps

Tungsten-halogen lamps employ the halogen cycle to keep tungsten from leaving the hot filament and depositing on the cold inside wall of the lamp jacket. The halogen cycle chemically converts the tungsten atoms boiled off the filament into tungsten-halide molecules in the low temperature region near the lamp walls. These molecules diffuse back to the tungsten filament where the high temperature disassociates them, thereby depositing tungsten back on the filament and freeing the halogen gas to repeat the cycle.

The halogen cycle allows operation of tungsten filament lamps at much higher temperatures than is possible in vacuum jackets. Typically, tungsten-iodine lamps operate at 3200^{o}K to 3400^{o}K with lifetimes of 100 hours compared to 2800^{o}K temperatures for similar lifetime, vacuum jacketed lamps. The 3400^{o}K temperature blackbody radiation from tungsten has an emission maximum near the 8000$\mathring{A}$ Nd:YAG pump bands. Unfortunately, the blackbody radiation is very broad band and the pump bands are quite narrow. Only moderate laser efficiency can, therefore, be expected from tungsten.

Tungsten-iodine lamps are low in cost. They are used in television, motion picture, and theater lighting and have been mass produced for some time. Electrically they are a simple resistive load and require an uncomplicated power supply. The first continuous Nd:YAG laser used tungsten lamps[1] and many commercial lasers employ them.

Figure 2-2 shows the radiometer set up for determining output radiation versus input power characteristic of the Q1000T3/4CL tungsten-iodine lamp. Only 0.73 to 1.0 micron Nd:YAG pump spectra region is measured. The experimental results are also shown in the figure. It should be noted that the intersect, P_o, which was defined in Section 2.3 is 180 watts. Similar experiments on a

number of these lamps have shown P_o to vary between 180 and 230 watts.

An experimental arrangement for determining the pump light absorption characteristics of Nd:YAG for a lamp is shown in Fig. 3-1. Light from the lamp is passed through a Jarrell-Ash $\frac{1}{2}$ - m Ebert monochromator and detected. Two different lengths of Nd:YAG are put in front of the detector to filter out the pump radiation. One Nd:YAG filter is 3 mm long and the other is 10 cm long. The detected spectrum is run first with no Nd:YAG filter in order to determine the transfer characteristics of the system. The spectrum is then repeated with each of the Nd:YAG filters.

The Nd:YAG absorption characteristics for the tungsten-iodine lamp is shown in Fig. 3-2. The 3 mm Nd:YAG filter which is typical of laser rod diameters is optically very thin. The pump bands have narrow fine structure and little radiation is absorbed in a single pass through 3 mm of Nd:YAG. The 10 cm long Nd:YAG filter produces wide deep absorption bands.

The combination of the 3 mm and 10 cm Nd:YAG filter data clearly shows what pump light spectra is effective in pumping Nd:YAG. We will find this technique is very valuable for evaluating line emitting pump lamps.

It should be noted that the detected spectral amplitudes in Fig. 3-2a, b, and c can not be directly compared. The gain of the electronics was independently adjusted for each spectrum in order to obtain a good curve and the data was not retained to allow intercomparison of the curves.

Tungsten-iodine lamp pumped 3 mm diameter Nd:YAG laser experiments, with several output transmission mirrors, as described in Section 2.5.1, have

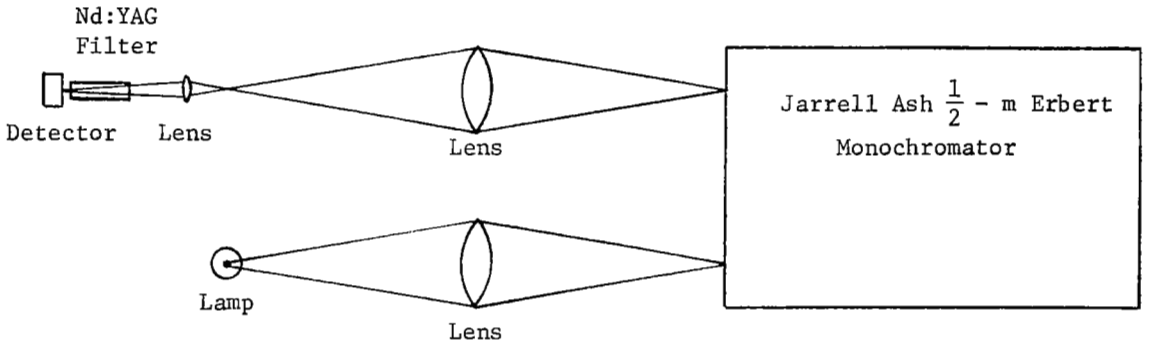

Figure 3-1 Experimental Arrangement for Determining the Nd:YAG Pump Band Absorption for Various Pump Lamps.

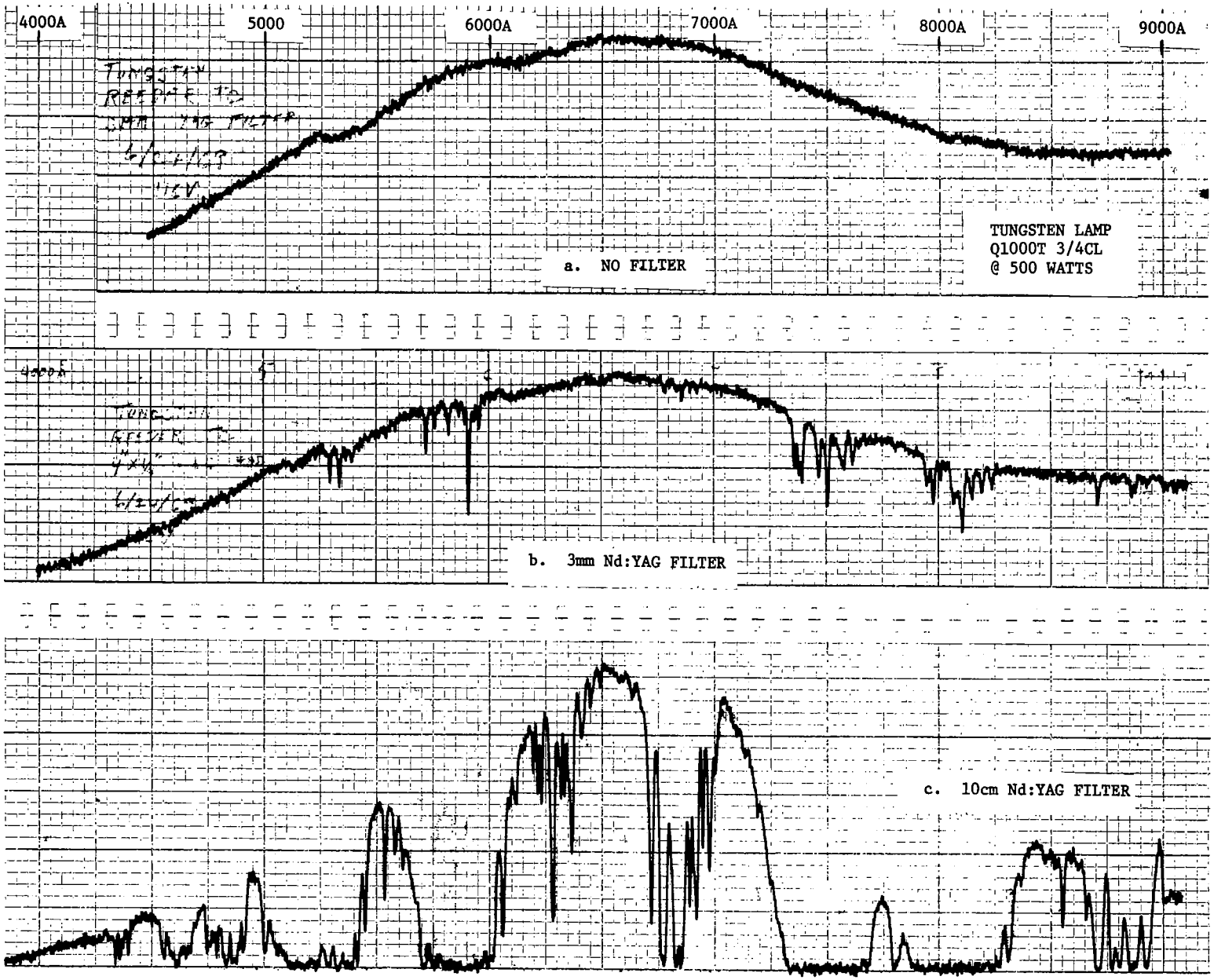

Figure 3-2 Nd:YAG Absorption of Tungsten Radiation

been run many times at Sylvania. The data has been variable, but in general has gotten better through the years as better Nd:YAG laser rods and better pump cavities have been made. We have carefully considered this data and have concluded that for high quality Nd:YAG rods in good pump cavities the constant dK for tungsten-iodine lamps is

$$(dK)_{WI} = 0.028 \frac{cm}{kW} \tag{3-1}$$

We should mention that this data was all taken with 3 mm diameter rods with 2 mm diameter lamp filaments. Data for other diameter rods was not available. We have assumed that dK is constant as our theory predicts and have used one set of dK data to determine the constant. We will show in the next section that dK is indeed constant for two different Kr arc pumped rod diameters.

The data for P_o from these experiments with 6.3 cm long lamps has been consistent with the radiometric data described in Section 2.3.

$$(P_o)_{\substack{WI \\ 6.3\ cm}} = 180 \text{ watts} \tag{3-2}$$

These tungsten-iodine pumped experiments together with all other pump lamp experiments have also determined the constants $\frac{2}{\beta A}$ and α_o that are dependent only on the laser material. We conclude that for good quality 1.0% Nd:YAG rods and good quality laser mirrors external to the laser rod in multimode operation,

$$\frac{2}{\beta A} = 1500 \text{ watts/cm}^2$$

and

$$\alpha_o = 0.006 \tag{3-4}$$

If the mirrors were on the rod ends α_o would be lower. For TEM_{oo} mode operation α_o would be greater because of higher diffraction losses.

The tungsten-iodine lamp has two characteristics that seriously limit it for space qualified laser application. First, the long delicate, coiled tungsten filament is particularly vulnerable to vibration test failure. A thirty minute vibration test-dwell at any frequency near a filament resonance is sure to destroy the filament. Second, the lifetime of tungsten-iodine lamps is typically less than 100 hours. A few thousand hours can be obtained by lower temperature operation which of course lowers the laser efficiency.

3.1.3 Krypton Arc Pump Lamps

The arc spectra of a number of the inert gasses are rich in line spectra in the near infrared. Xenon is most commonly used in arc lamps. The infrared line spectra of xenon misses all the Nd pump bands however. Read[11] was the first to note the superiority of Kr arcs for pumping Nd:YAG. Subsequent investigation[12] has confirmed this. Krypton arc pumped Nd:YAG lasers are currently the highest power and the most efficient[3] continuous lasers in the near infrared and visible spectral regions.

The narrow band 0.7 to 1.0 micron radiometric data for a 6 mm i.d., 10 cm long continuous Kr arc is shown in Fig. 3-3, compared with the tungsten lamp data. The intersect, P_o, for this water cooled lamp is 410 watts.

The Nd:YAG absorption characteristics for the Kr arc lamp is shown in Fig. 3-4. The two strongest Kr lines at 7600A and 8110A are both strongly absorbed by the Nd:YAG. The other Kr arc lines are not much absorbed. From these results we would expect the Kr arc lamp to be an effective pump lamp for Nd:YAG.

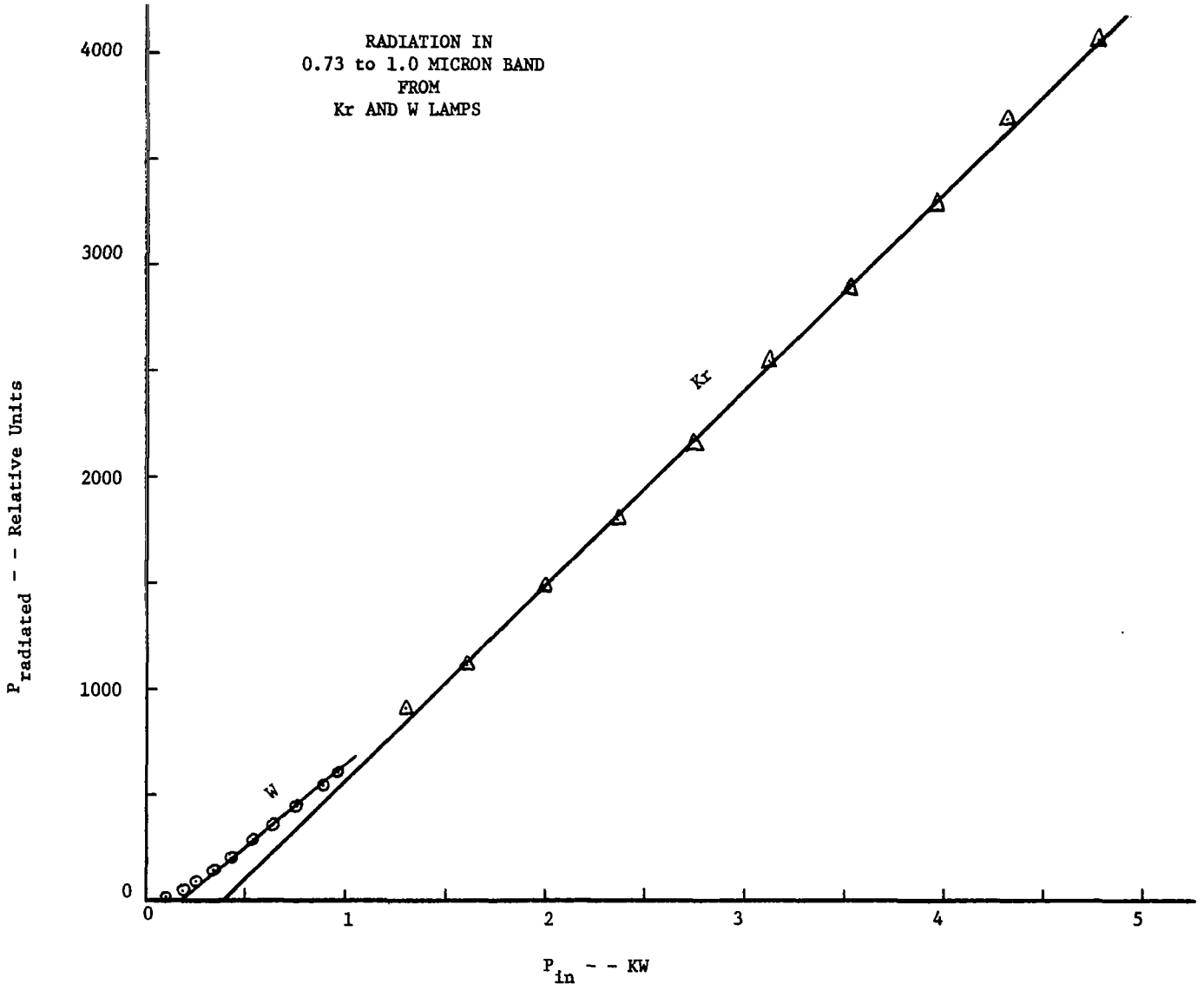

Figure 3-3 Narrow Band Radiation Output as a Function of Input for the Krypton Arc Lamp

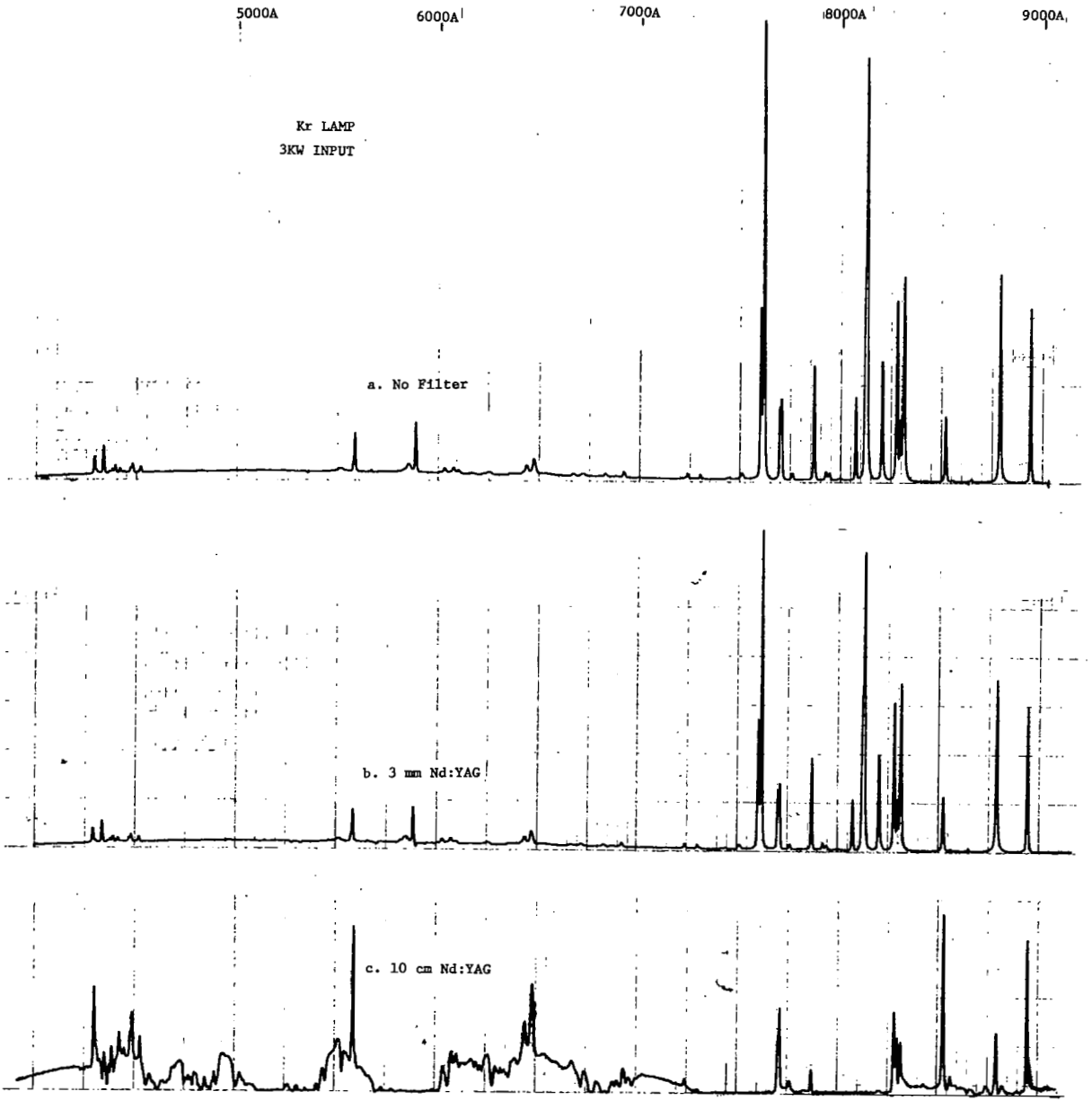

Figure 3-4 Nd:YAG Absorption of Krypton Arc Radiation

Krypton arc lamp pumped Nd:YAG laser experiments have been run with both 0.25 inch and 0.15 inch diameter laser rods. These experiments have been conducted with both 6 mm i.d., and 4 mm i.d. Kr arcs. The results have always been better with 6 mm lamps with both diameter laser rods. The reasons for this are not clearly known. One possibility is that the main luminous region of the Kr arc is smaller than the inside lamp bore as in the Hg arc[10] and that the arc for the larger bore more closely matches even the smaller laser rod. Another possibility is that the Kr arc does fill the bore (as it visibly appears to) and that wall losses are less for the larger bore lamps. In any case the best experimental results occur with the 6 mm bore Kr arc lamps.

Comparing the data obtained by using various mirror transmissions we find that dK for the 0.25 in. diameter and the 0.15 in. diameter laser rods (pumped with the 6 mm bore lamps) only vary by 8 percent. This is a remarkably small variation. It confirms our theoretical contention that dK is a constant for side pumped laser rods. The experimental data shows that dK for krypton arc lamps is

$$(dK)_{Kr} = 0.066 \frac{cm}{kW} \tag{3-5}$$

The data for P_o from these experiments on 10 cm lamps has been consistent with the radiometric data

$$(P_o)_{\substack{Kr \\ 10\ cm}} = 410 \text{ Watts} \tag{3-6}$$

The lifetime of Kr arc lamps has been much shorter than one would expect. Typical operating life is less than 100 hours. Failures are typically a breaking of the fused quartz lamp jacket or excessive sputtering of the lamp electrodes. This short life is inconsistent with the goals for a space qualified Nd:YAG laser. Also, the high P_o of water cooled krypton arc lamps produces higher laser thresholds than is desired for the space qualified laser.

3.1.4 Potassium-Mercury Arc and Potassium Arc Pump Lamps

The mercury arc lamps are the most developed lamp being manufactured. Elenbaas[10] has described the properties of these lamps in detail in his book. Lifetimes of these lamps are exceedingly long. Typical half-lives on Sylvania Lighting Division data sheets is 20,000 hours.

Mercury arcs can be doped with various elements to modify the spectral output of the lamps while maintaining the good mercury arc characteristics.[13,14] Doped Hg arc lamps are now used in almost all high intensity lighting such as street lights, sports arenas, etc. These lamps fall into two categories - metal doped Hg arcs and metal-iodide doped Hg arcs. The metal-iodide type lamps are very similar to conventional Hg arc lamps. Fused quartz lamp jackets are used and the lamps operate at temperatures and pressures typical of the low pressure Hg arcs. We will discuss application of these type lamps to Nd:YAG pumping in the next section.

The metal doped Hg arc lamps must be operated at temperatures above the boiling point of the metal dopant. The pressure of these lamps is also very high and the hot metal is usually very corrosive on the lamp jacket. The Na-Hg lamp is typical of a metal doped Hg arc lamp.[13] These lamps must use

sapphire jackets (typically polycrystalline) because of the high temperature and corrosiveness of Na gas. The lamps typically have metal end caps of niobium which matches the thermal expansion of sapphire. The niobium end caps must be protected to prevent oxidation at the high lamp operating temperature. The lamps are typically operated with a vacuum jacket. The output spectra of the Na doped Hg lamps are typical of Na and the Hg emission is almost completely suppressed. The high operating pressure considerably broadens the sodium emission lines. Na also strongly re-absorbs its own radiation. This produces a "reversal" in the emitted radiation. The wings of the broad spectral line are emitted but the center is almost completely self absorbed.

The potassium D lines are situated almost exactly between the two Nd:YAG pump bands. As a line emitter K would be very poor as a Nd:YAG pump lamp. In the high pressure metal doped arc, however, the broadened self reversed K lines have two wings that cover the two Nd:YAG pump bands. Liberman, Larson and Church[7] first recognized this fact. Because of the chemical similarity of K and Na, Na lamp technology could be applied to making K lamps and Nd:YAG lasers were successfully operated with the potassium lamp.

The luminous arc in a Hg or doped Hg arc lamp is much smaller than the lamp jackets inside the bore. Typically, the arc diameter is only 1/3 of the bore diameter.[15] Polycrystalline sapphire jackets scatter the radiation passing through and thereby greatly reduce the brightness of the lamp. A transparent single crystal sapphire jacket must, therefore, be used to achieve low threshold laser pumping[7].

The Sylvania Lamp Division has given us some polycrystalline sapphire jacketed K-Hg lamps. The narrow band 0.7 to 1.0 micron data for a 8 mm i.d.,

6.5 cm long, vacuum jacketed, continuous K-Hg arc operated at 60 Hz is shown in Fig. 3-5. Also shown in the Figure is the data for a RbI-Hg lamp that will be discussed later. The intersect, P_o, for this vacuum jacketed, radiation cooled, 6.5 cm long K-Hg lamp is 47 watts.

$$P_{o\ \substack{\text{K-Hg}\\ 6.5\text{ cm}}} = 47 \text{ watts} \tag{3-7}$$

The Nd:YAG absorption characteristics for this K-Hg lamp are shown in Fig. 3-6. The two broad wings of the potassium D lines overlap the Nd:YAG lins as desired. The lamp broadening in Fig. 3-6 is slightly greater than optimum. The lamp spectra as a function of input power is shown in Fig. 3-7. From this we can estimate that the optimum operating point for this 6.5 cm long lamp would have been about 450 watts.

Laser experiments were attempted with this polycrystalline jacked K-Hg lamp but the scattering in the lamp jacket prevented attainment of threshold. We were, therefore, unable to obtain laser data.

Liberman et al[7] gives comparative data for tungsten and K-Hg pumped lasers with a good quality pump cavity. Because of the excellence of their results, we can assume that they used a good quality Nd:YAG rod. We, therefore, know $2/\beta A \approx 1500$ watts/cm^2, $\alpha_o \approx .006$ and we know $P_o \approx 47$ watts. We also know P_o and K for the tungsten lamp. Using our model of the Nd:YAG laser and the known parameters we can fit our model to their data by adjusting dK for the K-Hg lamp. The resulting value of the dK for K-Hg was

$$dK_{\text{K-Hg}} = 0.08 \frac{\text{cm}}{\text{KW}}$$

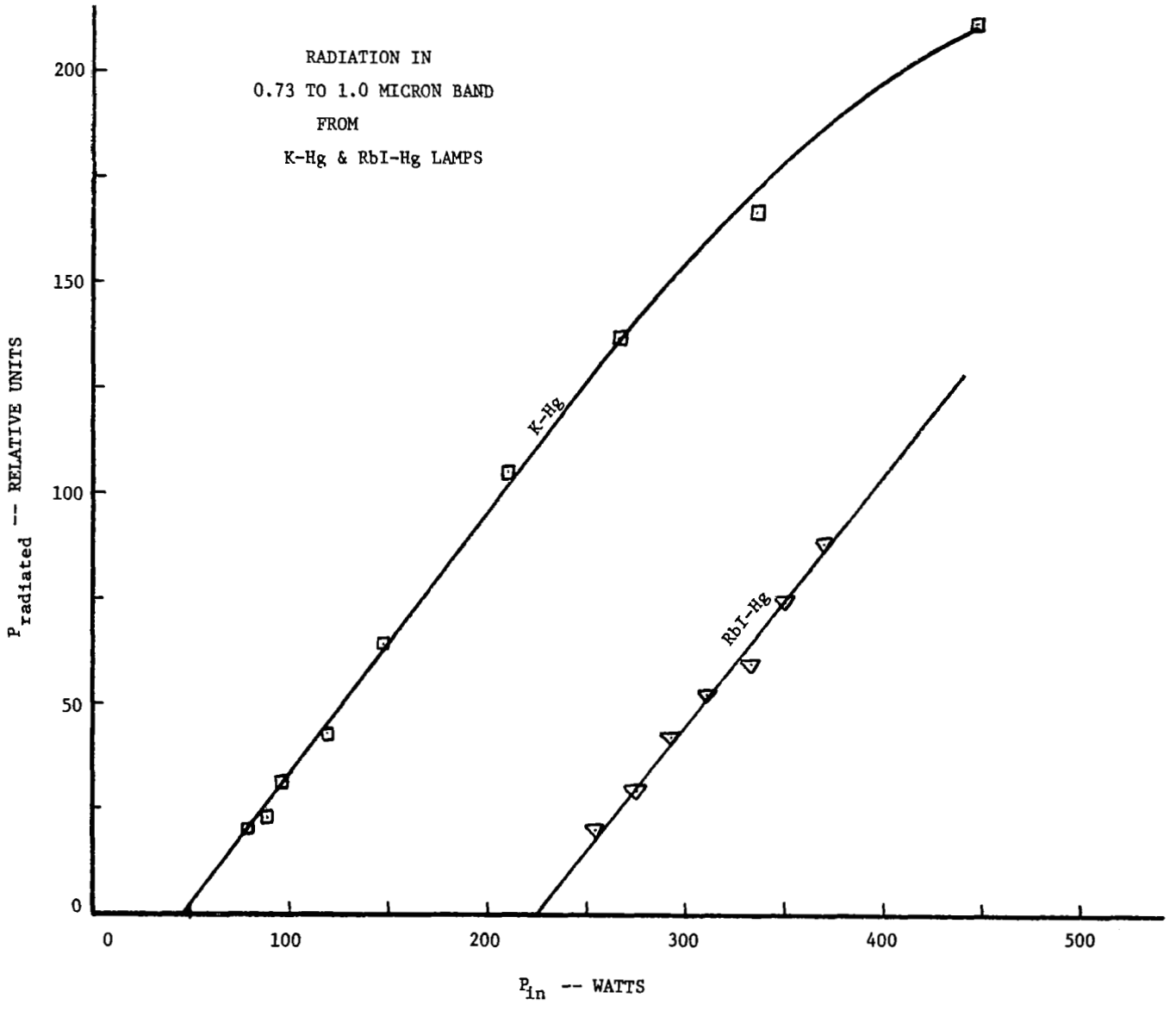

Figure 3-5 Narrow Band Radiation Output as a Function of Input for the Potassium-Mercury Arc Lamp and the Rubidium Iodide Mercury Arc Lamp.

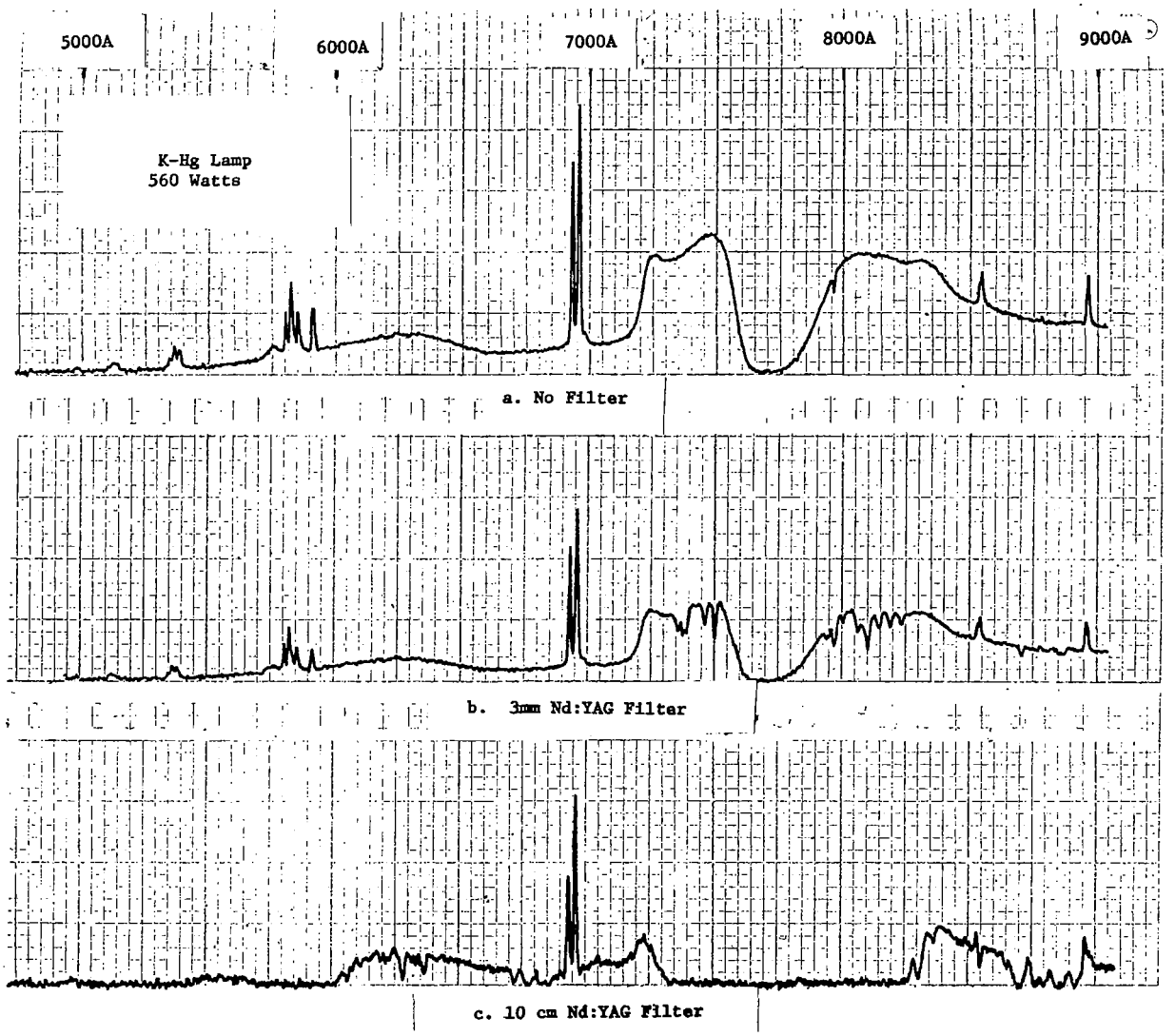

Figure 3-6 Nd:YAG Absorption of Potassium-Mercury Arc Radiation

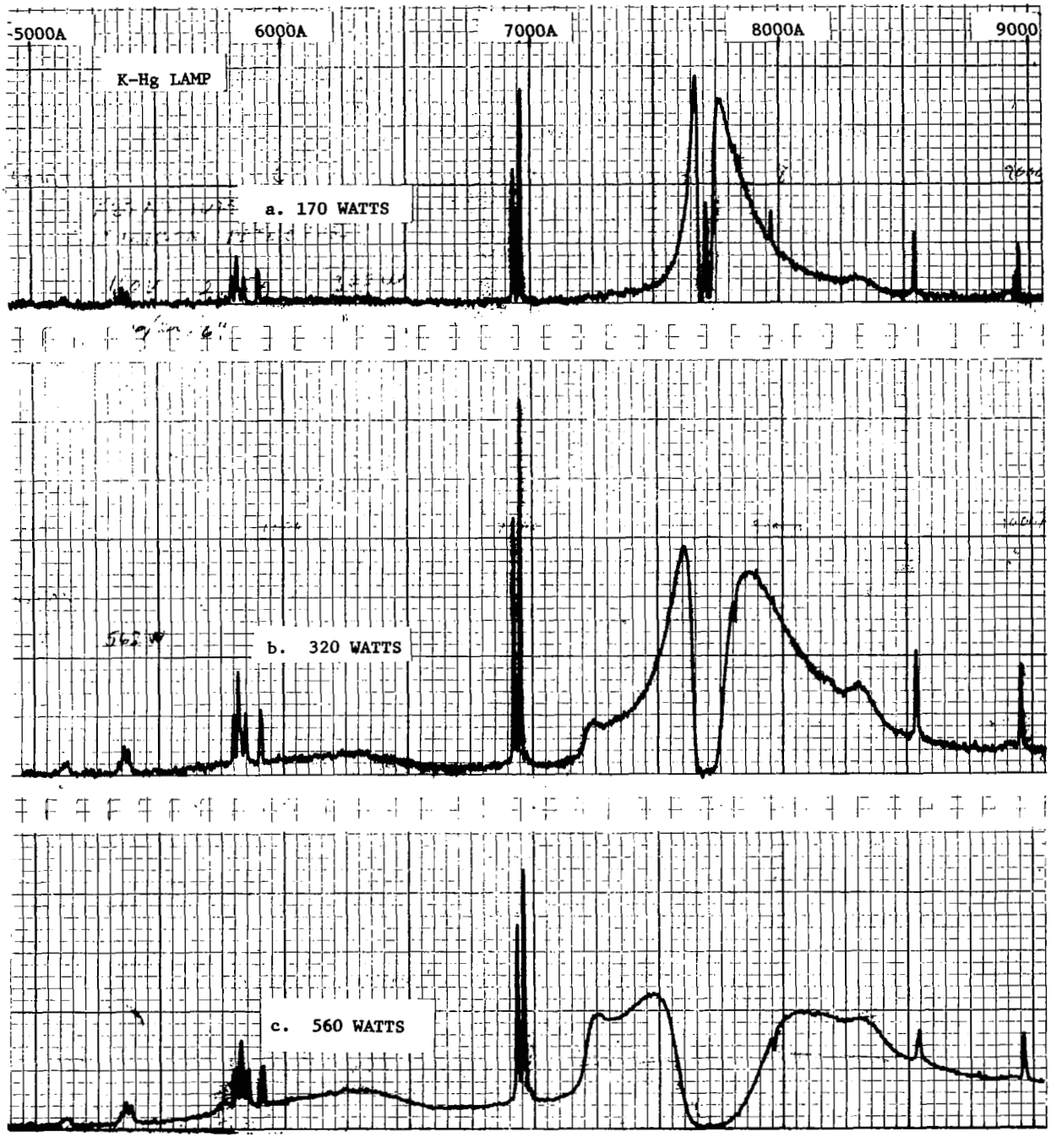

Figure 3-7. Potassium-Mercury Emission Spectrum for Varying Input Power.

The potassium-mercury lamp has the largest value of dK and the smallest value of P_o of any lamp we have considered. Fig. 3-8 shows the expected single-pass unsaturated gain, g_o, as a function of input power for a 3 mm diameter, 75 mm long Nd:YAG laser rod pumped by tungsten, krypton or potassium-mercury. The superiority of the K-Hg lamp is clearly demonstrated.

One curious aspect of the curves in Fig. 3-8 is the great variation in P_o for the various lamps. Elenbaas[10] has shown that P_o for a Hg arc lamp is represented by the heat loss from the lamp. He states that this heat loss is fixed per unit length and is unaffected by lamp diameter. He only considers the air convection cooled lamp in which side losses predominate, however. If we assume that P_o represents heat loss in all the lamps shown in Fig. 3-8 we note that this is consistent. The water cooled Kr arc has larger heat loss than the air cooled W lamp which has larger heat loss than the radiation cooled K-Hg lamp. We can then hypothesize that P_o is controllable in any lamp by changing the heat loss, i.e., the cooling. Liberman et al[7] not only developed a good spectral match lamp in K-Hg, but inadvertently by vacuum jacketing the lamp to protect the niobium end caps, they minimized P_o by insulating the lamp with the vacuum jacket.

One problem with the K-Hg lamp is that an A.C power supply must be utilized to prevent cataphoresis from separating the K and the Hg in the lamp. A 60 Hz power supply was used in our experiments. Liberman et al[16] found that 60 Hz produced ripple on the output and was less efficient than higher frequencies. They got their best results with 10 KHz power supply frequency. A high frequency A.C. power supply is a definite inconvenience and complication for a space qualified Nd:YAG laser.

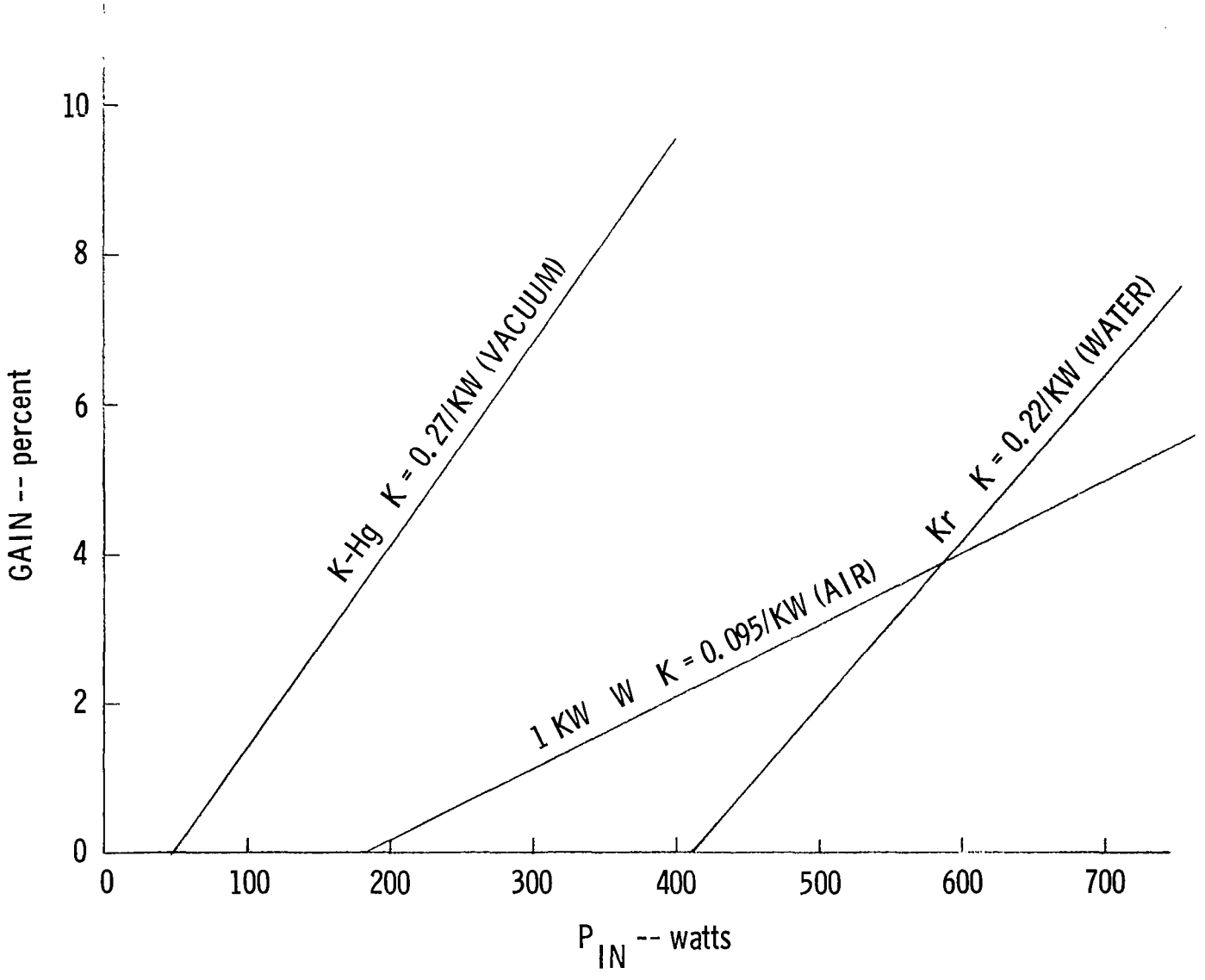

Figure 3-8. Theoretical Gain of 3mm x 75mm Nd:YAG for Various Pump Lamps.

Nobel[17] has recently developed potassium arc lamps containing no mercury. This work is being conducted under an Army contract with Ft. Monmouth, and is a continuation of the work started by Liberman et al[16]. The potassium arcs are essentially identical to the K-Hg without the complication of the two components. The luminous arc is about 1/3 the inner bore diameter. The spectral emission is identical to the K-Hg arc. The potassium arc can be operated DC with no cataphoresis problems.

Based upon estimates of the relative radiation heat loss from the sides and the ends of a radiation cooled K or K-Hg lamp we have estimated that P_o for a 6 mm bore, 2.54 cm arc length lamp would be 23 watts. Nobel[17] has recently tested such a lamp. He has kindly allowed us to use his data. He pumps a sample of Nd:YAG with radiation from the pump lamp and measures the 1.06 micron fluorescence as a function of input to the pump lamp. His data for a 1/4 inch diameter by 1.2 inch arc length is shown in Fig. 3-9. The intersect, P_o, for the lamp is 23 watts. The normal operating point for the lamp is 150 watts.

$$P_o = 23 \text{ W} \qquad (3\text{-}9)$$

Potassium
2.54 cm Arc Length

Na-Hg lamps are manufactured commercially by General Electric Corp. The half life of these lamps in their data sheets is quoted to be 8,000 hours. Since the K-Hg and K lamps are very similar to the Na-Hg lamps both technologically and chemically, we can make estimates of half life based upon the Na-Hg lamps. Commercial lamps are operated essentially in free space. In a laser pump cavity radiation is reimaged onto the lamp. This changes the lamp operating

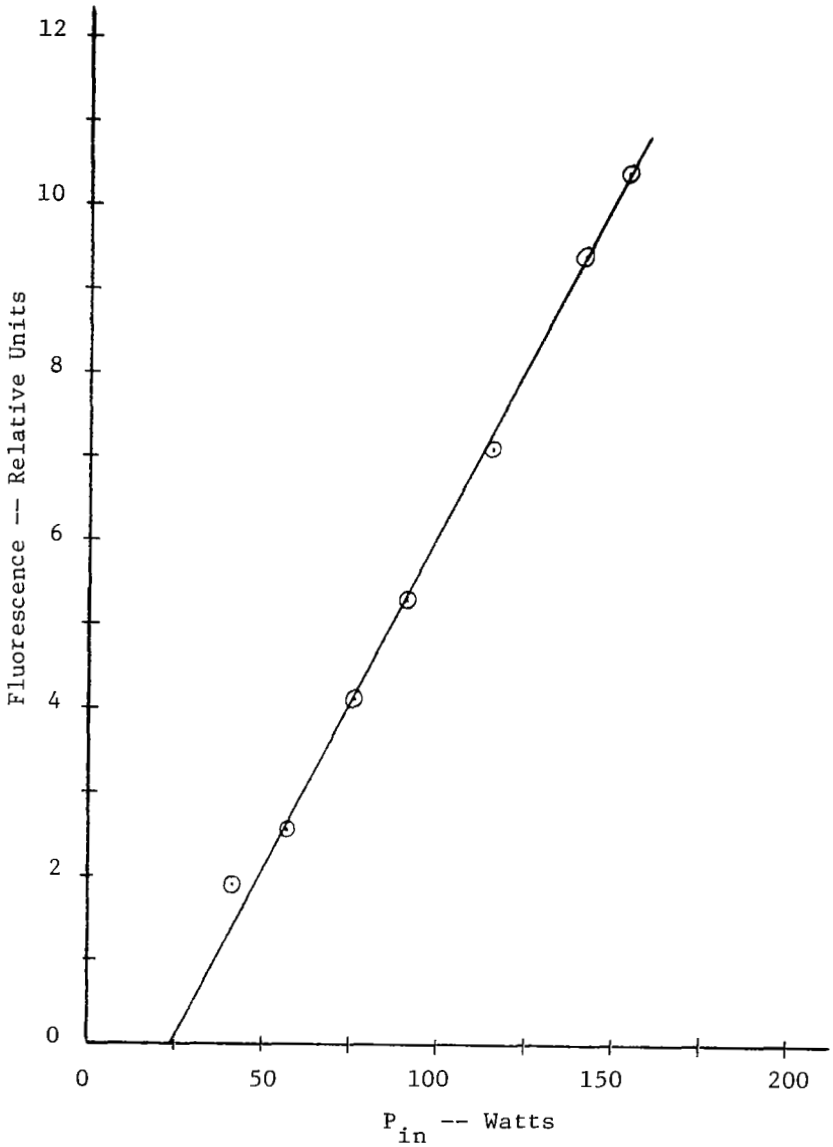

Figure 3-9. Nd:YAG Fluorescence as a Function of Input Power for a 1/4 Inch by 1 Inch Arc Length Potassium Arc Lamp (After Nobel[17]).

characteristics and might be expected to change the lamp lifetime.

To check lifetimes we took some commercial General Electric Na-Hg lamps and ballasts and deposited gold reflectors on the vacuum jacket concentric with the lamp. These reflectors simulated operation of the lamp in a laser cavity. We had to add inductance to the commercial ballasts to obtain stable lamp operation. The stable operating point of the lamps in the reflectors was at lower than rated input powers. Fig.3-10 shows a Na-Hg life test arrangement. Each lamp has an elapsed time meter that records operating time. The lamps are cycled three times a day. They operate for 8 hours, are turned off and allowed to cool for one-half hour, and repeat the cycle. At the time of writing this report the lamps have operated for over 4,000 hours with no failures. The lamp ratings, the operating power and the running hours on June 1, 1970 are listed in Table 3-1.

TABLE 3-1

Na-Hg Life Test Data in Reflectors

Lamp No.	Power Rating	Operating Power	Running Time (3-8 hr. cycles/day)
1	400	300	6044 (1800 hr. was at 200W)
2	275	240	4248
3	275	130	4224
4	400	300	4241

We can, therefore, say quite certainly that potassium pump lamps for a space qualified Nd:YAG laser will last several thousand hours. We suspect that with careful quality control and selection 10,000 hour lifetimes can be obtained. This can only be proved of course by development of the lamps which is one of the things we will recommend at the end of this report.

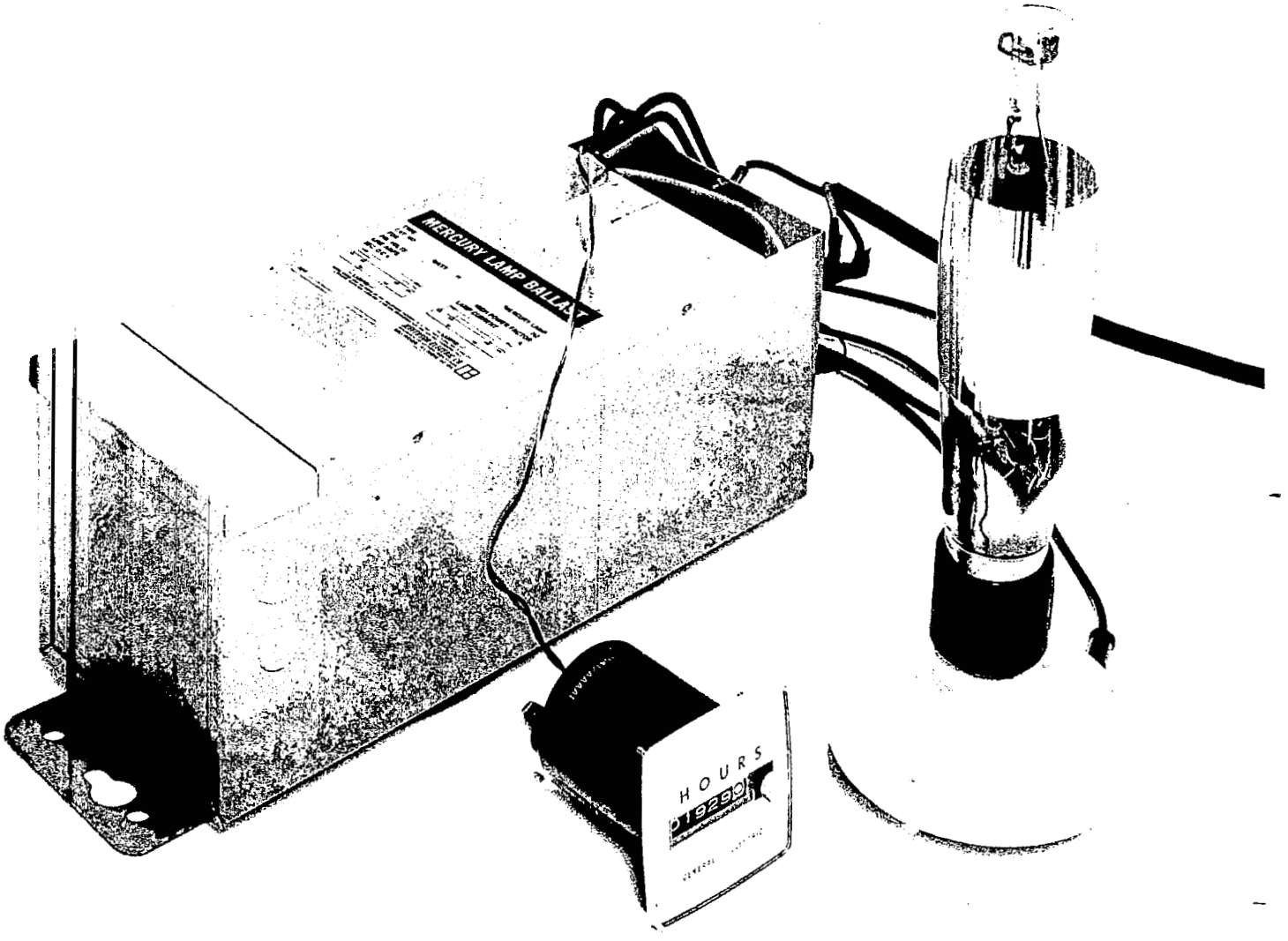

Figure 3-10. Life Test on Na-Hg Lamps in Reflective Cavities.

3.1.5 Rubidium Iodide-Mercury Arc Pump Lamps

The boiling point of metal-iodides is much lower than that of metals. Metal-iodide can be used to dope a metal in a mercury arc lamp for much lower temperature and pressure operation than the direct metal doped mercury arc. Metal iodide lamps produce a narrow line emission due to the lower pressures. Little pressure broadening and reversal occurs. For metal-iodide doped Nd:YAG laser pump lamps the line emission must be in the Nd:YAG pump bands. Rb-I has two strong lines near 8000Å and is a possible Nd:YAG pump lamp as was recognized by Liberman et al[16]. The metal iodide lamps are not corrosive and can be made with fused quartz jackets.

The Sylvania Lamp Division gave us a RbI-Hg lamp with 8 mm bore fused quartz jacket and 6.3 cm arc length. The narrow band 0.7 to 1.0 micron radiation from this lamp was shown in Fig. 3-5. The intersect, P_o, for this air-cooled lamp was 225 watts. This is consistent with the heat loss hypothesis since air-cooled tungsten lamps have P_o between 180 watts and 230 watts.

$$\left.P_o\right)_{\substack{\text{RbI-Hg}\\ \text{6.3 cm Arc Length}}} = 225 \text{ W} \qquad (3\text{-}10)$$

The Nd:YAG absorption characteristics for this RbI-Hg lamp are shown in Fig. 3-11. It will be noted that one of the Rb lines is strongly absorbed and a second is somewhat absorbed. The Na D line shows up as an impurity and is strongly absorbed. The Cs impurity lines are not absorbed.

This RbI-Hg lamp was compared with a tungsten lamp in a rather poor laser. The RbI-Hg lamp had lower threshold and higher slope efficiency than the

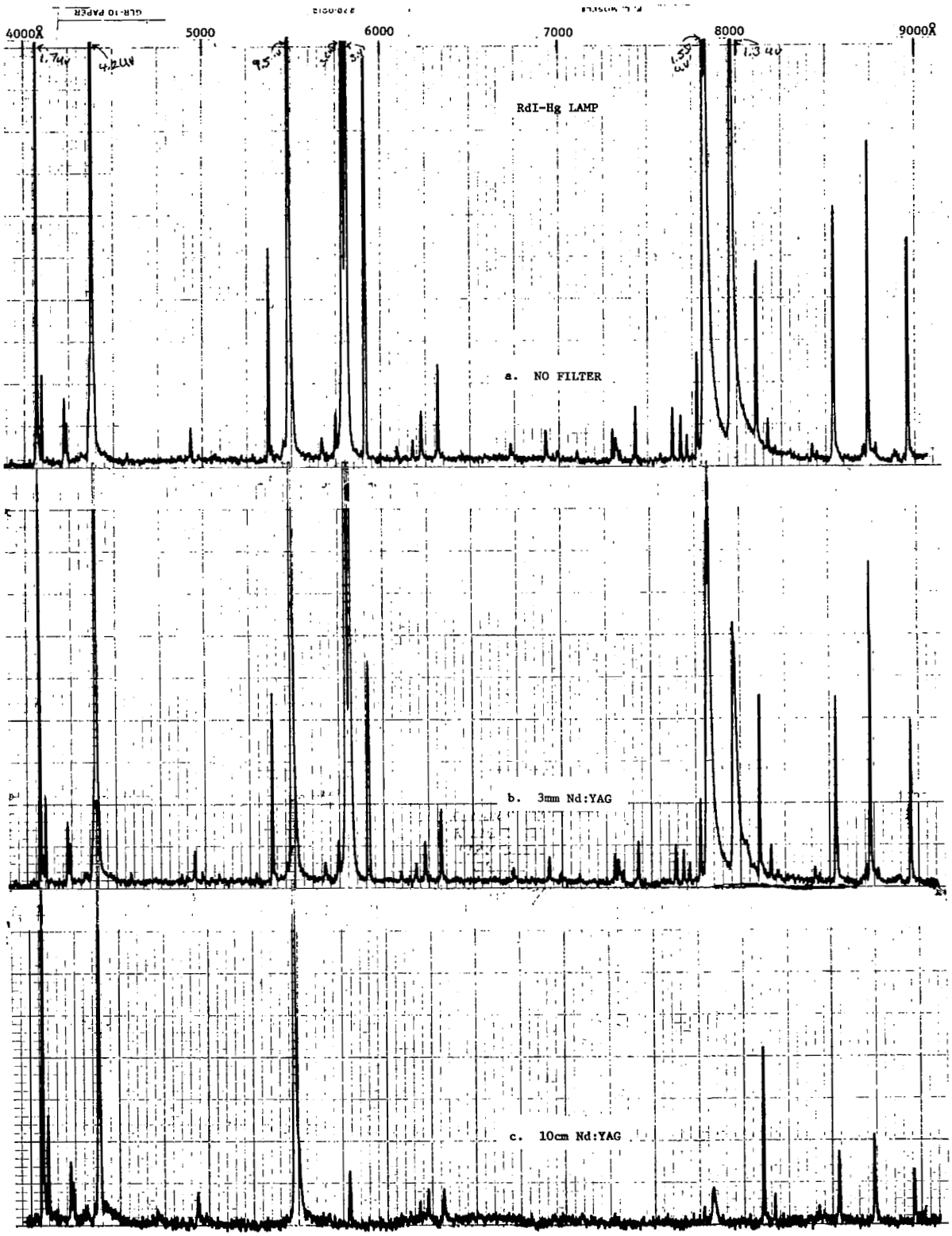

Figure 3-11. Nd:YAG Absorption of Rubidium Iodide-Mercury Radiation

tungsten. Reducing the relative data and interpolating to the best tungsten laser data, we determined the constant dK for RbI-Hg was

$$dK)_{RbI - Hg} = 0.046 \frac{cm}{kW} \qquad (3\text{-}11)$$

We therefore conclude that RbI-Hg is not as good as Kr or K but is better than W for pumping Nd:YAG.

During these experiments the lamp was observed to bulge, indicating the operating temperature was dangerously close to the melting point of fused quartz.

The Sylvania Lighting Division gave us a second RbI-Hg lamp with a concentric tabulated jacket around the side but not over the lamp ends. We took narrow band 0.7 to 1.0 micron radiometric data in the manner of Fig. 2-2 on this lamp. First we took data with air in the side jacket. We then evacuated the side jacket and took data again. We then removed the jacket and took data in free air. We then put a full vacuum jacket over both the side and ends of the lamp and took data. In each case we only took relative data to find P_o. The data could not be inter-compared to determine relative radiation intensity for the various cases except in the two side jacketed experiments in which the experimental arrangement was not disturbed in evacuating the jacket. Fig. 3-12 shows the data from these experiments plotted. It will be noted that P_o decreased each time the lamp was further insulated and that in the full vacuum insulating jacket case P_o is 47 watts identical to that for the same size K-Hg lamp in vacuum jacket.

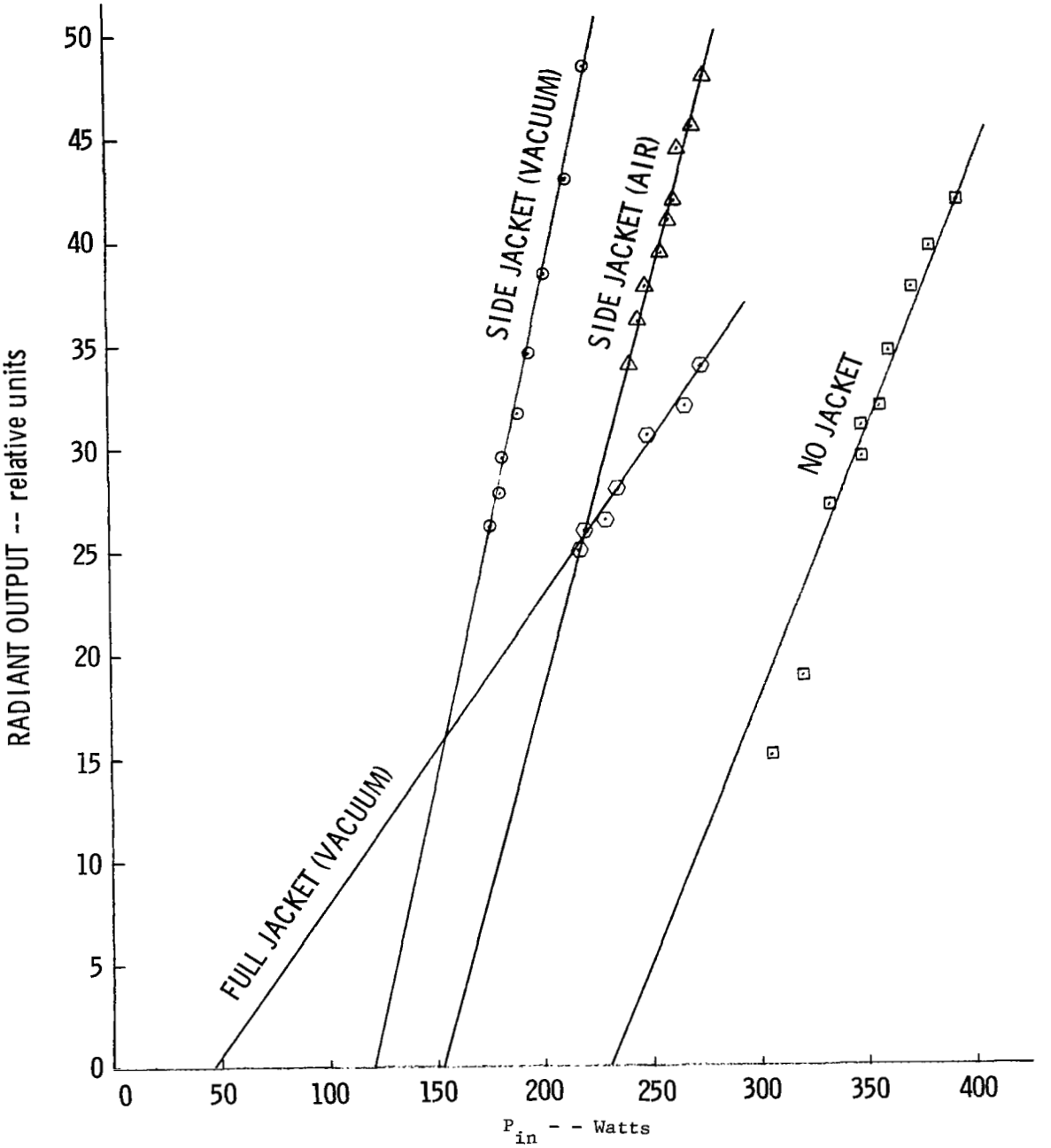

Figure 3-12. Narrow Band Radiation Output as a Function of Input to the Rubidium Iodide-Mercury Lamp for Several Heat Insulation Conditions.

These experiments verify that P_o is nothing but the heat loss from the lamp. If we want low heat loss we must insulate the lamp. Insulating the lamp of course causes the lamp to operate hotter and we again had bulging in the fused quartz jacket when we vacuum jacketed the lamp. We conclude then that *fused quartz is not acceptable for use in a vacuum jacketed lamp. Sapphire is* required. Since potassium can be used in sapphire and potassium is superior to Kr or RbI we conclude that sapphire jacketed potassium lamps are preferable for space qualified Nd:YAG.

We did try two vacuum jacketed fused quartz krypton arc lamps. In both cases the lamp immediately blew up even at less than 100 watts input power. We suspect the reason for this is the tendency of the Kr arc to fill the lamp bore, thereby, heating the walls more than RbI-Hg does.

3.2 Characteristics of an Optimum Lamp Pumped Nd:YAG Laser

We have developed a theoretical model for the Nd:YAG laser and we have determined that potassium arc lamps are the best known pump lamps for a space qualified Nd:YAG laser. We have determined the laser material and potassium lamp constants that are required in our theoretical model. In this section we will utilize this data to find the laser operating characteristics we can expect from a space qualified Nd:YAG laser.

First, let's gather together the equations we will need from the side pumped theoretical model and the lamp and material constants.

$$P_{out} = \frac{T}{\beta} \left(\frac{g_o}{\alpha} - 1 \right) \qquad (2\text{-}29)$$

$$\alpha = \frac{T}{2} + \alpha_o \tag{2-30}$$

$$g_o = K (P_{in} - P_o) \tag{2-43}$$

$$\eta_d = \frac{KT}{\alpha\beta} \tag{2-45}$$

$$P_{th} = P_o + \frac{\alpha}{K} \tag{2-46}$$

$$P_{out} = \eta_d (P_{in} - P_{th}) \tag{2-47}$$

$$T_{op} = 2 (\sqrt{g_o \alpha_o} - \alpha_o) \tag{2-57}$$

$$\frac{2}{\beta A} = 1500 \ \frac{\text{watts}}{\text{cm}^2} \tag{3-3}$$

$$dK)_{\text{Potassium}} = 0.08 \ \frac{\text{cm}}{\text{kw}} \tag{3-8}$$

$$P_o)_{\substack{\text{Potassium} \\ 2.54 \text{ cm}}} = 23 \text{ watts} \tag{3-9}$$

$$A = \frac{\pi}{4} d^2 \tag{3-12}$$

Assuming we have the highest quality laser rod and external mirrors, the lowest dissipative loss, α_o, we can expect is

$$\alpha_o = 0.006 \tag{3-4}$$

We can of course introduce more dissipative loss with lower quality laser components or by additional elements such as modulators or frequency doublers inside the laser cavity.

Utilizing the equations we have gathered we have as a function of rod diameter, d, calculated P_{th}, P_{out}, and g_o for the lowest dissipative loss (3-4), optimumly coupled (3-57) Nd:YAG laser. We have assumed a 1 inch arc length potassium lamp with a rated input power of 150 watts. The results are plotted in Fig. 3-13. The power output reaches a broad maximum of $\sim$ 1.25 watts at a rod diameter of $\sim$ 4 mm. The unsaturated single pass gain, g_o, is very low for the larger rod diameters and rises at an accelerating rate as the rod diameter is reduced. The laser threshold is lowest for the small diameter rods and rises more or less linearly as the rod diameter is increased.

The output characteristics of the small diameter laser rods is saturation dominated. The output characteristics of the larger diameter laser rods is gain and loss dominated.

A very low gain laser that is extremely loss sensitive would not have reliability characterisitcs required for space qualification. The smallest additional loss would make such a laser inoperable. Nd:YAG lasers with external mirrors are typically operated reliably with g_o = 5%. We, therefore, believe that output power must be traded for increased gain to achieve a minimum of 5% gain in the space qualified Nd:YAG laser.

Based upon Fig. 3-13 we predict that a 2 mm diameter, side pumped, best quality Nd:YAG laser rod in the best quality pump cavity will have a reliable 5 percent unsaturated single pass gain. The output power achievable will

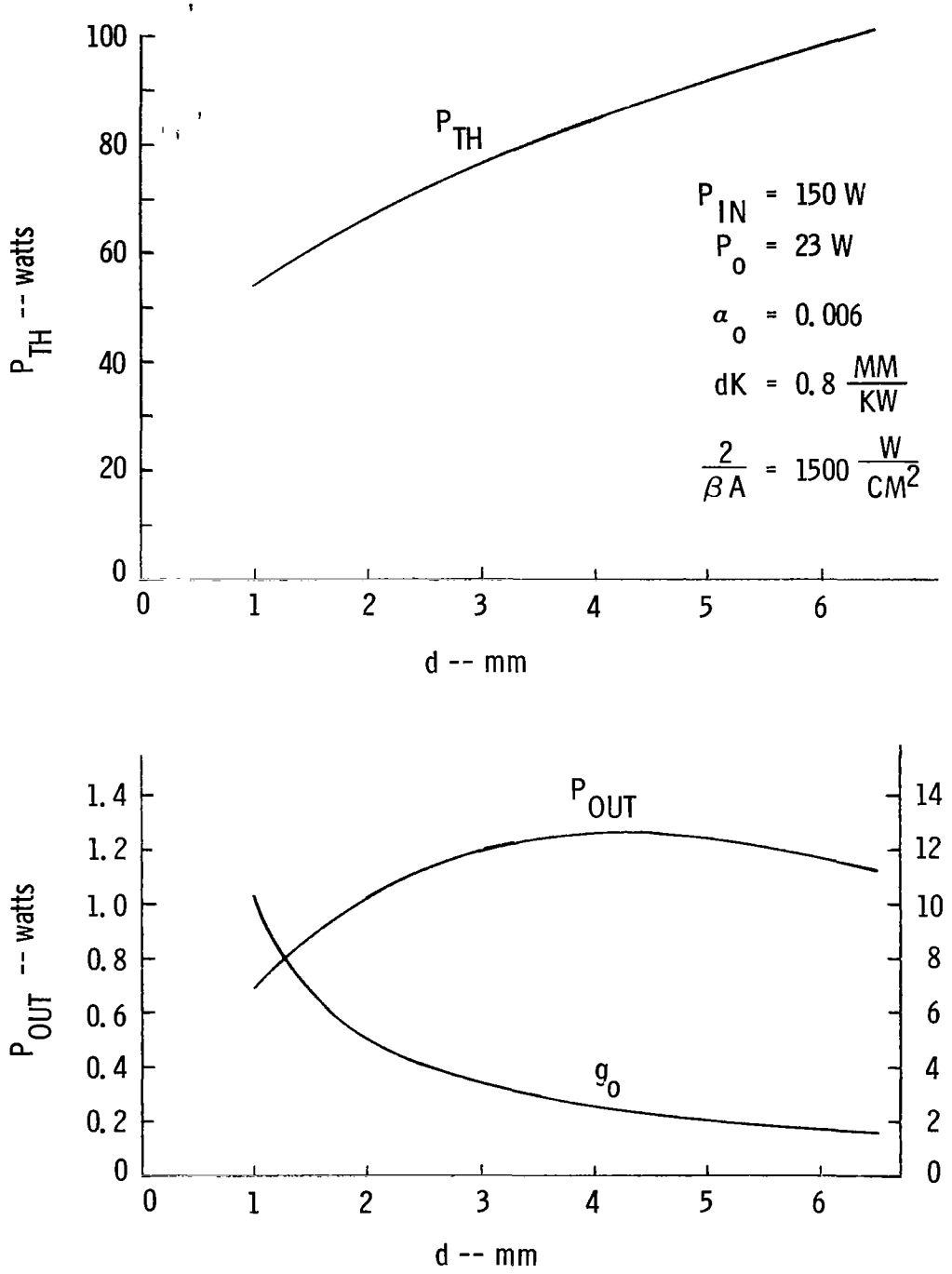

Figure 3-13. Theoretical Most Optimistic Estimate of K-Hg Pumped Nd:YAG Laser Performance.

be $\sim$ 1 watt with 150 watts input into a 1 inch long potassium pump lamp. The overall efficiency will be 0.66 percent. Laser threshold with an optimum output coupling mirror of T = 2.2% will be 66 watts. This represents the lowest input power Nd:YAG laser capable of 1 watt output with external mirrors that we can contemplate.

Let's consider the optimum gain, g_o, for a Nd:YAG laser with a given dissipative loss. Assume that the laser rod diameter is adjusted to achieve this gain. We can write equation (2-43) as

$$g_o = \frac{dK}{d} (P_{in} - P_o)$$

Rearranging

$$d = \frac{dK}{g_o} (P_{in} - P_o) \qquad (3\text{-}13)$$

This gives the diameter required for gain, g_o, with input power, P_{in}, into lamp with intersect, P_o, and constant dK. Considering optimum output transmission equations (2-29), (2-30), (2-57), (3-12), and (3-13) may be combined and rearranged to get

$$P_{out} = \frac{2}{\beta A} (dK)^2 \frac{\pi}{4} (P_{in} - P_o)^2 \left(\frac{\sqrt{g_o} - \sqrt{\alpha_o}}{g_o} \right)^2 \qquad (3\text{-}14)$$

Replacing all the constants by a single constant Q,

$$P_{out} = Q \left(\frac{\sqrt{g_o} - \sqrt{\alpha_o}}{g_o} \right)^2$$

We may find the maxima of P_{out} as a function of g_o for given α_o by setting $\frac{d P_{out}}{d g_o} = 0$ and considering the extremum where $\frac{d^2 P_{out}}{d g_o^2} < 0$. The result is

$$g_o)_{op} = 4 \alpha_o \tag{3-15}$$

Figure 3-13 is consistent with this. The maximum P_{out} occurs at a diameter where $g_o = 2.4\%$ which is 4 times $\alpha_o = 0.6\%$.

Assume that optimum gain and rod diameter are utilized. Substituting (3-15) into (3-14) the optimum output for a laser with dissipative loss, α_o, is

$$P_{\substack{out \\ op}} = \frac{\pi}{64} \left(\frac{2}{\beta A} \right) \frac{(dK)^2}{\alpha_o} (P_{in} - P_o)^2 \tag{3-16}$$

The optimum laser efficiency $\varepsilon_{op} = \frac{P_{\substack{out \\ op}}}{P_{in}}$ is

$$\varepsilon_{op} = \frac{\pi}{64} \left(\frac{2}{\beta A}\right) \frac{(dK)^2}{\alpha_o} \left(P_{in} - 2 P_o + \frac{P_o^2}{P_{in}} \right) \tag{3-17}$$

We must use this equation with some caution. At low input powers the rod diameters will become very small in order to maintain the gain constant. Very small rods can neither be fabricated nor efficiently pumped. We should, therefore, limit use

of equation (3-17) to input powers such that d given by equation (3-13) is greater than 1 mm. Also, Nd:YAG rods are not practical above 9 mm diameter, so we should impose this upper limit.

Fig. 3-14 shows the optimum theoretical efficiency for various dissipative losses plotted versus input power. The curves have been discontinued at the low power end where the rod diameter becomes 1 mm and at 9 mm or the high power end. The drastic effect that intracavity dissipative loss, α_o, has on Nd:YAG laser performance is clearly shown in the figure. If one remembers that typical electro-optic and non-linear crystals introduce 2 to 3% loss when inserted in Nd:YAG lasers with high circulating laser powers, the difficulties involved with electro-optic modelocking, intracavity frequency doubling, and cavity dumping is clearly demonstrated.

Before leaving Fig. 3-14, we should again emphasize that each point on the curves represents a theoretically optimized potassium arc lamp pumped Nd:YAG laser. Each point represents a different optimum diameter laser rod and different optimum transmission laser mirrors.

Let us now consider the effect of different dissipative losses, α_o, on a laser rod of fixed diameter and fixed input power that produces gain, g_o. Combining equations (2-29) and (2-57) and rearranging

$$P_{out} = \frac{2}{\beta}\left(\sqrt{g_o} - \sqrt{\alpha_o}\right)^2 \tag{3-18}$$

The efficiency, ε, is

$$\varepsilon = \frac{2}{\beta P_{in}}\left(\sqrt{g_o} - \sqrt{\alpha_o}\right)^2 \tag{3-19}$$

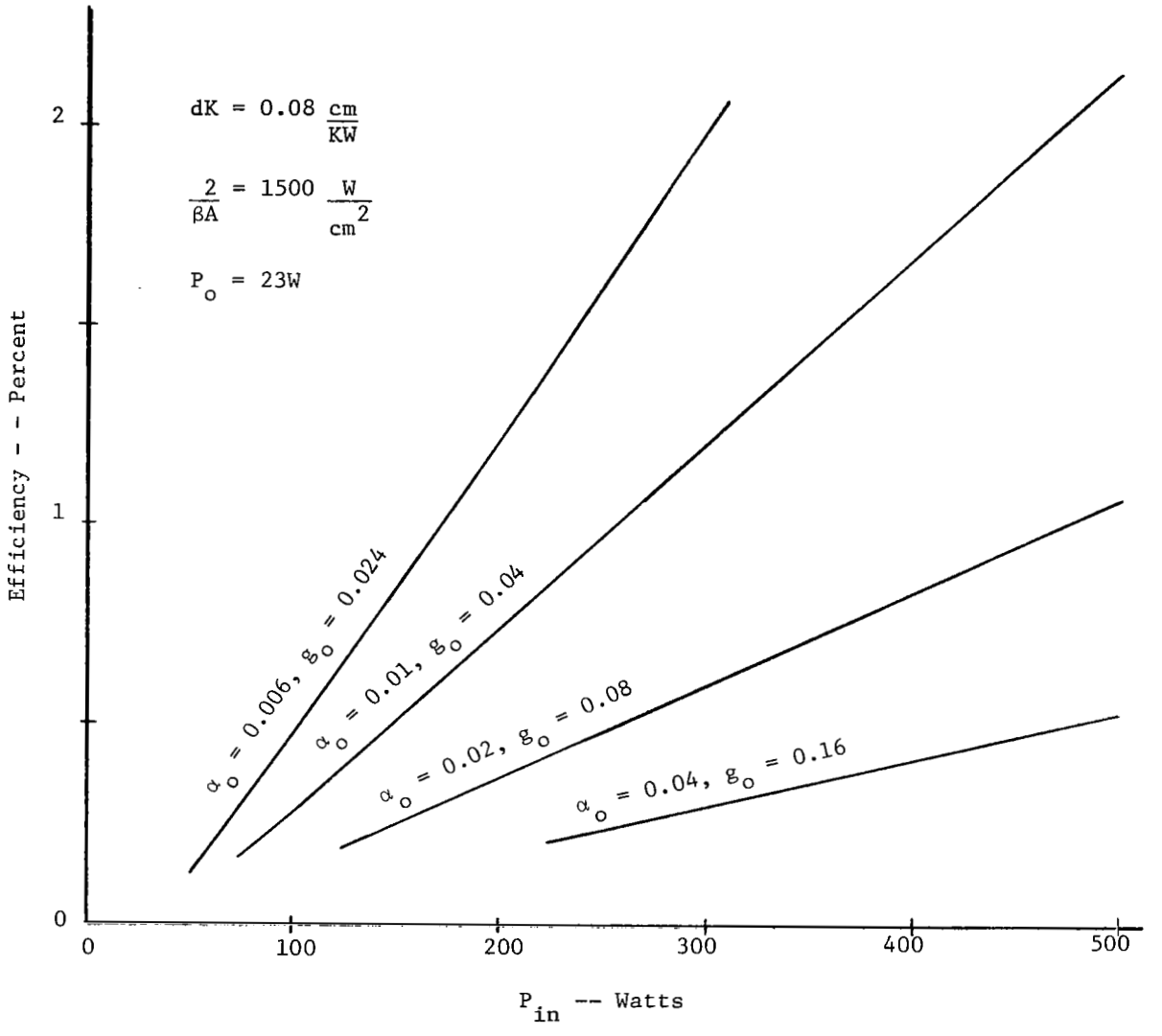

Figure 3-14. Optimum Theoretical Efficiency for Various Dissipative Losses for Potassium Arc Pumped Nd:YAG.

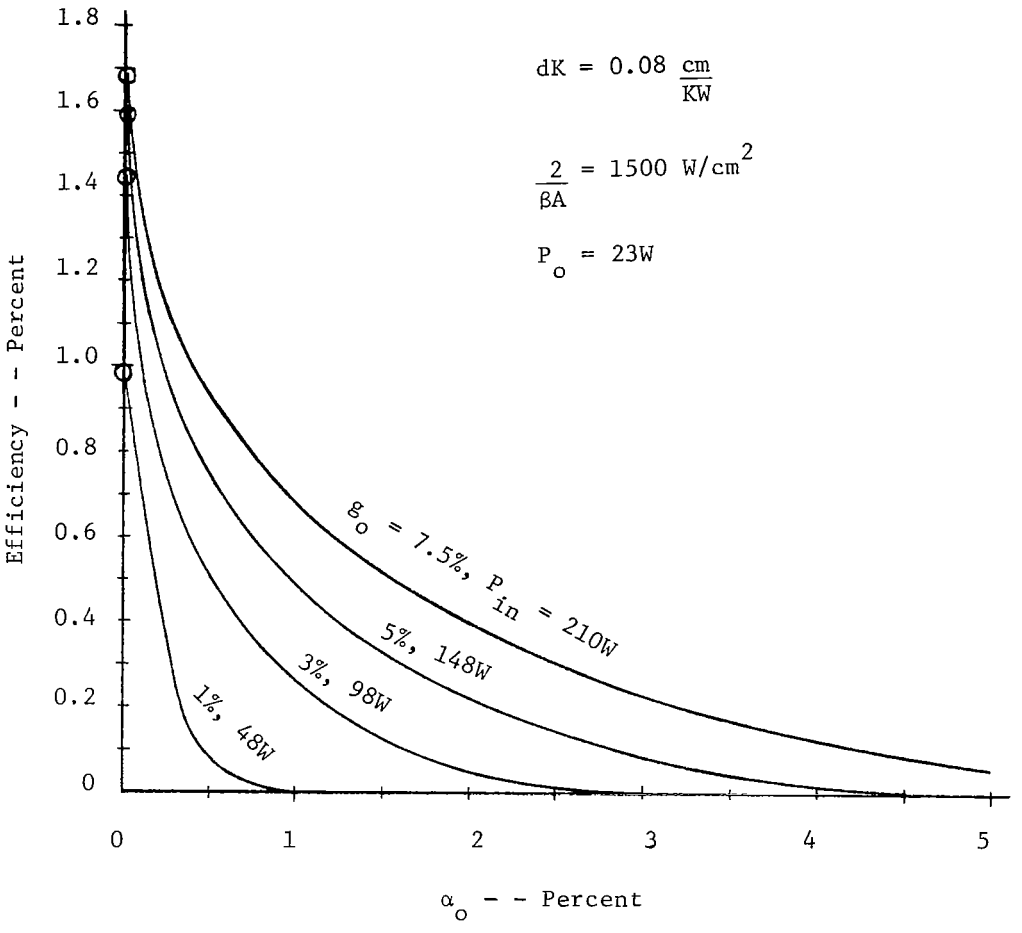

Figure 3-15. Efficiency of 2mm Nd:YAG Laser as a Function of Dissipative Loss, α_o, for Various Gains or Input Powers to a Potassium Arc Lamp.

Assume we have a 2 mm Nd:YAG rod pumped with a 1 inch potassium lamp. In Fig. 3-15 the efficiency for this laser is plotted versus the dissipative loss, α_o for several different gains achieved with various input powers. Each point on these curves represents a different optimum mirror transmission but the same laser rod.

Again we see the drastic effect of dissipative loss on laser performance. The Nd:YAG laser is a low gain laser when operated at a few watts of output power. The technology of the space qualified Nd:YAG laser will, therefore, be that of achieving low dissipative loss.

SECTION 4

INCOHERENT SEMICONDUCTOR DIODE PUMPED Nd:YAG LASERS

The idea of luminescent diodes as the pump lamp for a Nd:YAG laser is extremely appealing. The simplicity, reliability and long life associated with all solid state electronic systems immediately comes to mind. In this section we will analyze the present and future prospects and characteristics of diode pumped Nd:YAG.

4.1 Effect of Temperature on Nd:YAG Laser Performance

Most incoherent semiconductor diode pump Nd:YAG lasers operated up to the present time have been at cryogenic temperatures. Temperature was not included in our parametric analysis in Section 2. Therefore, we must now consider temperature in order to clearly understand these diode experiments.

First, consider the effect of temperature on pump band absorption. The fine structure of the Nd pump bands narrows and peak absorption increases as the temperature is lowered. Kaminskii[18] has measured these effects and has found that the integrated pump band absorption remains constant, independent of temperature. The narrowing of the pump band fine structure is compensated by its increased peak absorption. This is, of course, only true for an optically thin pumping arrangement with pump radiation that is wide compared to the fine structure of the pump bands. The emissions from $GaAs_{1-x}P_x$ and $GaAl_xAs_{1-x}$ diodes and potassium arc lamps are wide

compared to the pump band fine structure, however, and side pumped, low power Nd:YAG lasers are optically thin to the pump radiation. We may, therefore, assume that the pumping rate for $GaAs_{1-x}P_x$ and $GaAl_xAs_{1-x}$ diodes or potassium arc lamp pumped Nd:YAG is independent of temperature and may apply pumping rate information obtained at one temperature to another temperature.

Second, consider the effect of temperature on threshold and saturation in the Nd:YAG laser. Holloway, et al.,[20] have shown that Nd laser thresholds vary inversely with the peak fluorescent intensity. They measured peak fluorescent intensity as a function of temperature, and their results compared favorably with the reduction in laser threshold between 295°K and 77°K. In addition, two separate experiments have been conducted to measure the laser threshold as a function of temperature,[19,21] using 77°K GaAsP diodes to pump a variable temperature Nd:YAG laser rod. We are indebted to Ostermayer and Geusic[21] for giving us a copy of their data prior to publication. Figure 4-1 shows the replotted data from each of these investigators. There is some variation in the rate of threshold drop with temperature. All agree, however, that the threshold decreases quite rapidly with temperature and then levels off at about 0.25 of the room temperature value. If we restrict our investigations to 77°K and room temperature, we can confidently conclude that threshold will be less by 1/4 at 77°K compared to room temperature.

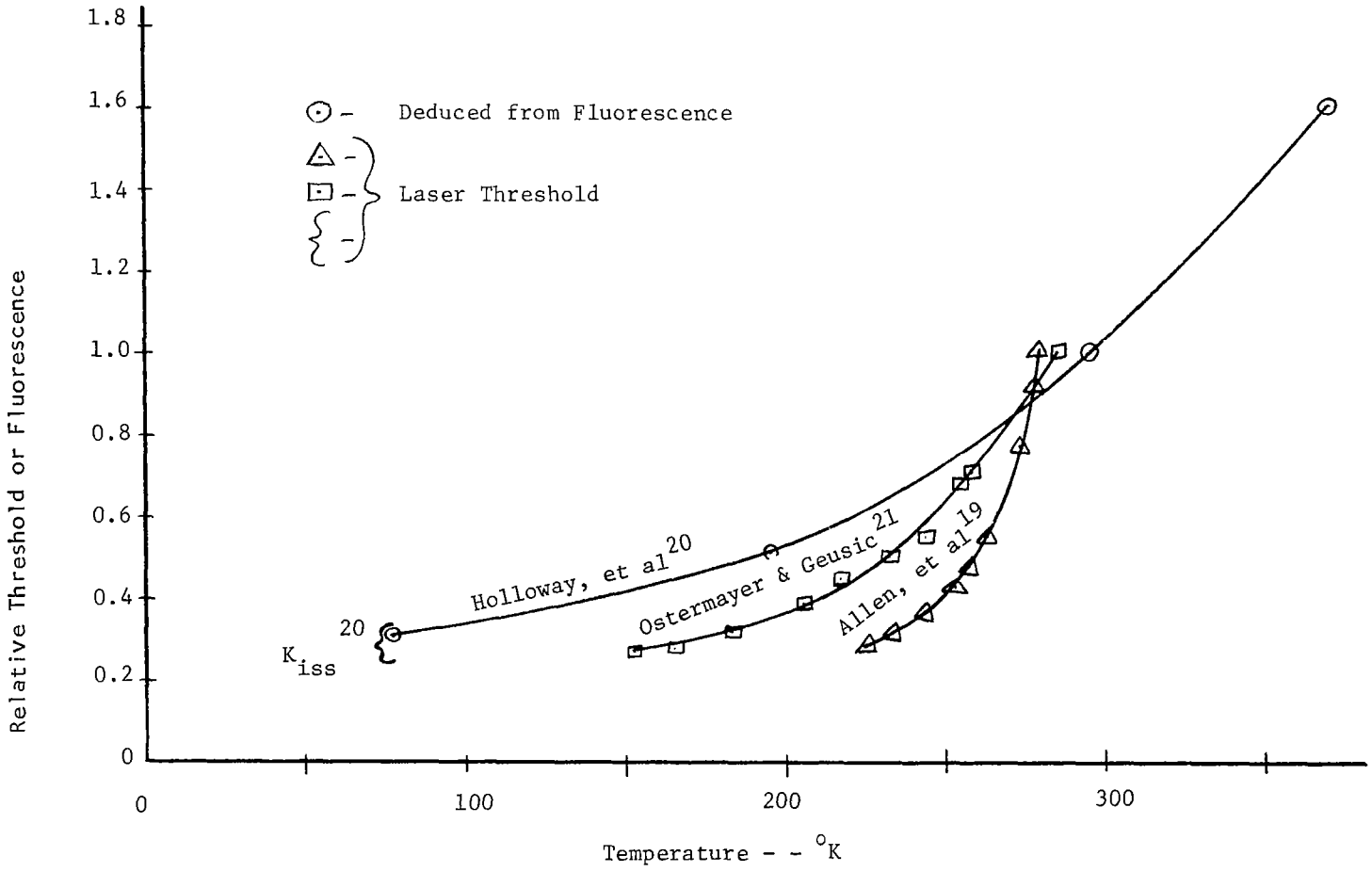

Figure 4-1. Effect of Temperature on Nd:YAG Laser Threshold.

The laser threshold with GaAsP diodes will be given from equation (2-46) by

$$P_{th} = \frac{\alpha}{K} \tag{4-1}$$

since $P_o = 0$ for electroluminescent diodes. The gain constant K must then be affected by temperature. Consider equation (2-42)

$$K = \frac{\sigma_p k_p k_r \eta N_1 \sigma \tau_T}{2h\nu_p d} \tag{2-42}$$

The narrowed, more intense fluorescence at lower temperatures would be expected to increase the stimulated emission cross section σ in equation (2-42). All other factors would be expected to remain constant. We, therefore, conclude that σ increases by 4 in reducing the temperature from room temperature to 77°K. Considering equation (2-28),

$$\beta = \frac{2\sigma\tau_T}{Ah\nu_L} \tag{2-28}$$

we conclude that both β and K increase by 4 when Nd:YAG is reduced from 295°K to 77°K.

Before considering diode pumped lasers, it will be instructive to consider the theoretical performance of a potassium lamp pumped laser with the laser rod maintained at 77°K. Using our factor of 4

$\frac{2}{\beta A} = 375 \frac{\text{watts}}{\text{cm}^2}$ and $dK = 0.32 \frac{\text{cm}}{\text{kW}}$. Assuming optimum output coupling, we have used equation (3-17) to calculate the optimized efficiency as a function of input power for $\alpha_o = 0.003$ and $g_o = 0.012$. This is plotted in Figure 4-2. The graph has been terminated at low powers for a 1 mm diameter rod. We will use these results later to compare with diode pumped 77°K Nd:YAG.

4.2 $GaAs_{1-x}P_x$ Diode Pumped Nd:YAG

Continuous operation of a Nd:YAG laser at 77°K using incoherent GaAsP diodes as the pump source has been demonstrated by Allen and Scalise;[8] they have reported achieving 1% efficiency. In this section we will determine the constant dK for GaAsP diodes and will use our theoretical model to predict performance of these devices.

For diode pumping, a laser pump band with significant absorption and with wavelength near the laser transition is desired. The 8100Å pump band best meets these requirements in Nd:YAG.

We made the high resolution spectrophotometer transmission measurements of the Nd:YAG pump bands shown in Figures 4-3, 4-4 and 4-5. Resolution was less than 1Å throughout these traces. A 5.13 mm long sample of nominally 1% Nd:YAG was used; the highest absorption was clearly resolved. We will use this data to predict diode laser performance with incoherent diode pump sources. We will assume that the radiation makes two or more passes through the laser rod, so that the data for the 5 mm thick sample shown may be used directly.

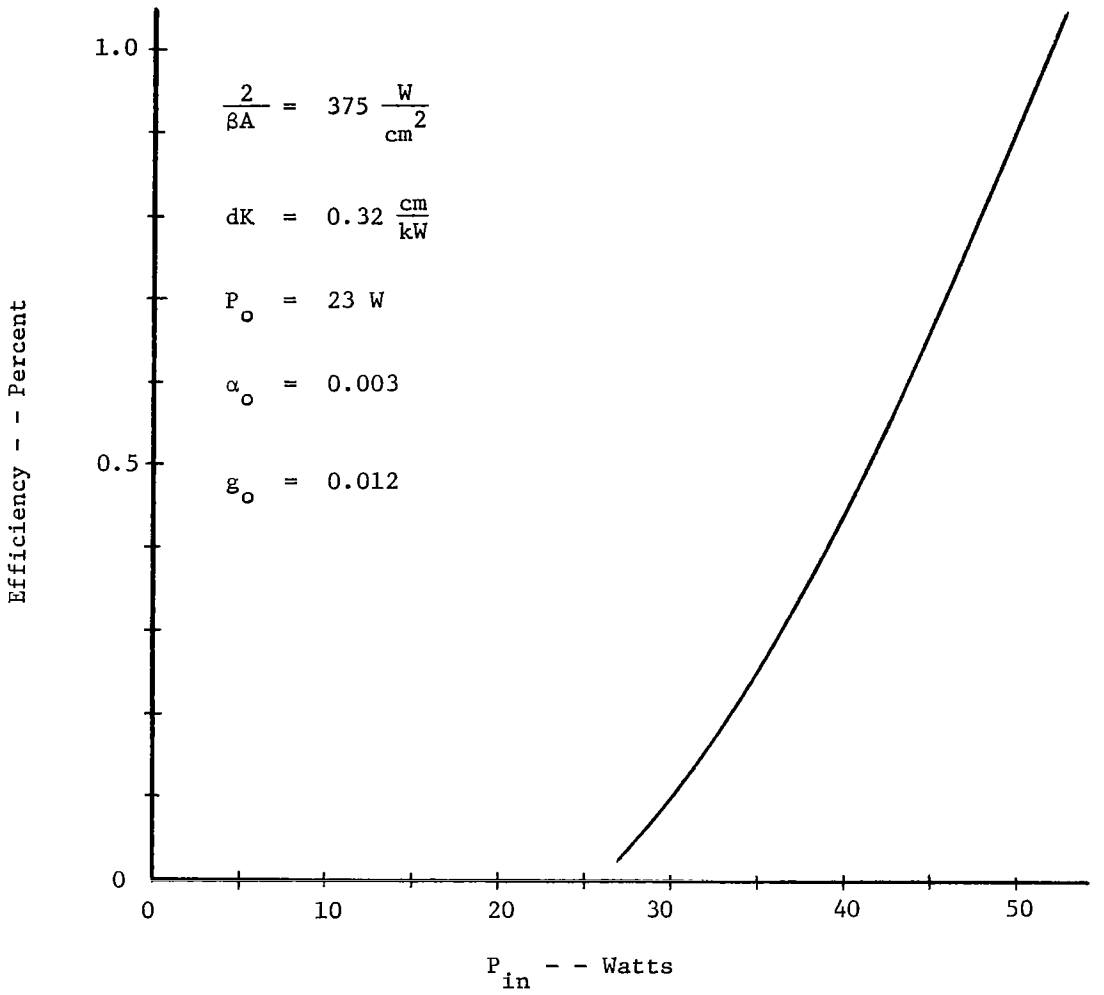

Figure 4-2 Optimum Efficiency of Potassium Arc Pumped 77^{o} Nd:YAG Laser

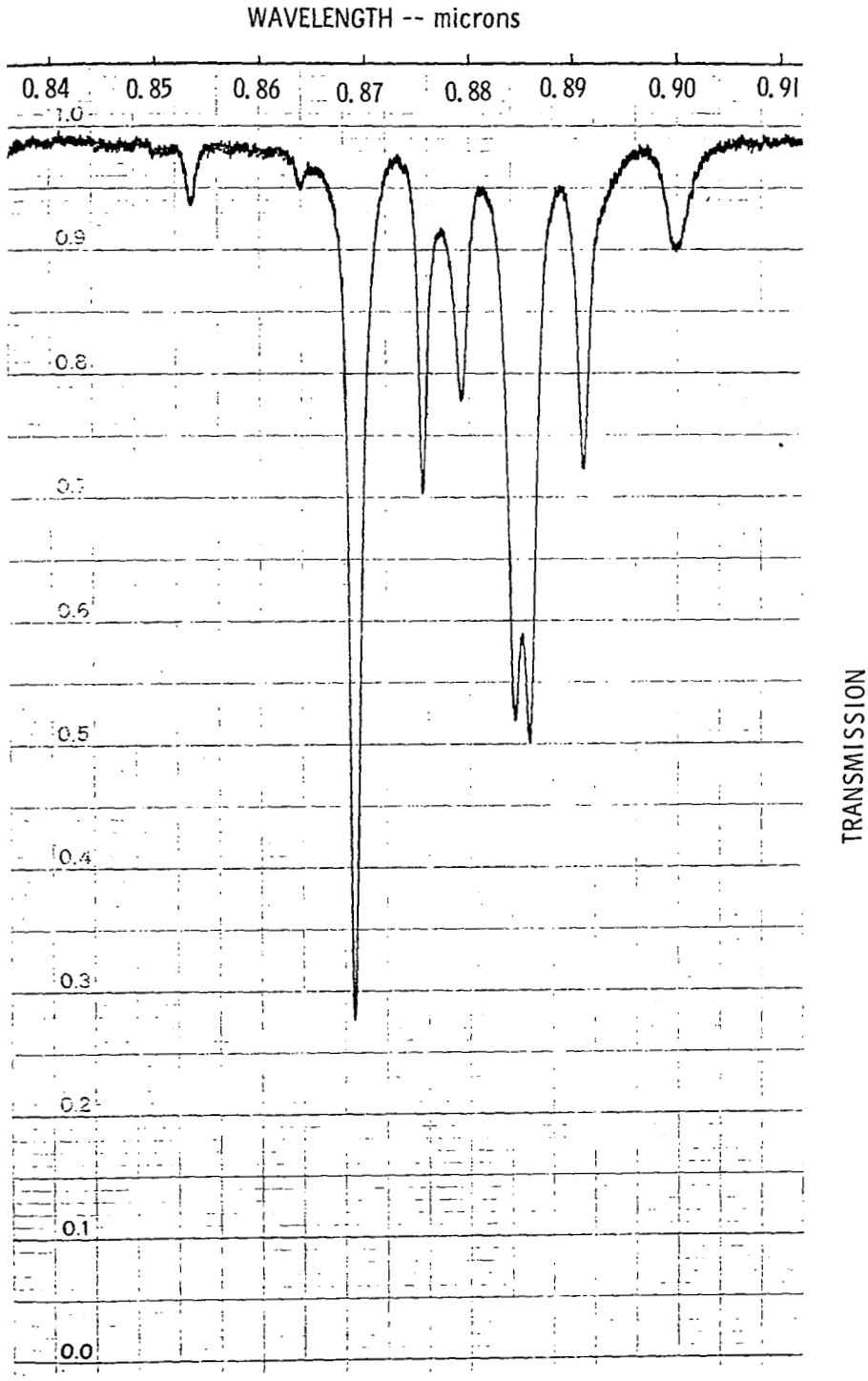

Figure 4-3 Absorption Spectrum of 8800 A Pump Band for 0.203 ", 1% Nd:YAG.

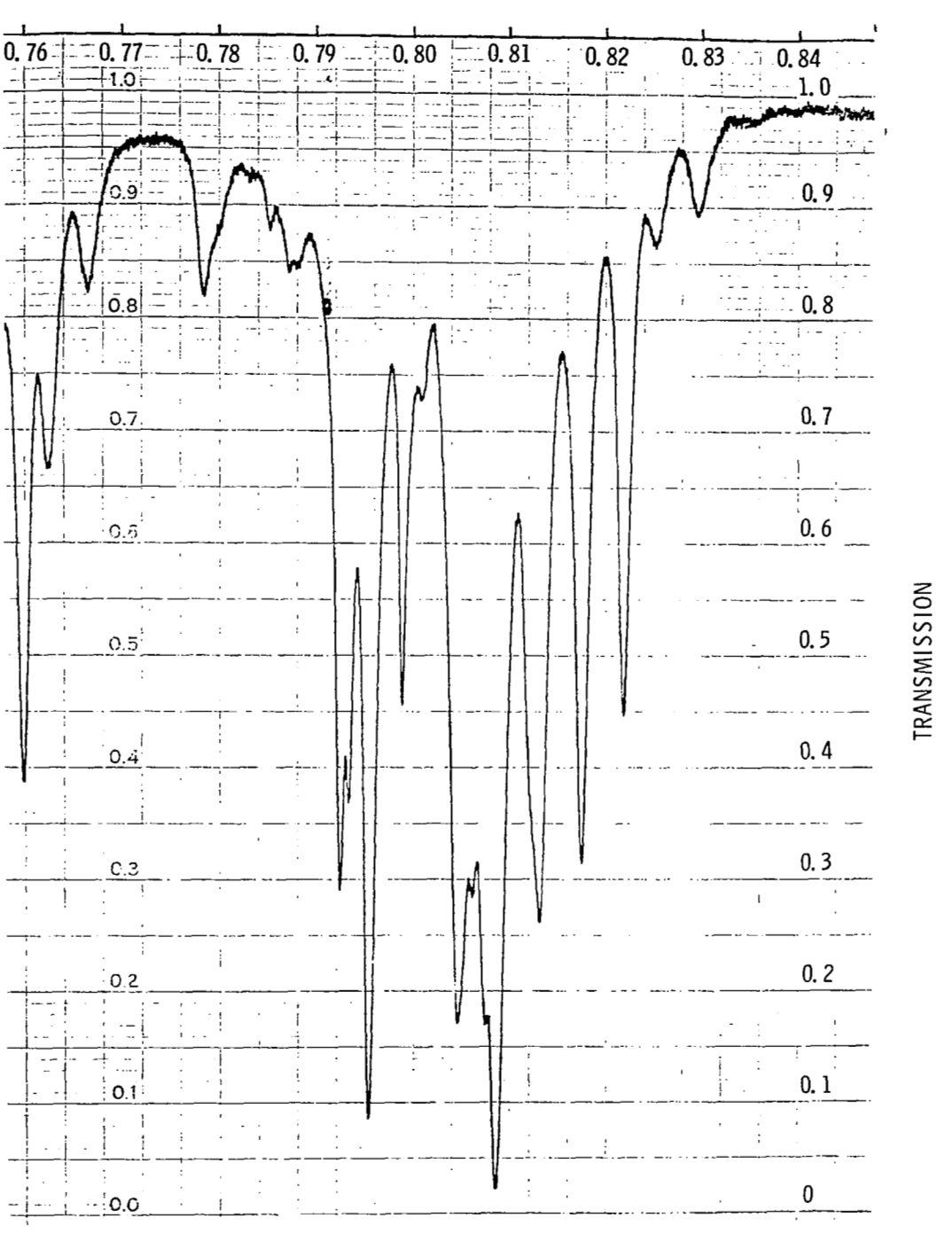

Figure 4-4 Absorption Spectrum of 8100A Pump Band for 0.203 ", 1% Nd:YAG.

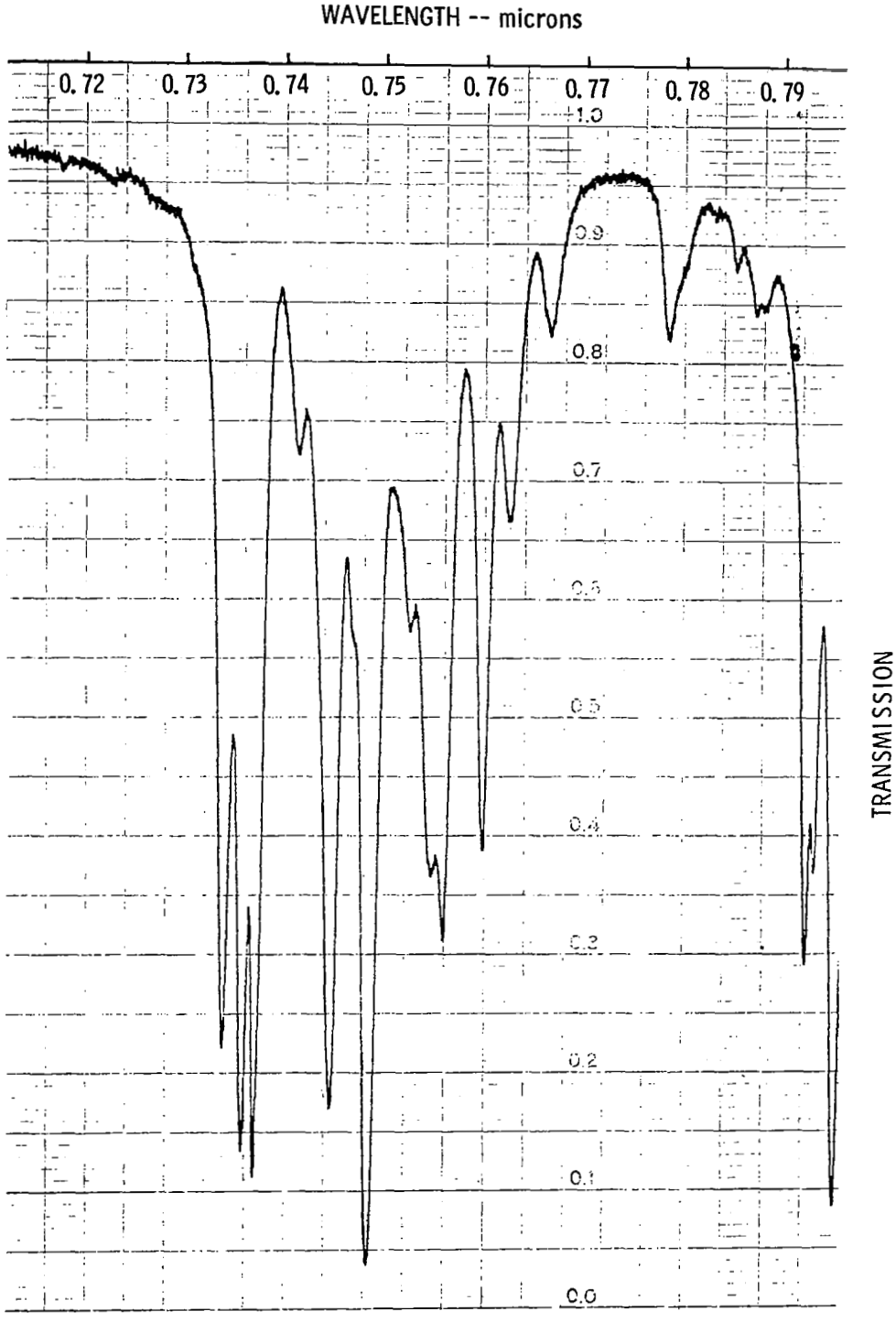

Figure 4-5 Absorption Spectrum of 7500A Pump Band for 0.203 ", 1% Nd:YAG.

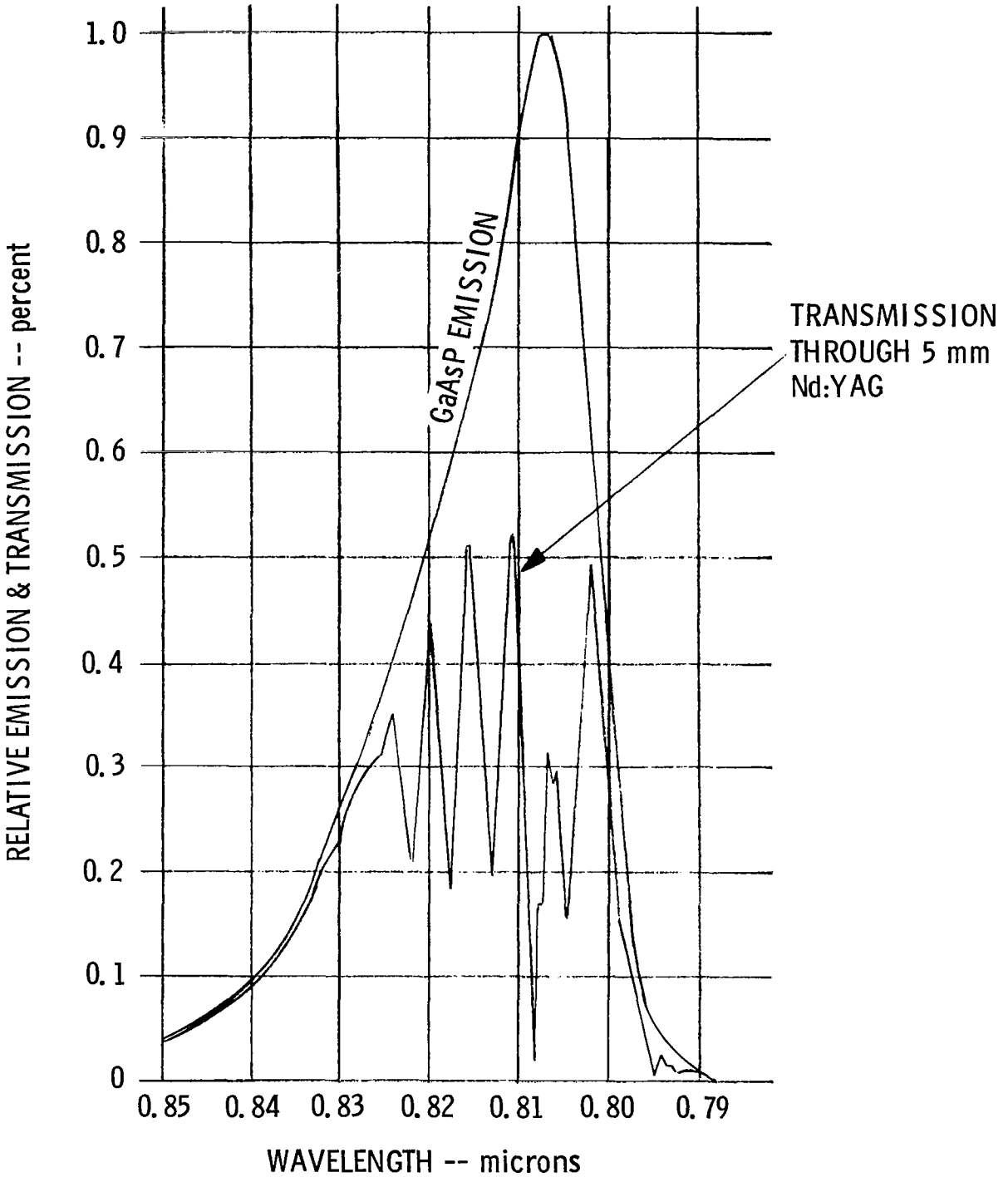

Figure 4-6. $GaAs_{1-x}P_x$ Emission and Computed Transmission Through 5mm of Nd:YAG

$GaAs_{1-x}P_x$ diodes are normally operated with the output through a thin p layer on a thicker n substrate.[22] The cw laser pump diodes used to date have been fabricated into a dome[19] from the substrate side and have emitted through the thicker, slightly more absorbing n material. The dome is used to reduce the angle of incidence at the exit surface and thus reduce the total internal reflection loss at the high refractive index exit surface.

The output spectrum from one of these domed diodes[19] centered on the 8100Å pump band is redrawn in Figure 4-6. Figure 4-6 also shows the product of the diode spectrum and the laser rod transmission (from Figure 4-4). This represents the pump light not absorbed by the laser rod. Graphical integration of these curves shows that 48% of the diode emission should be absorbed in this hypothetical laser. (Note this is a 77°K diode and a room temperature laser rod.) The quantum efficiency due to the difference in absorption and emission wavelengths (0.81 and 1.06 microns) is 0.77. Assuming negligible threshold, the conversion efficiency from diode emission to laser output would then be 0.37. For diodes with 10% external quantum efficiency, the overall efficiency would then be 3.7%. Remembering that the integrated pumping efficiency was independent of laser rod temperature since peak fluorescent intensity variation explained the threshold variation with temperature, we may use this number for the rod at 77°K as well. We conclude then that 3 to 4% efficiency is the best attainable with 77°K $GaAs_{1-x}P_x$. This assumes negligible threshold and perfect coupling of the diode emission into the rod.

Experimentally, 0.5 to 1.0% efficiency has been obtained.[8,19,21]

Let's make an estimate of the constant dK at 77°K for GaAsP pumped Nd:YAG based upon our above analysis. Assume optimum output coupling. From equations (3-18) and (2-43)

$$P_{out} = \frac{2}{\beta} K P_{in} \left(1 - \sqrt{\frac{\alpha_o}{g_o}}\right)^2$$

Therefore,

$$K = \left(\frac{P_{out}}{P_{in}}\right)\left(\frac{\beta}{2}\right) \frac{1}{\left(1-\sqrt{\frac{\alpha_o}{g_o}}\right)^2} \qquad (4-2)$$

Assume that α_o is negligible for the 2.5 mm diameter laser rod. Use our value of 0.37 for diode emission to laser output and assume 10% efficient diodes,

$$\frac{P_{out}}{P_{in}} = 0.037$$

Operation at 77°K will make $2/\beta A = 375$ watts/cm^2. Using the area of our assumed 2.5 mm diameter laser rod,

$$\frac{2}{\beta} = 18.4 \text{ watts/cm}^2$$

Correcting K for Nd concentration (N_1 in equation (2-42)) since our sample was 1% instead of the normal 1.5%, we then get

$$\left(dK_{\substack{GaAsP \\ 77°K}}\right)_{max} = 0.75 \text{ cm/kw} \tag{4-3}$$

Let us now estimate dK for GaAsP based upon the experiments reported in the literature. The highest efficiency device was reported by Allen, et al.[19] They achieved an output of 48 mw at 1% efficiency with the diodes and the laser rod operated at 77°K. Iteratively solving equation (4-2) with the condition $g_o = KP_{in}$ and assuming $\alpha_o = 0.003$, we find that for their 1.5 mm diameter laser rod experiment,

$$dK_{\substack{GaAsP \\ 77°K}} = 0.61 \text{ cm/kw} \tag{4-4}$$

This agrees well with our estimate (4-3). An inconsistency, however, is the threshold level we estimate using our theory. We conclude the laser would only be 3.5 times threshold and not 20 times threshold as we understand is common.[21] We also have to assume $\alpha_o = 0$ for the 1 mm rod reported by Allen, et al.[8] to calculate a minimum threshold of 410 mw compared to their measured 300 mw. We, therefore, must consider with some reservations the dK values we have estimated for GaAsP.

We will show in Section 6 on heat removal that operation of a laser at 77°K is impossible in a spacecraft due to the extremely heavy space radiator that would be required. Let us now consider room temperature operation of GaAsP diodes. The diodes used by Allen, et al.[19] had only 1% external efficiency at room temperature. Even then, thermal tuning shifted the wavelength such that more phosphorus was required to obtain 8100Å emission. Higher phosphorus content, of course, further reduces the external quantum efficiency. Room temperature laser operation, therefore, appears impossible with this class of GaAsP device.

Graded junction techniques should be possible in $GaAs_{1-x}P_x$, as in $Ga_{1-x}Al_xAs$. The technology has not been developed in the 8100Å wavelength region, but several firms are producing efficient red-emitting $GaAs_{1-x}P_x$ display diodes. Red-emitting graded-junction GaP diodes with 7% external efficiency have recently been reported.[26] We therefore expect that graded junction technology can be (or has been) developed to produce diodes with outputs comparable to that of $Ga_{1-x}Al_xAs$, which we will discuss in the next section.

4.3 $GaAl_{1-x}As_x$ Diode Pumped Nd:YAG

GaAlAs is made by liquid phase epitaxy. High efficiency room temperature incoherent diodes have been made from this material.[23,24] In Figure 4-7 we have replotted a typical room temperature emission spectrum[24] of a $Ga_{1-x}Al_xAs$ diode centered on the 8100Å Nd:YAG laser pump band. Also shown is the product of the diode spectrum and the laser rod transmission from Figure 4-4. Again this represents the pump light not absorbed by the laser rod in our model of a double pass through a 2.5 mm rod.

Graphical integration of these curves shows that 37% of the diode emission should be absorbed. Again the quantum efficiency (due to absorption at 0.81 micron and emission at 1.06 microns) is 0.77. Assuming negligible threshold, the efficiency of diode emission to laser output would be 0.28. Assuming a room temperature diode with 8% quantum efficiency[25] and negligible threshold, the maximum overall efficiency would be 2.2 percent.

Let us make an estimate of the constant dK at room temperature for GaAlAs pumped Nd:YAG. Using equation (4-2), assuming $\alpha_o = 0$ for a 1.5% Nd rod, assuming 0.28 emission to output for 8 percent diodes, and using the room temperature value of $2/\beta$, we get

$$\left(\frac{dK_{GaAlAs}}{20°C}\right)_{max} = 0.114 \text{ cm/kw} \qquad (4\text{-}5)$$

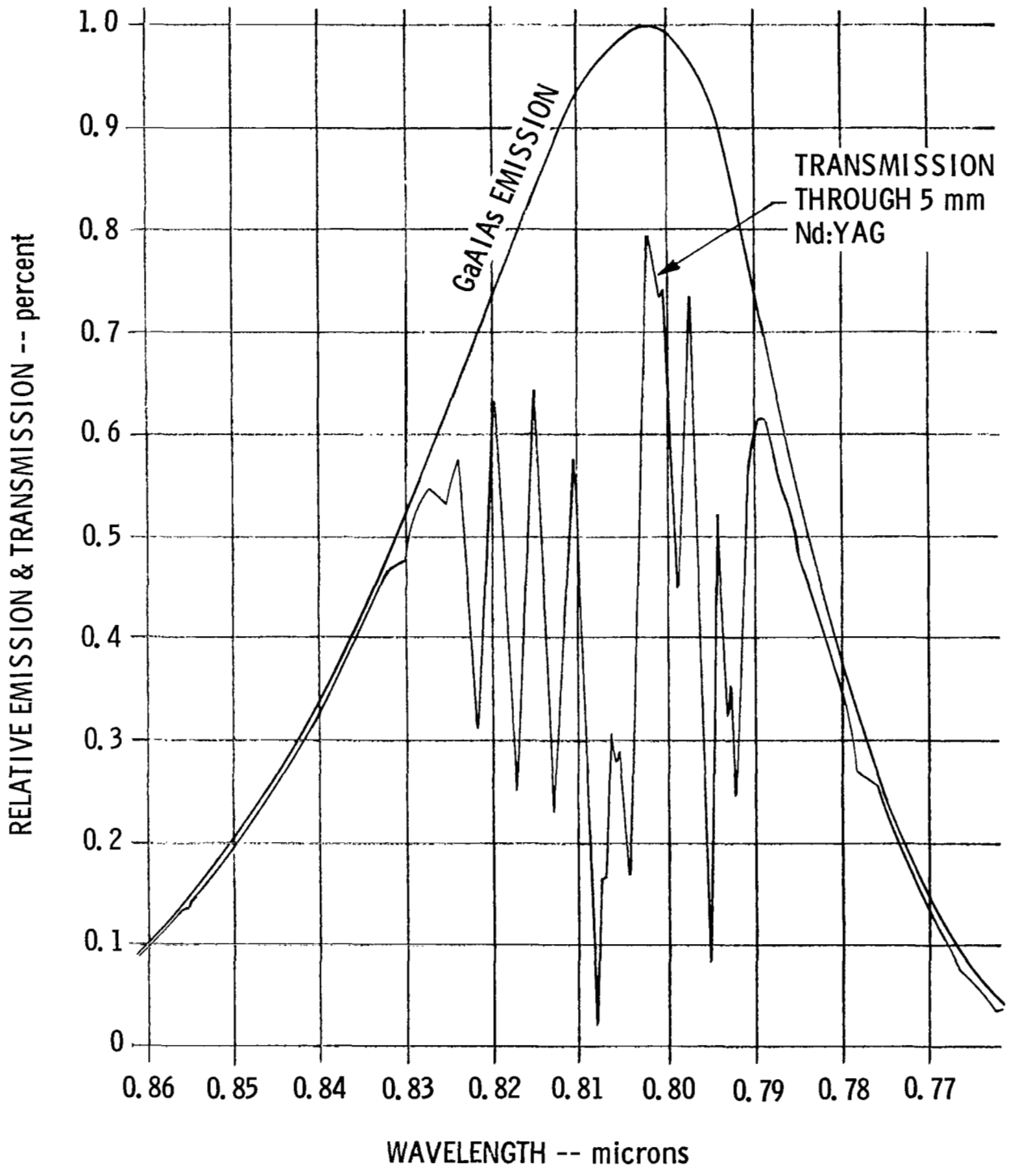

Figure 4-7. $Ga_{1-x}Al_xAs$ Emission and Computed Transmission Through 5mm of Nd:YAG

Assuming we can realize 0.8 of this maximum dK value as we estimate has been accomplished at 77°K with GaAsP, our best guess for GaAlAs room temperature diodes is

$$dK_{\substack{GaAlAs \\ 20°C}} = 0.09 \text{ cm/kw} \qquad (4\text{-}6)$$

4.4 Characteristics of an Optimum Incoherent Diode Pumped Nd:YAG Laser

We can now use our theoretical model and the dK constants we have estimated for diode pumped Nd:YAG to estimate laser performance. First, consider operation at 77°K using GaAsP diodes. Utilizing equations (3-17) and (4-4), we have plotted in Figure 4-8 the expected laser efficiency versus input power for an optimum laser with mirrors on the laser rod having $\alpha_o = 0.003$ and $g_o = 0.012$. Again, we have been careful in employing the optimized equation (3-17). At the low input powers we have restricted the laser rod size to not less than 1 mm. At the high input powers, we have restricted the maximum efficiency to 1% because of the uncertainty in our theoretical understanding of diode pumped lasers and the problems which will occur in coupling large diode arrays to the laser rod. Also shown for comparison in the figure is the data from Figure 4-2 for potassium arc lamp pumped 77°K Nd:YAG. Figure 4-8 shows that extremely good Nd:YAG laser performance is possible at low input powers for the laser operated at 77°K with either diode or potassium lamp pumping. We will show in Section 6 that heat removal considerations prohibit operation at such low temperatures. We must then look at higher temperature operation.

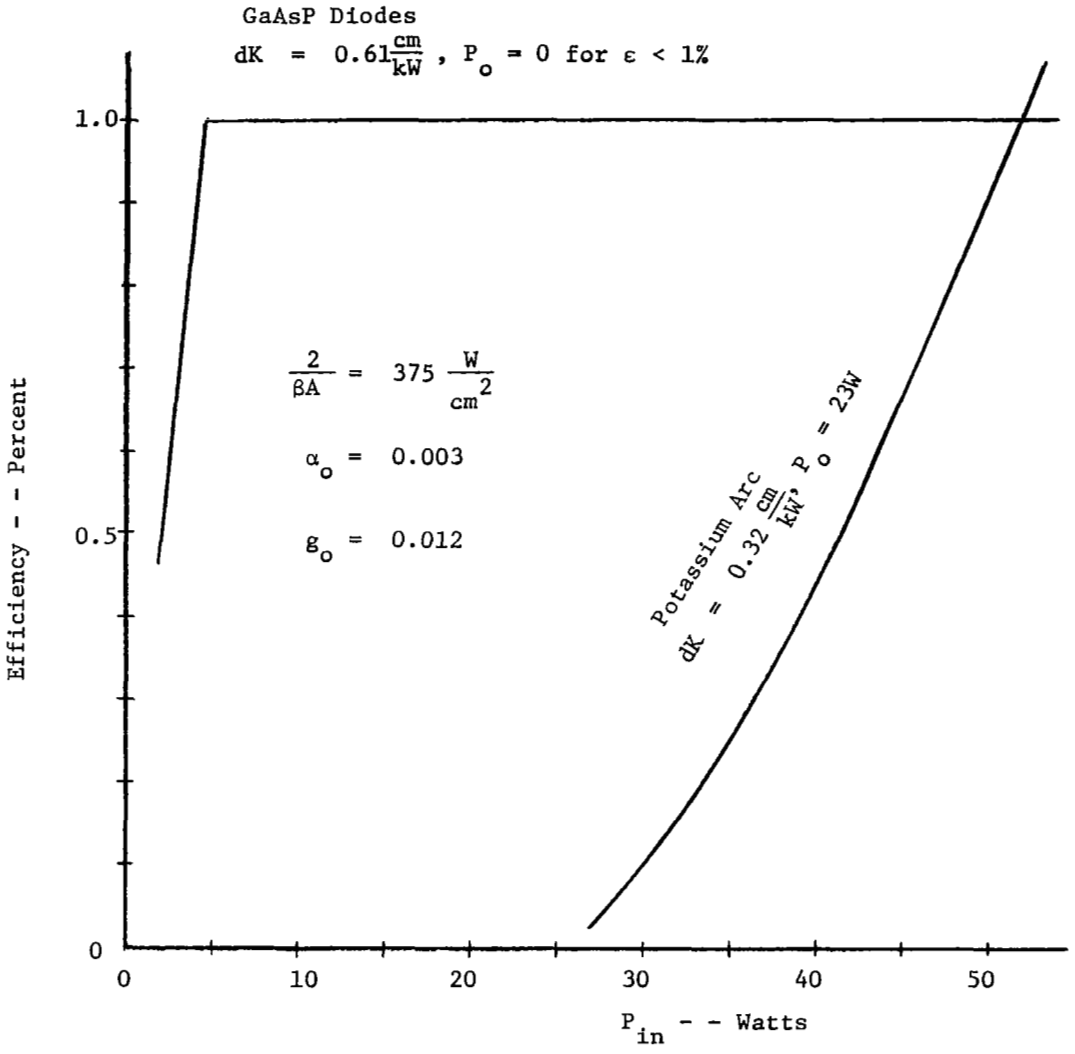

Figure 4-8 Theoretical Efficiency of 77°K GaAsP Diodes and Potassium Arc Pumped 77°K Nd:YAG Laser.

Utilizing equations (3-17) and (4-6) we have plotted in Figure 4-9 the expected laser efficiency versus input power for an optimum 20°C GaAlAs diode pumped 20°C Nd:YAG laser rod. An external mirror laser with several values of dissipative loss, α_o, has been considered. Again, powers lower than those with optimum laser rod diameters less than 1 mm have not been included and a maximum laser efficiency of 1% has been assumed. In Figure 4-10 we have compared the room temperature GaAlAs diodes and the potassium arc lamp pumped room temperature Nd:YAG efficiency versus input power estimates from Figures 3-13 and 4-9 for the best performance $\alpha_o = 0.006$ and $g_o = 0.012$ conditions. GaAlAs diode pumped Nd:YAG has about 0.3% efficiency at only 30 watts input. The efficiency for the diodes is higher than for the potassium arc up to an input power of 170 watts where the two become equal. Above this input, we estimate the potassium arc pumped Nd:YAG to be more efficient.

The number of diodes required for a laser pump depends, of course, on the diode design. Considering the IBM $Ga_{1-x}Al_xAs$ technology,[27] a 0.012 x 0.036 diode operated at ~ 250 amp/cm^2 current density could produce 90 mW total emission at 8 percent efficiency. An output power of 1 watt requires 100 watts of input power according to Figure 4-10. We then estimate that an array of about 90 GaAlAs diodes is required for a room temperature 1 watt Nd:YAG laser operating at 1 percent efficiency at 1.06 microns wavelength.

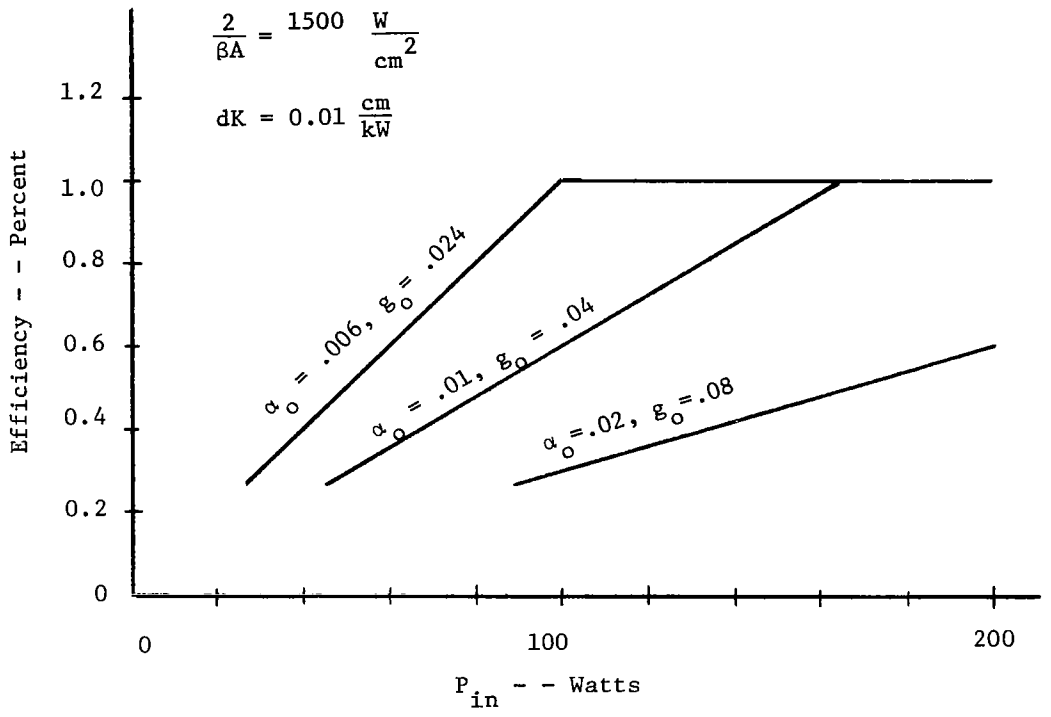

Figure 4-9. Efficiency of 20°C GaAlAs Diodes Pumped Nd:YAG Laser.

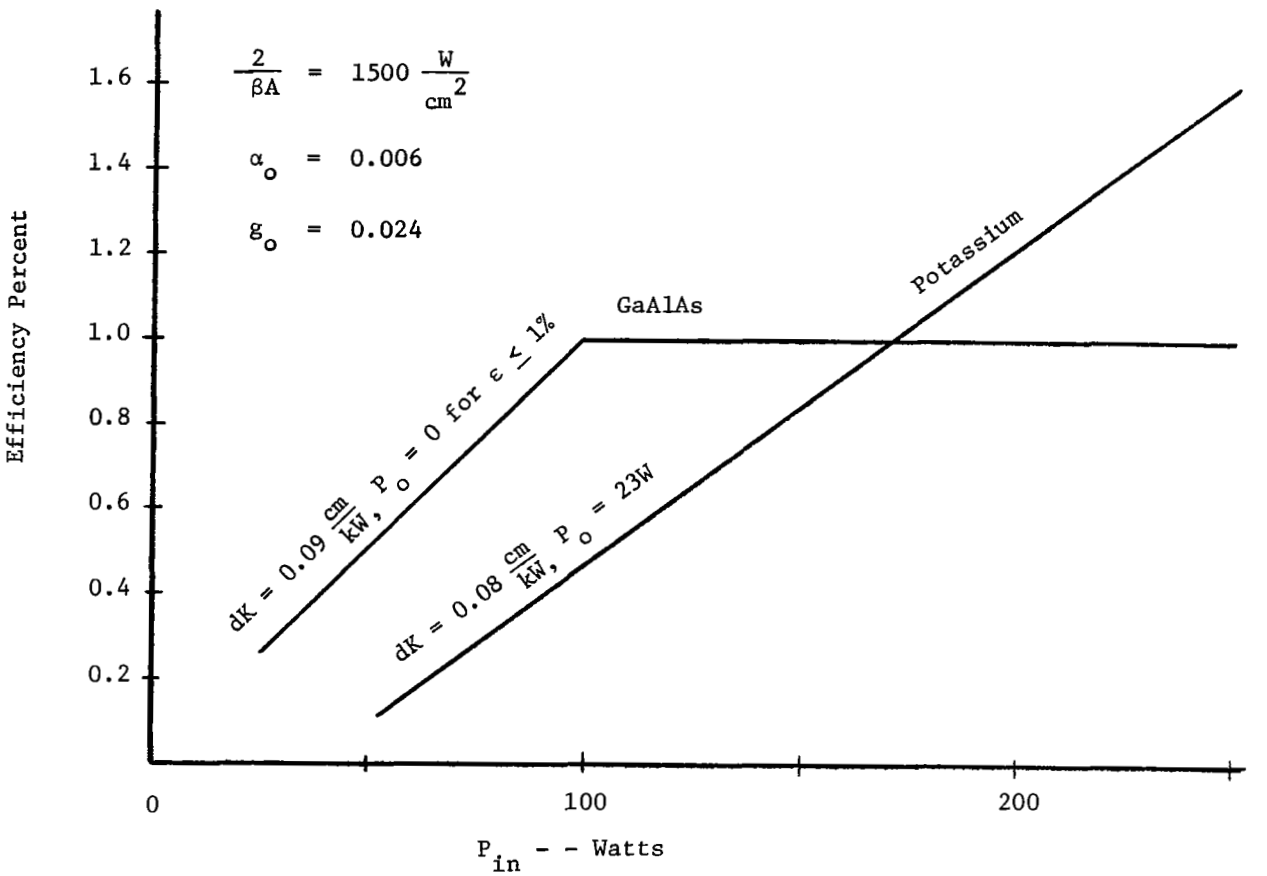

Figure 4-10. Efficiency of 20°C GaAlAs Diodes and Potassium Arc Lamp Pumped 20°C Nd:YAG.

4.5 Expected Life of Room Temperature GaAlAs Laser Pumping Diodes

Little life data is available on room temperature GaAlAs diodes. Data is available on GaAs diodes, however, and we can assume it will apply to future GaAlAs devices. Diode life depends on operating current density.[28] We have assumed operating current densities of 250 amps/cm^2 in our estimate of 90 diodes for 1 watt output. Konnerth,Marinace, and Topalian[29] have recently published life data on both liquid-epitaxy and zinc diffused GaAs diodes operated at current densities of 250 to 500 amps/cm^2. We have taken the liberty of reproducing their best data in Figure 4-11. Most of these diodes were operating at better than 80 percent of their initial output luminescence at 22,500 and 30,000 hours. The half life of these diodes appears to be greater than 90,000 hours. Electroluminescent diodes can, therefore, be made with extremely long life. This is a very important property for a space qualified Nd:YAG laser. Least we become over-confident, however, Konnerth, et al.[29] show curves of diodes with half lives of less than 3,000 hours. Development effort must occur for long-lived room temperature GaAlAs diode pumping arrays for Nd:YAG to be available.

LONG-LIVED ELECTROLUMINESCENT GaAs DIODES

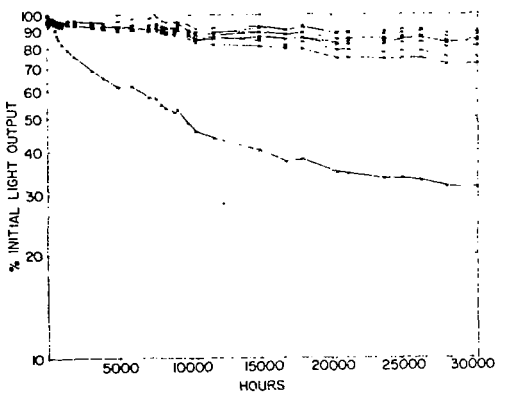

Operating life characteristic of ten unpotted diodes fabricated by the liquid-epitaxial growth of *n*-type GaAs upon a Zn-doped GaAs substrate.

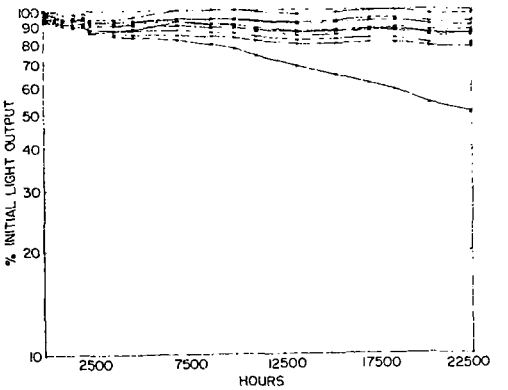

Operating life characteristic of ten unpotted diodes fabricated by the diffusion of Zn for four hours at 750°C +45 min at 850°C into GaAs with a donor concentration of 2×10^{18} Sn/cm^3.

Figure 4-11. Konnerth, Marinace and Topalian's[29] Data on Life of Liquid-Epitaxy and Zinc Diffused GaAs Incoherent Diodes.

SECTION 5

SUN PUMPED Nd:YAG LASERS

A number of research efforts on sun pumped lasers have been completed over the years.[30,31,32,33,34,35,36] Most of these studies were completed before good quality Nd:YAG was available and the results were in general not spectacular. With materials and techniques now available, efficient sun pumping of Nd:YAG lasers should indeed be practical. The weight required to directly sun pump a space qualified Nd:YAG laser should be significantly less than weight required for solar cell structures and power supplies for an electrically pumped Nd:YAG laser.

A problem with exclusive sun pumping is that the sun is occasionally occulted in most satellite orbits. Optical communication systems may be required when the laser is in the dark. For this reason, a dual pumping arrangement is preferred, whereby, a space qualified Nd:YAG laser can be sun pumped at most times, but can be electrically pumped when in the dark. We will describe such a dual pumping scheme later in this section and our lamp pumped space qualified Nd:YAG laser design which will be described in section 8 is compatible with dual pumping.

5.1 Consideration of Previous Sun Pumping Research

Considerable research (both theoretical and experimental) has been done on sun pumping various materials. The staff of American Optical Company has performed three studies under contract for the

U.S. Air Force.[30,31,34] They have defined a theoretical merit factor, G which is essentially the degree above threshold for a given sun-pumping level. In calculating G they have assumed a collector area of $1m^2$. We feel that a better comparision is to assure an area of $0.29m^2$, equal to that of the 24-inch solar collector used in the American Optical experiments. Consulting the three American Optical final reports [30,31,34] and converting the most recent theoretical predictions of G for various materials to the $0.29m^2$ area, the merit factors are as shown in Table 5-1 for Nd:YAG, Nd:Glass, Nd:$CaWO_4$ and ruby. Also shown in Table 5-1 are the experimental values of the merit factor (or degree above threshold) for various materials as determined by various sun-pumping investigators. Again, the values have been converted to a solar collector area of $0.29m^2$ or 24-inch diameter.

Table 5-1. Sun-Pumping Merit Factor, G(Degree Above Threshold), for a 24-Inch Solar Collector and Laser Material at Room Temperature

Material	G,Theoretical	G,Experimental
Ruby	0.3[30,31]	Never Lased
Nd:$CaWO_4$	1.2[31,34]	1[36]
Nd:Glass	12[34]	Intermittent Lasing
Nd:YAG	20	2[36], 3[35]

The data in Table 5-1 show that ruby will not lase with the 24- inch solar collector. A collector of about 40 inches in

diameter theoretically should just achieve threshold. This result is not at all surprising. Ruby is a three-level laser material and has been operated CW with the brightest lamp available, the high-pressure Hg capillary arc.

Nd:$CaWO_4$ has been made to lase with sun pumping by workers in Russia.[36] Their experimental results agree extremely well with American Optical Company's theoretical predictions.[31,34]

Nd:Glass has been made to lase intermittently by American Optical Company. Simpson[32] was able to reach bursts 0.5 second in length. Young[35] was able to get 7-millisecond bursts.

Nd:YAG has the highest figure of merit shown in Table 5-1. It has been successfully sun pumped by RCA[33] and American Optical.[34] The Russians recommend it as the best material for sun pumping.[36] Recently, Rothrock[37] has grown Nd:YAG with 0.1% Cr which has excellent optical quality. Nd:Cr:YAG with 1% Cr[38] was extensively investigated by Pressley. The optical quality of this material was poor and prevented exploitation of the large Cr pump bands that cross relax to the Nd ions. The high optical quality 0.1% Cr:Nd:YAG is essentially identical to Nd:YAG in side pumping arrangements. With the long pump light path available in end pumping, however, significant pump light can be absorbed by 0.1% Cr. This new material is an attractive candidate for dual pumped lasers using solar end pumping and potassium lamps or GaAlAs diodes for side pumping. The solar pumping figure of merit, G, for this material is estimated to be 30 for this material end pumped with a 24-inch solar collector.

5.2 Dual Pumped Laser Design Approach

We have designed a Coude sun-pumping attachment for a space-qualified side-pumped laser. This attachment brings the solar pump energy to the laser rather than bringing the laser to the solar energy as is commonly done in research experiments. The solar collector has been assumed to be a 24-inch telescope. A design layout of the sun-pumped laser is shown in Figure 5-1, 5-2, and 5-3. The 24-inch primary collects the incident sunlight and brings it toward a focus where it is intercepted by a cassegrainian secondary mirror. The secondary increases the focal length producing a nearly collimated beam. This beam is deflected at a right angle and down the axis of the hollow elevation adjusting shaft. A mirror centered on the shaft deflects the beam to another mirror centered on the azimuth rotation axis. The beam exits through the hollow azimuth adjusting shaft; it is now completely independent of the solar collector. Regardless of the elevation and azimuth position of the solar collector, the exit beam position remains unchanged.

A mirror now deflects the beam to a lens. The solar image produced by the primary and secondary mirror falls approximately at the lens. The lens brings an image of the entrance aperture of the solar collector onto a cone frustrum "trumpet" light concentrator[39] that changes diameter down to the diameter of the Nd:YAG laser rod in the space-qualified laser. The trumpet concentrator is made of undoped YAG material and is optically contacted to the end of the Nd:YAG laser rod. A small laser mirror is deposited on the large end of the concentrator. The solar rays are totally internally reflected

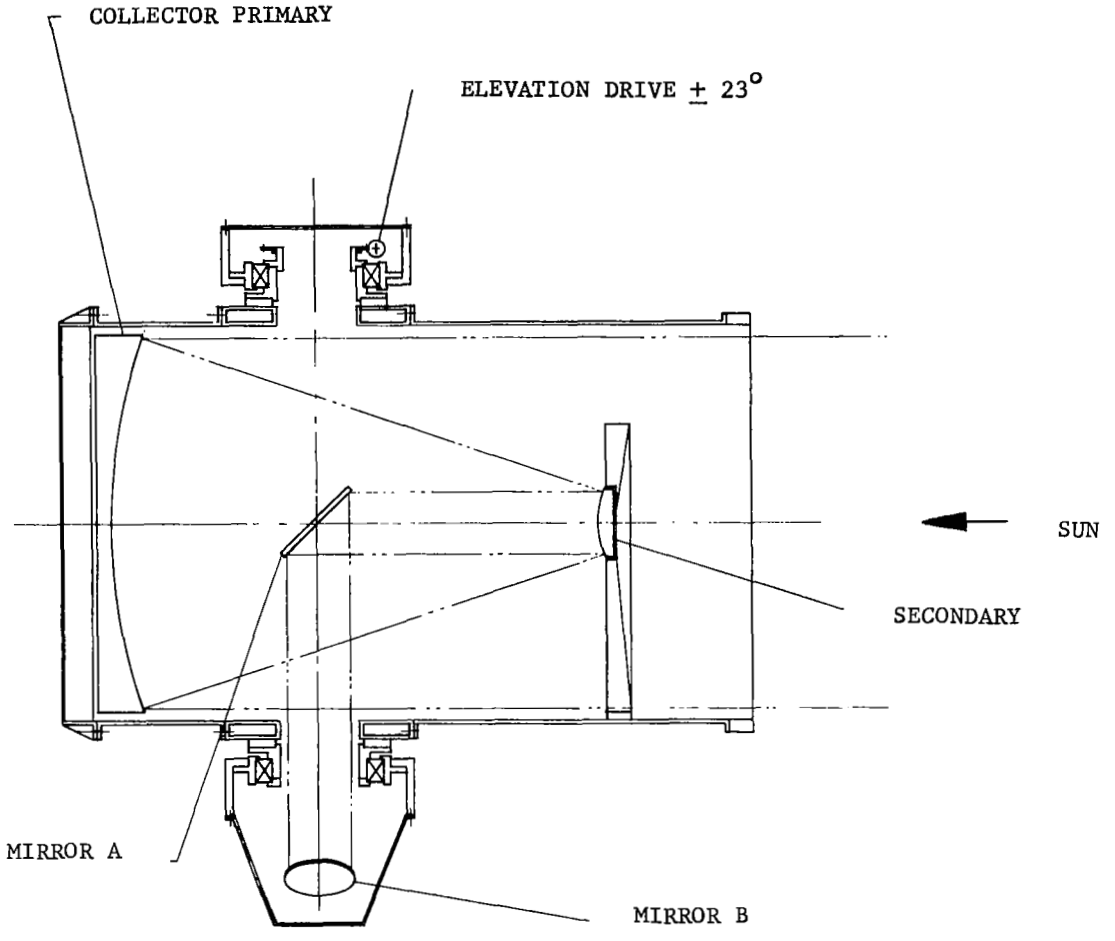

Figure 5-1 Sun-Pumped Laser Design

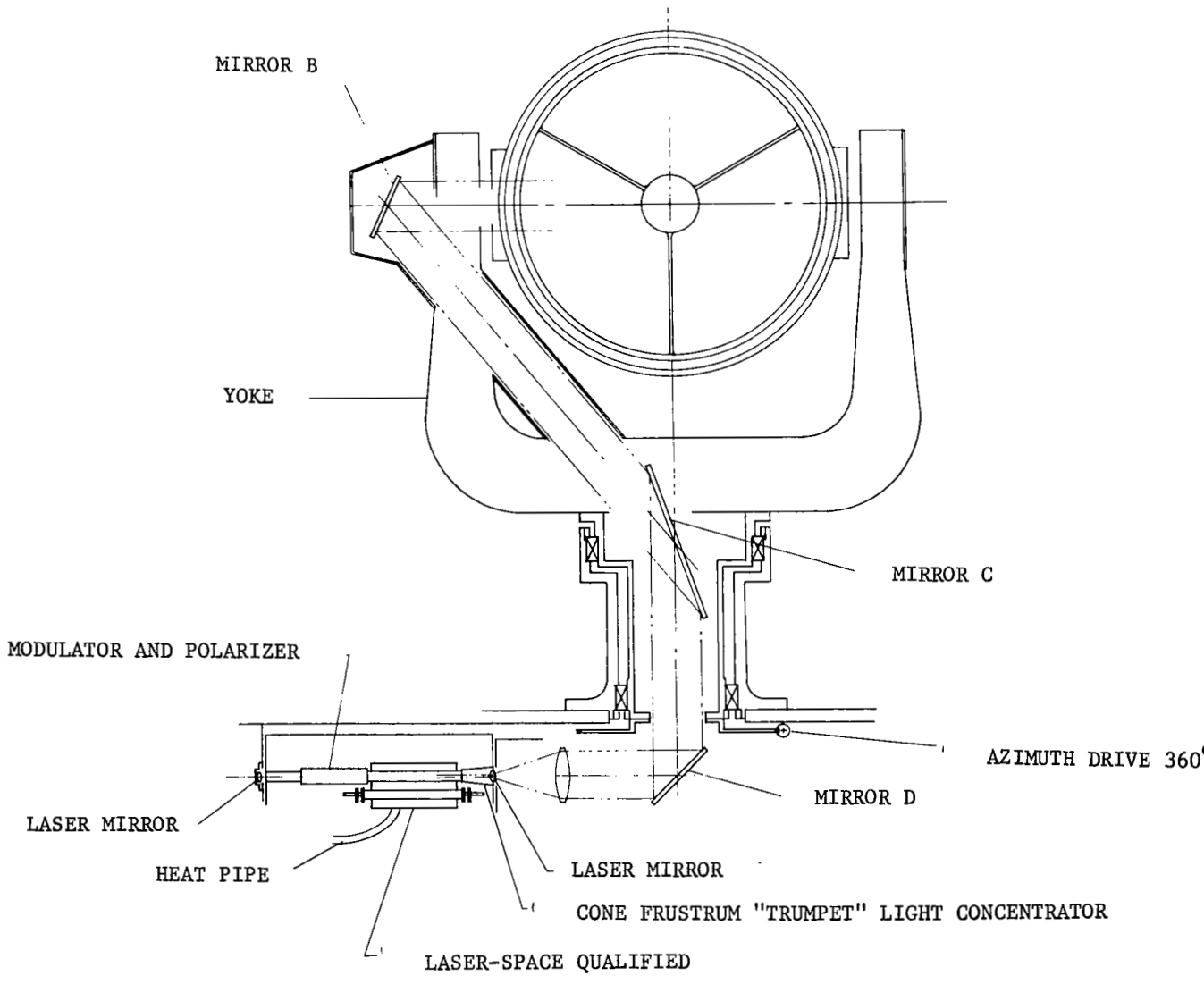

Figure 5-2. Sun-Pumped Laser Design.

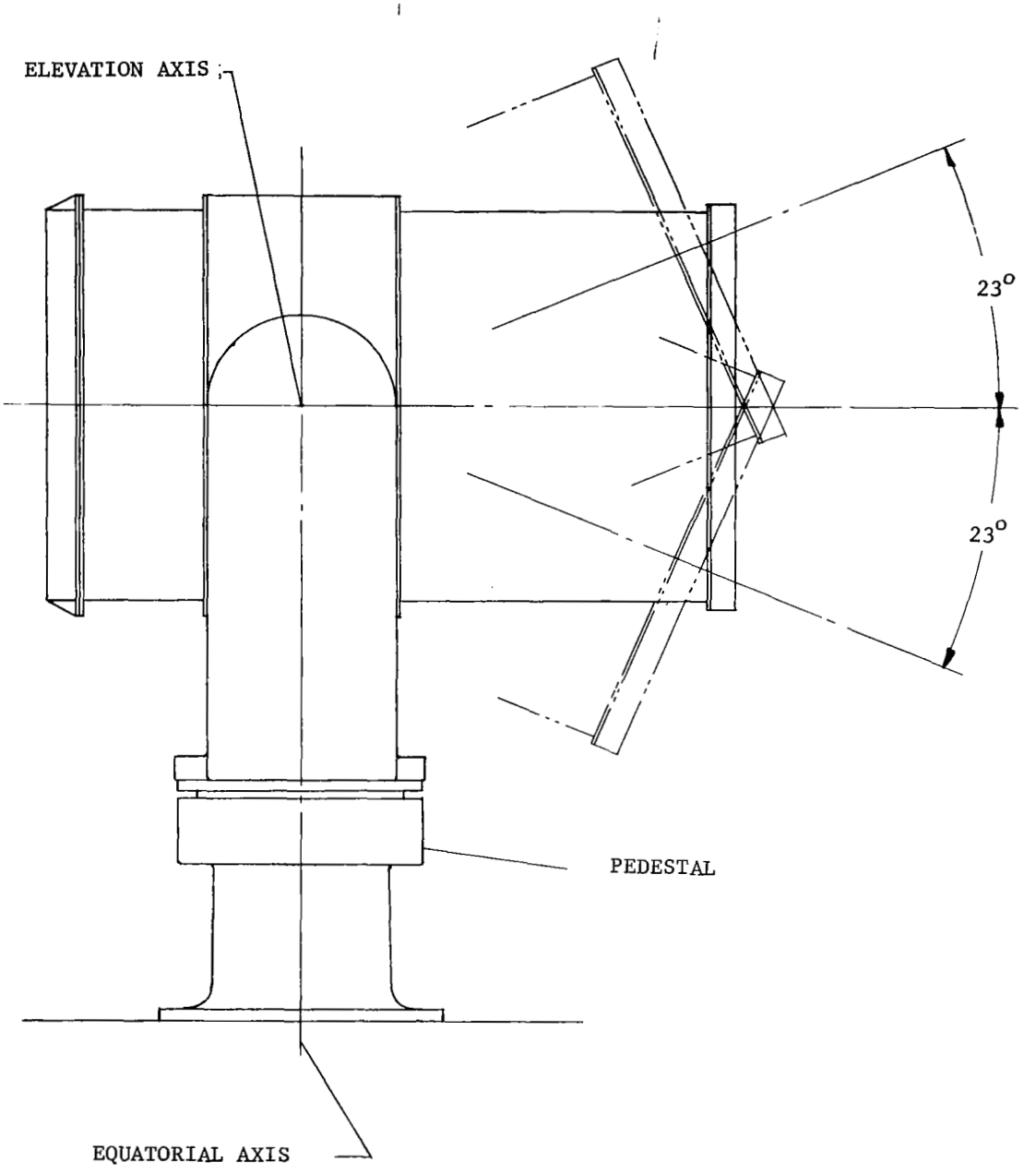

Figure 5-3. Sun-Pumped Laser Design.

in the cone until they enter the end of the laser rod. The four-level Nd:YAG laser material is pumped more intensely at the entrance end than at the opposite end. This is no problem however, because Nd:YAG is quite transparent to its own laser emission. (With a three-level material such as ruby, this would be a critical problem because the laser energy would be reabsorbed at the far (unpumped) end of the rod.) All reflective surfaces are optically coated with high reflection dielectric or enhanced metal coatings for the Nd:YAG pump bands.

This design is unique. It achieves end pumping with a nearly all-reflective optical system. The laser is mounted completely independent of the solar collector pointing and tracking. The laser can be both sun pumped and lamp pumped.

SECTION 6

HEAT REMOVAL FROM Nd:YAG LASER IN SPACE

Most Nd:YAG lasers are cooled by flowing water around the surface of a cylindrical laser rod. The thermal stresses induced by this method of cooling with cylindrical symmetry severely limit low order spatial mode laser performance,[3] and it has been suggested that cooling with cartesian symmetry would be better. Circulating liquid cooling is not a favored technique for space-borne systems either. Conductive and liquid-filled heat pipe cooling techniques have much longer life and are more reliable. Conductive and heat pipe cooling were, therefore, chosen for the space qualified Nd:YAG laser design. These cooling devices were assumed to terminate in radiative heat exchangers that dumped the heat into space.

The space qualified Nd:YAG laser has been designed with conductive cooling of the laser rod from one side in a cartesian relationship. This design will be described in detail in Section 7. In this section, we will analyze the problem of heat transfer from the space laser, will describe some of the laser design details required for our thermal analysis, and will describe some of the heat removal experiments conducted during the program.

The symbols used in equations in this section will reuse some of those used earlier. We have done this to be consistent with the nomenclature normally used in the heat transfer literature. The earlier symbol definitions are used throughout the rest of the report; those used in this section are used only in this section.

6.1 Laser Rod Mounting

The mounting structure for the YAG rod is constructed of pure niobium, having a thermal coefficient of expansion which closely matches that of YAG. The coefficient of YAG had previously been determined to be 6.9 in/in/°C.[40] The coefficient of niobium is 6.88 in/in/°C to 7.38 in/in/°C, depending upon the melt and manufacturer. Niobium is one of the refractory metal family, having a melting temperature of 4379°F. It has a density of 535 lbs/ft.^{3}, approximately the same as brass. The thermal conductivity is reasonably high, 31 BTU/hr. ft.^{2} °F/ft., a desirable property in this application. The YAG rod mounting is shown in Figure 6-1.

The mounting surface for the rod is a machined radiused groove to provide intimate contact with the rod over 90° of its periphery. The rod is soldered into this groove. Niobium cannot be wet and soldered with ordinary fluxes due to the inertness of the oxide coating; therefore, plating of the niobium was attempted. It was found that cleaning the material in hot H_2SO_4, applying a nickel strike with a 50 x 10^{-6} inch thick layer of copper followed by a final gold flash provides good solderability and corrosion resistance.

The YAG rod is plated over 90° of its periphery. It was found that the proprietary technique of Liberty Mirror Division of Libby Owens Ford produced a vacuum deposited gold highly-reflective second surface mirror with the best adherence of a number of techniques we investigated. Nickel is applied over this to provide coating thickness and solderability without scavenging. The YAG rod is soldered to the support block using

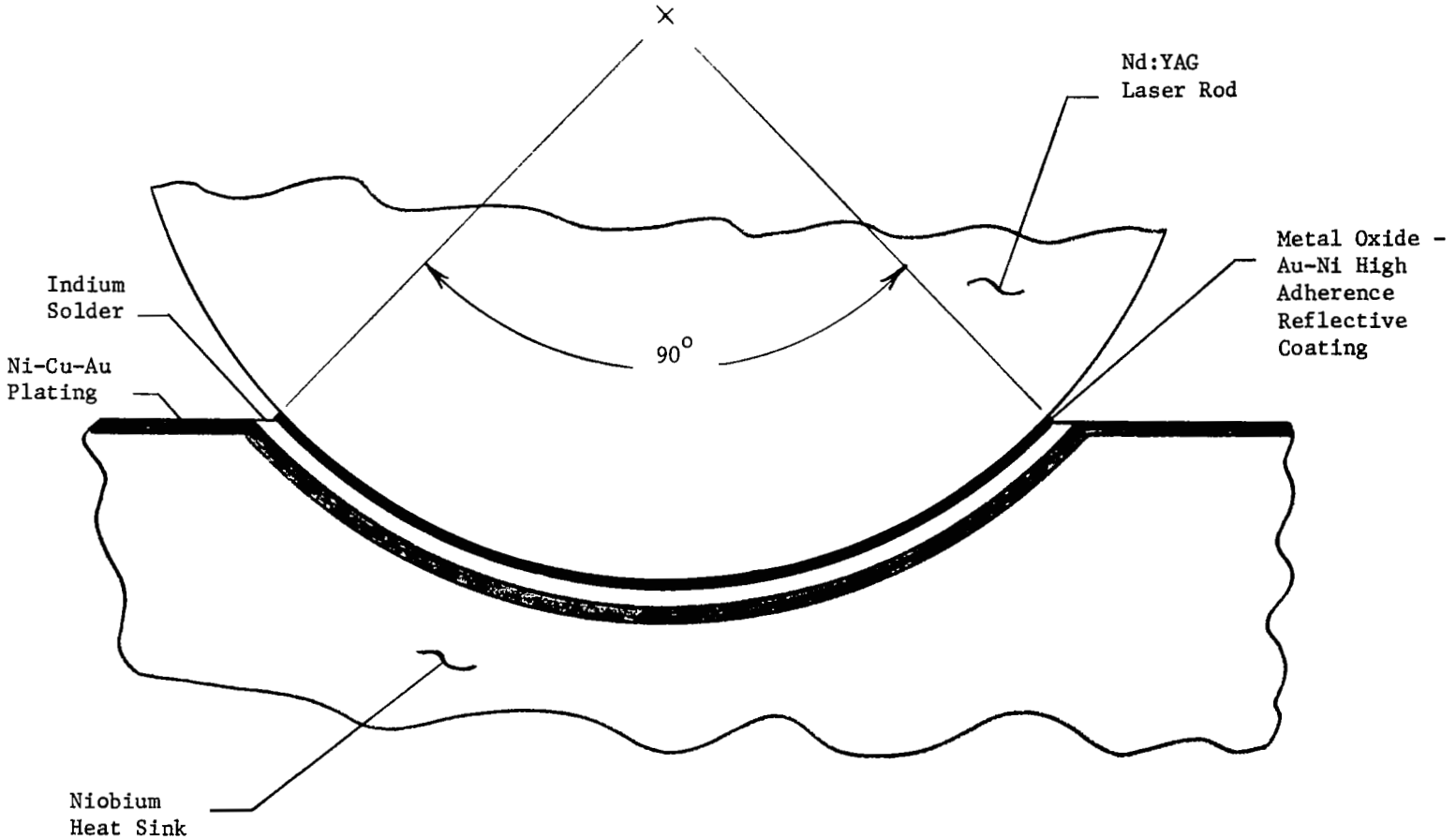

Figure 6-1. Conductively Cooled Nd:YAG Laser Rod Mounting Arrangement.

pure indium solder which has a low melting point, high ductility, and minimum scavenge to the nickel and gold during soldering. The solder bond between the rod and block is maintained at .004" - .005" thickness. This results in maximum joint strength and low thermal resistivity.

One of the problems is adherence of the gold mirrored surface to the YAG rod. We considered a number of techniques of applying this high internal surface (second surface) reflecting coating which must have minimum thermal impedance. We ran test samples on what appeared to be the three most promising techniques. The first was the proprietary vacuum deposited oxide undercoating and gold technique of Liberty Mirror Division of Libby Owens Ford Corporation. The second was sputtering of oxide undercoatings and gold. Electrotec Corporation produced samples with Al_2O_3 and TiO_2 undercoatings using the sputtering technique. The third was the fired-on "liquid gold" formulations of Engelhard Industries.

The sample substrates used in these experiments were of fused quartz. It was used because of the similarity of the adhesion and reflection problem with YAG and the lower cost and availability. Table 6-1 shows the reflectivities measured for the various samples using a 6328Å He-Ne laser.

Samples with the 88% reflecting Liberty Mirror coating and the 80% Al_2O_3 undercoated Electrotec coating were soldered successfully with no degradation of the coatings. We then decided to utilize the Liberty Mirror coating in our experiments because of its higher reflectivity.

TABLE 6-1. Internal Surface Reflectivity of Various High Adherence Gold Coatings on Fused Quartz Plates.

Coating Description	Coating Manufacturer	Internal Surface Reflection
Proprietary vacuum deposited oxide undercoated gold with nickel overcoat	Liberty Mirror	88%
Sputtered Al_2O_3 under Gold with nickel overcoat	Electrotec	80%
Sputtered TiO_2 under Gold with chromium, then nickel overcoat	Electrotec	45%
Hanovia liquid gold bright white, No. 1	Engelhard Industries, Hanovia Liquid Gold Div.	37%
Hanovia liquid gold bright, No. NW	Engelhard Industries, Hanovia Liquid Gold Div.	60%
Reference vacuum deposited gold (external surface)	Sylvania	98.5%

A 2 mm diameter Nd:YAG rod was coated over 90° of its periphery with the Liberty Mirror coating and was soldered to the niobium mounting with indium solder. About 50% of the coated surface was removed by the soldering. We believe that nickel overcoat layer was not as thick as required and that the indium solder scavenged the gold coating. Further development is required in order to produce reliable joints between the Nd:YAG rod and the niobium.

6.2 Heat Pipe Considerations

The heat pipe was selected as a means to remove heat from the rod mounting structure because the high thermal conductance, fifty or more times better than a solid metallic conductor, and low weight and high anticipated reliability seem ideal for use in spacecraft applications. The heat pipe as used for this purpose consists of an outer circular housing, an inner screen to carry the fluid, and the working fluid. The fluid is vaporized in the evaporator end by heat input, travels down the center of the assembly to the other end which must be cooled in some manner to cause condensation of the fluid which then travels to the evaporator end by surface tension forces in the screen wick. The pipe is completely closed, forming a hermetic seal between the working fluid and the outside environment.

Practical considerations in the application of heat pipes are those of required conductance length, thermal flux densities in the input and output surfaces, total heat flux conductance, and desired working temperature. A pipe's maximum thermal conductance is a function of the working fluid, pipe diameter and wick configuration. In the absence of

a gravity field, the thermal conductance is directly proportional to the latent heat of vaporization of the fluid, to the cross sectional area, to the square root of the surface tension and the vapor density of the fluid,[42]

$$\frac{Q}{A} \simeq h_v \sqrt{\rho_v \gamma} \qquad (6\text{-}1)$$

where Q = axial heat flux

A = area of vapor flow passage

h_v = latent heat of vaporization

ρ_v = density of vapor

γ = surface tension.

Assuming operation in a gravity field, the maximum length for a given pipe diameter, wick material and fluid is determined by the available pressure head or

$$\Delta P_C = \Delta P_G + \Delta P_L + \Delta P_V$$

where ΔP_C = pressure head generated by the capillary structure

ΔP_G = pressure head due to gravity

ΔP_L = viscous pressure loss in liquid

ΔP_V = viscous and inertial pressure loss in vapor.

In the above equality, the liquid and vapor drag and the gravity forces equal the surface tension forces in the capillary structure. The gravity force could either assist or impair operation on the ground, depending upon pipe orientation, but would not be a factor in outer space.

Optimum lengths for different combinations of fluid and wick have been determined and are available commercially. Longer lengths for a given diameter suffer a linear loss in efficiency due to the greater pressure gradients in the longer flow path. Circular heat pipes with 90° bends are available from several vendors who have solved the problem of liquid return through the curved portions.

A useful expression for the overall design of a heat pipe is as follows:[42]

$$\frac{Q}{A} = h_v \left[\frac{2g_o}{\lambda} \rho_v (\Delta P_C - \Delta P_G) \left(1 + \frac{\phi^2}{2} \left(1 - \left(1 + \frac{4}{\phi^2}\right)^{1/2}\right)\right)\right]^{1/2} \tag{6-2}$$

where $\phi = \dfrac{a}{(\Delta P_C - \Delta P_G)^{1/2}}$ and $a = \dfrac{\nu}{g_o} KA \sqrt{\dfrac{2g_o}{\lambda} \rho_v}$

g_o = gravitational constant

λ = a constant

ν = kinematic viscosity

K = wick configuration factor.

The maximum thermal density for the input and output to a heat pipe is determined empirically and is the point at which heat transfer ceases due to the fact that the capillary structure can no longer deliver sufficient return fluid to the evaporator section per unit time. For the pipes used in this program, the maximum thermal density has been determined by the manufacturer to be 15-20 watts/in.^{2} on the input end and 30 watts/in.^{2} on the output end.

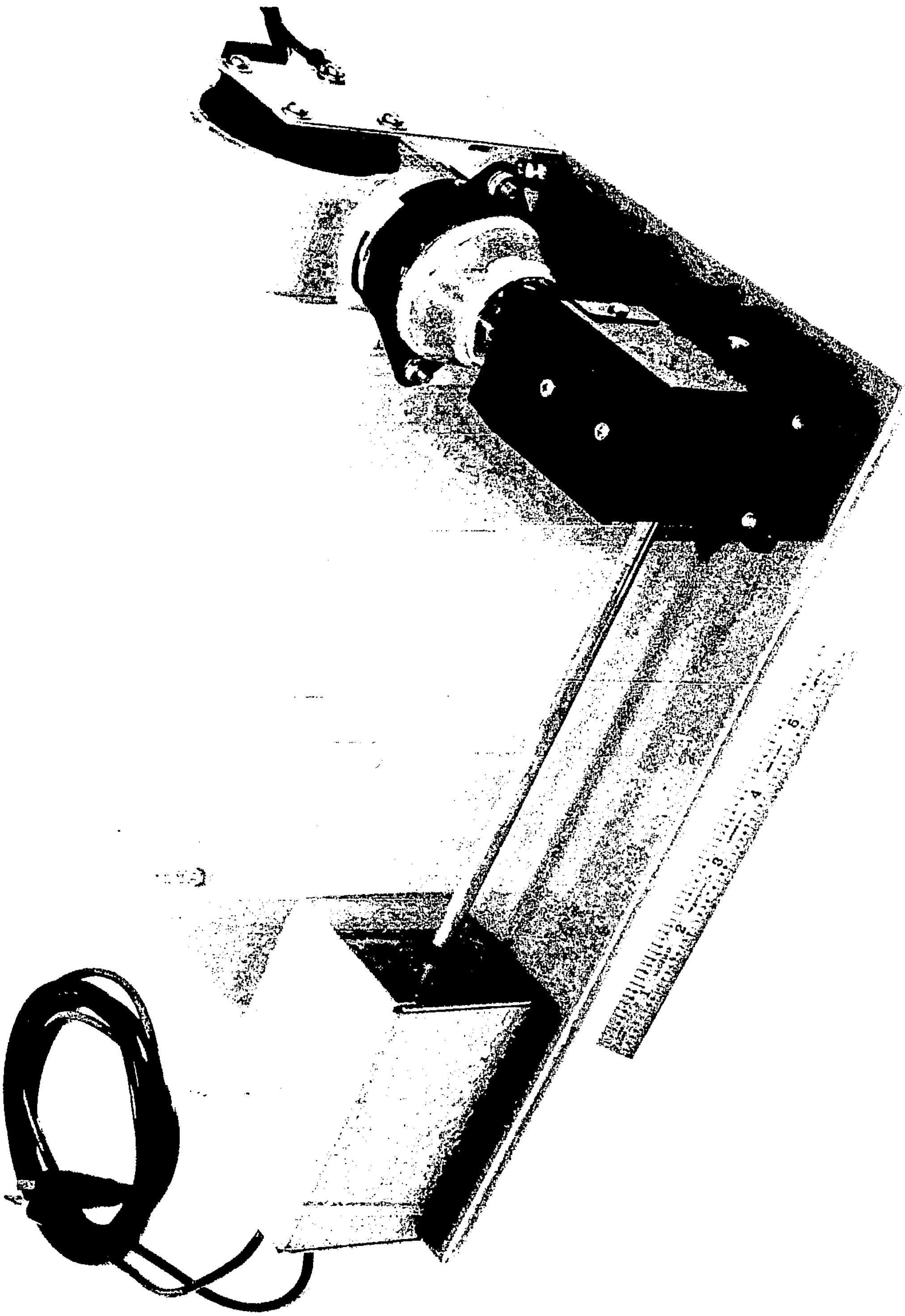

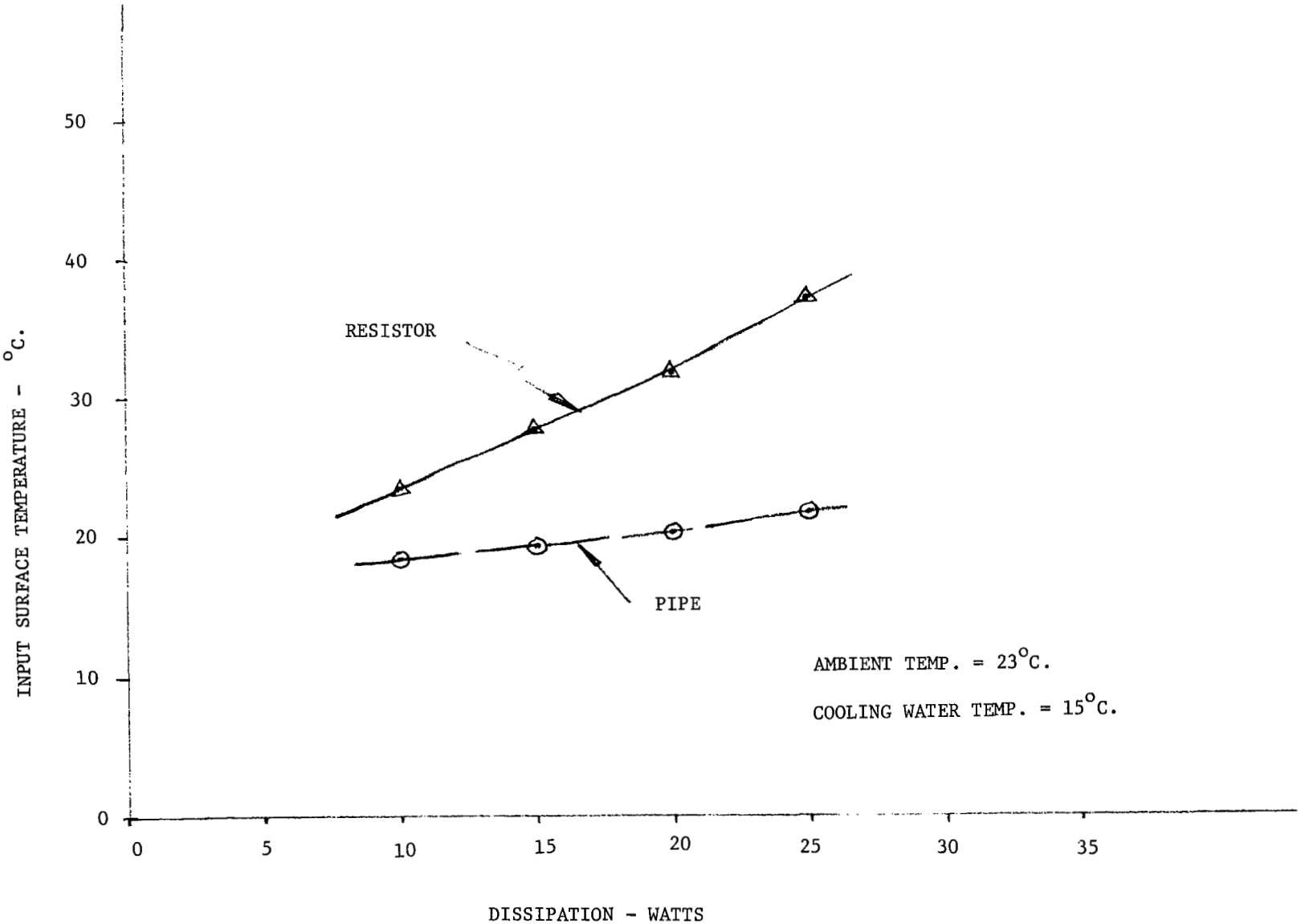

Figure 6-3. Test Results for Anhydrous Ammonia Heat Pipe - 25" Dia. x 12" Long
(Purchased from Energy Conv. Systems)
Pipe-Horizontal

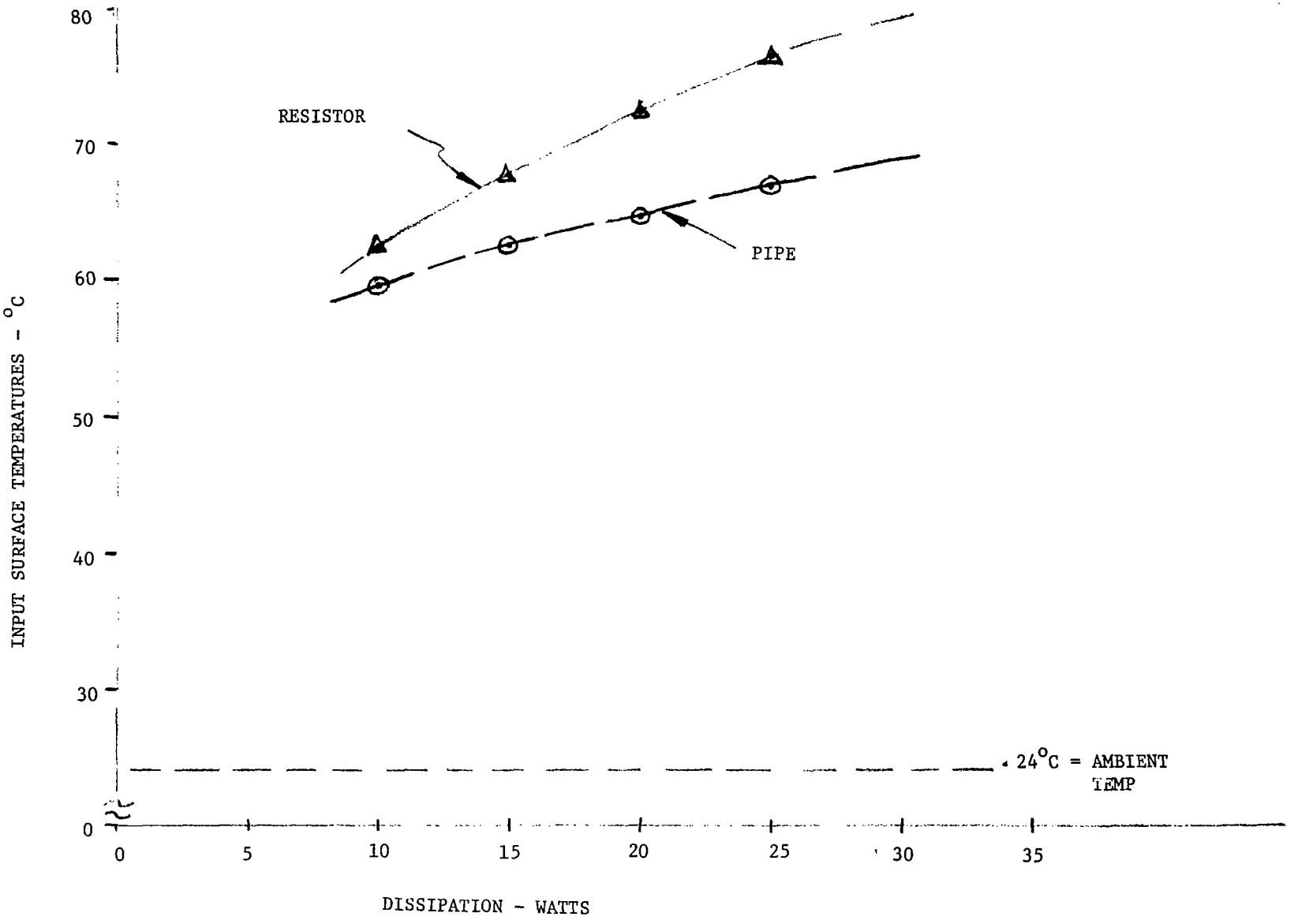

Figure 6-4. Test Results for Methanol Heat Pipe - .25" Dia. x 12" Long (Purchased From Energy Conv. Systems) Pipe - Horizontal

With consideration of the above parameters, the pipe selected was a .25" diameter by 12" long stainless steel pipe filled with anhydrous ammonia. Test apparatus to simulate laser rod thermal input levels is shown as Figure 6-2. Test results for the anhydrous ammonia pipe are shown in Figure 6-3. A .25" diameter by 12" long copper pipe filled with methanol was also tested. The test results are presented as Figure 6-4.

6.3 Thermal Resistance from Laser Rod to Radiation Cooler

Total heat path thermal resistance from the rod to the radiation device consists of a number of series resistances. These consist of metallic resistivities, inefficiencies in the heat pipe and interface resistances. Values were calculated for two distinct cases, 2 watts dissipation and 20 watts dissipation into the heat pipe. Results are plotted in Figure 6-5.

The first two resistances encountered by thermal energy from the rod are the indium solder joint and the material of the niobium block. For heat loss through these materials with no heat loss from the sides, resistance can be calculated as:[43]

$$R = \frac{3.414\ L}{AK} \qquad (6\text{-}3)$$

where R = thermal resistance °F/watt

L = path length - ft.

A = path area - $ft.^2$

K = material conductance - $\frac{BTU\ ft.}{hr.ft.^2\ °F}$

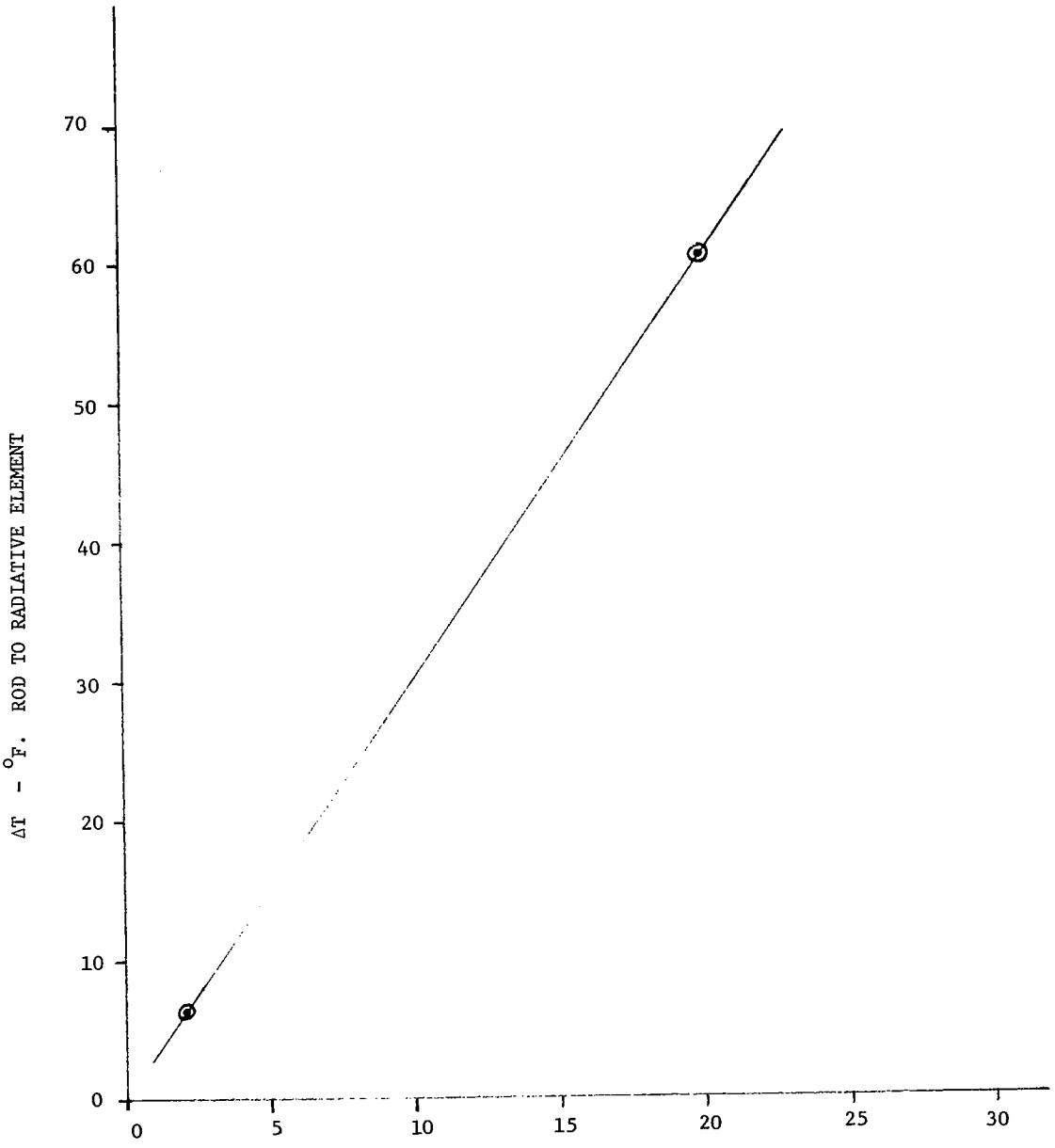

Figure 6-5. ΔT - Laser Rod to Radiator

The next resistance encountered will be that across the metal-to-metal interface of the mounting block to the heat pipe and will be calculated as a metal-to-metal interface in a vacuum by the following equation:[44]

$$R_{CV} = \frac{(8+e^{d})\,(Y_e \times 10^{-3}+16)^{.34}}{(3\times10^{3})(8.9\times0.1e^{d})} \quad \frac{(\omega_o \times 10^{3}+10)^{1.7}}{F(P_a)G(S_F)} \qquad (6\text{-}4)$$

where R_{CV} = thermal contact resistance, °F ft.^{2}/watt

P_a = apparent contact pressure, psi

d = distance between clamping points, inches

S_f = surface finish of lower yield point surface, μ in.

Y_e = initial yield point of material on hot side of interface, psi

ω_o = initial total flatness, in.

$F(P_a)$ = 1.8 + 0.034 P_a, at contact pressures above 30 psi

$G(S_F)$ = 1.0 for surface finishes between 12 and 46 micro-inches.

Calculated values for the thermal resistances into heat pipes give extremely low values; these have not been borne out in practice.[42] A conservative value of .5°F in.^{2}/watt will be assumed for the evaporator end and .02°F in.^{2}/watt for the condenser end. These cover losses through the container wall and the film resistance for either vapor or condensate.

Total thermal resistance of any configuration can be seen to be linear with input. This is shown by the equations and the test results with simulated loads on heat pipes in Figure 6-3 and Figure 6-4.

The individual thermal resistances are tabulated below for the Nd:YAG rod to space radiator:

Indium joint =	.1 °F/watt
Niobium block =	1.76 °F/watt
Block to heat pipe =	1.08 °F/watt
Vapor end of pipe =	.36 °F/watt
Liquid end of pipe =	Nil
Pipe to radiator interface =	.65 °F/watt.

For purposes of the calculations it is assumed that for all cases, one half of the thermal energy dissipated through the heat pipe is generated in the rod and one half is energy leakage into the niobium block from the shell. Thus, in calculating the temperature difference between rod and radiator, only one half of heat pipe total passes through the indium and niobium block resistances. In the lamp pump laser design presented in Section 7, the shell has been designed to minimize this unwanted input; however, due to the close proximity of the high temperature lamp, it is impossible to eliminate it.

Similar thermal resistances are encountered in the cooling systems required for the laser pump lamps or pump diodes. We will not repeat the detailed calculation for these cases, however.

6.4 Dissipation of Energy by Radiation

The surface area required to radiate heat into space at a maximum value will occur if the entire radiating surface temperature is uniform and the radiating surface is convex or flat so that every element of it can see a hemisphere of directions and no other bodies such as the Sun or other parts of the spacecraft can be seen by the surface. The minimum radiator area required under these conditions is then determined by the relation:[43]

$$Q = A \sigma F_e T_s^4 \qquad (6\text{-}5)$$

where Q = heat flow BTU/hr.

A = area, $ft.^2$

σ = Stefan-Boltzmann Constant,

$$1.732 \times 10^{-9} \frac{\text{BTU}}{\text{hr.ft.}^2(^\circ\text{R})^4}$$

F_e = emissivity factor

T_s = source temperature, °R.

When heat is to be dissipated from a concentrated source, as from the condenser end of a heat pipe, distributing the heat uniformly over the radiator surface is a problem. We will assume the heat is uniformly distributed along the edge of a good conducting fin, and will assume that the fins project out in both directions from the heat pipe in the base, and that radiation is possible from both sides of the fins.

To determine the exact variation in temperature along the fin outward from the base requires solution of a non-linear differential equation containing an expression with the 4th power of the temperature. An attempt has therefore been made to simplify the solution by assuming linearity over a small temperature range.[45]

The base temperature of the fin will be a known value and the temperature at the outer end assumed. Then an average can be determined and a linear expression incorporating emissivity and radiant heat flow per unit area can be derived. This term would be equivalent to the convection factor in the linear first order differential equation case which is solvable.

This approximation is usable if the base temperature remains constant, the receiver temperature is fixed, and there is negligible temperature drop over the length of the fin. The fin efficiency as a function of temperature base excess versus fin thickness and height can be determined and plotted as in reference (45). Figure 6-6 shows the radiating fin configuration we have assumed. Additional assumptions and limitations are:

1. The heat flow is steady.
2. The fin material is homogeneous.
3. The coefficient of heat transfer is based on an average over the total fin.
4. The receiver is at a constant temperature.
5. There are no temperature gradients along the fin other than along the height.
6. There is no resistance to flow of heat into the fin, and there are no heat sources within the fin.

7. There is a negligible amount of heat transferred by radiation from the ends and edges of the fin. The sides of the fin are the surfaces that dissipate heat by radiation.

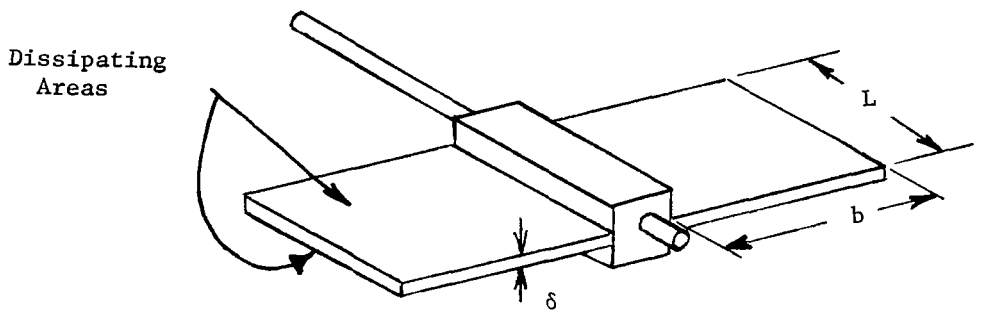

Figure 6-6. Radiating Fin Configuration

Using these assumptions we find that[45]

$$\eta = \frac{\tanh mb}{mb} \qquad (6\text{-}6)$$

η = fin efficiency

$m = \sqrt{\frac{2h_r}{K\,\delta}}$

b = fin height, ft.

h_r = heat transfer coefficient by radiation

BTU/ft.^{2} hr./°F

K = thermal conductivity of fin material,

BTU/hr.ft.^{2} °F/ft.

The efficiency curve plotted from equation (6-6) is shown in Figure 6-7. If the configuration has an efficiency of 65 percent, we can consider 65 percent of the total extended surface to be operating at the base temperature.

6.4.1 Laser Rod Heat Dissipation

We can now calculate the radiation cooler area and weight required to dissipate waste heat into space. Consider first a one-watt potassium arc lamp pumped space qualified Nd:YAG laser. In Section 8 we will describe the design of such a laser. This design maintains the laser rod at 68°F. An estimated 3 watts of heat is generated in the laser rod, and an estimated 12 watts of heat leaks into the laser rod mounting block from the lamp and pump cavity reflectors. In Section 6.3, we have estimated that the thermal drop in transporting heat from the rod to the heat pipe interface is 1.86 °F/watt or 6.5 °F for 3 watts, and that the thermal drop from the interface into the heat pipe and on to the radiation cooler is 2.49 °F/watt or 37.4 °F for 15 watts. The temperature at the fin base in the radiation cooler must be then 417 °R.

If we then assume the base temperature to be 417 °R, the outer fin end temperature to be 397 °R, and the fin emissivity factor to be 0.9, the arithmetic average $\bar{h}_r$ can be calculated

$$h_r = \frac{Q}{AT} = \sigma F_e T_s^4$$

$$\bar{h}_r = \frac{\sigma F_e (T_1^4 + T_2^4)}{2} \qquad (6\text{-}7)$$

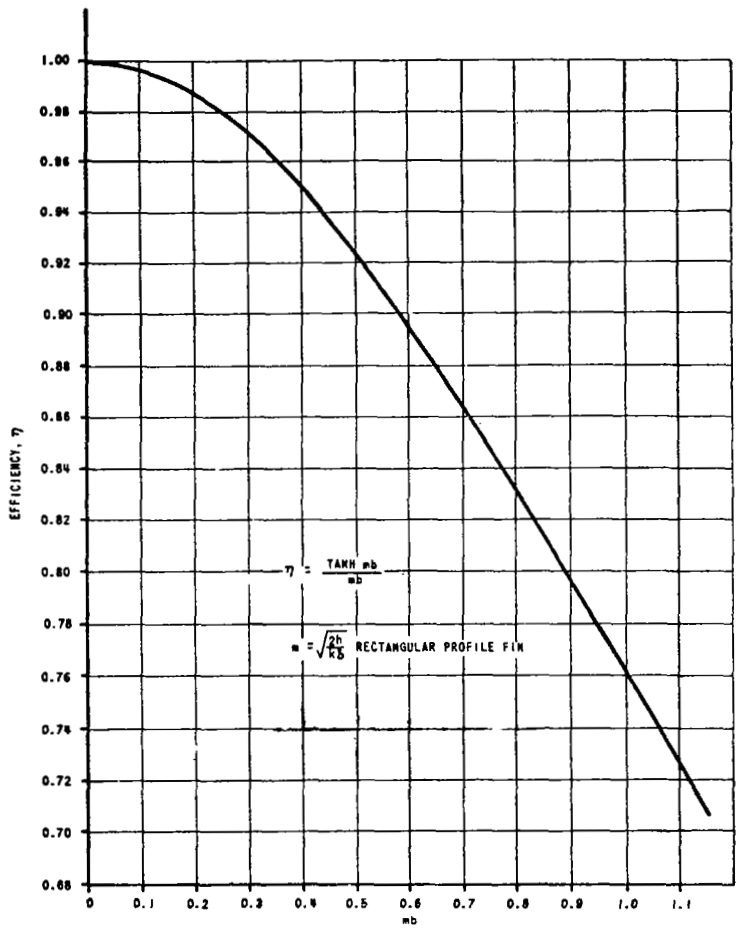

Figure 6-7. Efficiency of longitudinal fin of rectangular profile.

where T_1 = the fin base temperature

T_2 = the fin tip temperature.

We get $\overline{h}_r = 0.105.$

Assuming the fin to be made of 6061T6 aluminum with K = 90 BTU/hr.ft.^{2} °F/ft. and the fin thickness, δ, to be 0.125 inches

$$m = 0.473.$$

Assuming the fin height, b = 12 in. in equation (6-6),

$$\eta = 0.93$$

Rearranging equation (6-5), the area required for 15 watts dissipation using a 0.93 efficiency factor for 417 °R base temperature is 1.1 ft.^{2} The fin length required for the required area from the two sides of the two fins is 3.3 in.

The weight of such a space radiation cooler at the condenser end of the heat pipe would be about 0.9 pounds. Further calculations show that a lighter weight but larger size radiation cooler can be made using 0.62 inch fins. Choice of the optimum tradeoff depends upon the application and vehicle in which the laser is mounted.

By the same technique, it can be shown that attempting to operate the rod at cryogenic temperatures, as an example 77 °K (138 °R), would not be feasible from a size and weight standpoint without a mechanical cooling unit of some type. As an example, if we assume the same approximate dissipation (rod losses will probably decrease but lamp leakage into the mounting surface would increase), the same approximate thermal resistance loss could be anticipated. With the initial rod temperature to be maintained at 138 °R, a 43 °F loss to the base of the radiating fins could be expected. Thus, for the initial calculation, let's assume the complete radiative device is at 138° - 43° = 95 °R. The minimum required surface area would then be:

$$A = \frac{Q}{\sigma F_e T_s^4} = 403 \text{ ft.}^2$$

This, of course, assumes that the fin was at uniform temperature; considering loss of fin efficiency due to conduction losses to outer parts of the fin or fins, it would be ridiculous to attempt maintaining the rod at 77 °K without some type of mechanical cryogenic cooler. We must then conclude that the good laser performance achievable by operating the laser rod at 77 °K is not worth the added weight required to dissipate the waste energy into space.

6.4.2 Potassium Arc Lamp Heat Dissipation

The potassium arc lamp is operated at a very hot temperature (1200 °F) and is only cooled by radiation. This heat shows up in the laser pump cavity reflectors. The reflectors may be operated at a high temperature and still perform satisfactorily. The waste heat from the pump lamps can, thereby, be removed from a high temperature source, greatly reducing the radiation cooler requirements.

The radiative dissipation device required for the lamp reflectors can be calculated as previously shown for the condenser end of the laser rod heat pipe. In the case of the lamp waste heat, we assumed that the base temperature of the fin is 600 °F or 1060 °R and the device must radiate 150 watts to the interior of the spacecraft which would be assumed to be at 70 °F or 530 °R or to space at 0 °R. Some form factor and total emissivity of source and receiver must be assumed. For our purpose, assume $F_a = 0.9$ and $F_E = 0.8$.

Again, a fin will be assumed to project from each side of the laser housing with radiation possible from both sides of each fin.

Assuming all of the fin at the base temperature, the area required is

$$A = .346 \text{ ft.}^2$$

If we assume the base temperature to be 1060 °R and the outer fin end temperature to be 1040 °R, the average h_r can be determined.

$$\bar{h}_r = 2.74 \text{ BTU/hr.ft.}^2/\ ^\circ\text{F}$$

Assuming a fin of .125" thick 6061TG aluminum, and b = 6" long,

$$\eta = \frac{.8342}{1.205} = 0.69$$

Again, the total fin surface will be the two sides of the two fins, each with a height of 6" extending along the lamp axis a distance L = 3 inches. The weight of the fins would be approximately .44 lbs. Optimization would be possible after the final position and configuration were known.

6.4.3 Diode Array Heat Dissipation

To assume a diode pumped laser operating with 1% efficiency and one watt output will require that 90 watts of thermal energy be dissipated from the diode array. We could assume a heat pipe is utilized to remove the energy from the immediate area of the array to such a point outside the spacecraft where it will be ultimately dissipated by radiation. If it is desirable to maintain the array at 20 °C (68 °F), it could be assumed that resistive loss into and out of the heat pipe would be similar to those shown previously for the case requiring maintenance of the laser rod at 20 °C for the lamp cooled version. The heat pipe required would be significantly larger than the 1/4" diameter unit assumed before, possibly as much as 5/8" diameter and filled with anhydrous ammonia.

The minimum required area to dissipate the 90 watts, assuming all of the extended radiating surface attached to the condenser end of the heat pipe is operating at the base temperature, is as follows:

$$A = \frac{Q}{\sigma F_e T_s^4}$$

Assume $F_e = .9$

Assume T_s = [460 + 68] - 60 °F resistance loss

$$T_s = 468\ ^\circ R$$

$$Q = 90 \text{ watts}$$

$$A = \frac{90(3.414)}{(1.732\text{x}10^{-9})(.9)(468)^4} = \frac{307}{1.56\text{x}10^{-9}(48.0\text{x}10^{9})}$$

$$A = \frac{307}{75} = 4.1 \text{ ft.}^2$$

Assuming the same average radiation transfer coefficient as used in the determination of fin size and efficiency for the previously determined laser rod dissipator,

$$\overline{h}_r = .1425 \text{ BTU/hr.ft.}^2/\ ^\circ F.$$

Assuming fins extending out 24 inches on each side of the heat pipe condenser end and constructed of 3/16" thick 6061T6 aluminum, then

$$m = \sqrt{\frac{2\,\bar{h}_r}{K\,\delta}} = \sqrt{\frac{2(.1425)}{90(\frac{.187}{12})}} = \sqrt{\frac{.285}{1.4}}$$

$$m = \sqrt{.204} = .452$$

with b, the fin height equal to 24 inches,

$$mb = .452\ (2.0) = .904$$

$$\tanh mb = .7183$$

$$\text{efficiency } \eta = \frac{.7183}{.904} = .795$$

The total fin surface required would be the two sides of the two fins, each of height two ft. and extending along the heat pipe a distance L.

So, $$2[2(2.0\ \text{ft.} \cdot L)] = \frac{4.1\ \text{ft.}^2}{.795}$$

$$8.0\ \text{ft.} \cdot L = 5.16\ \text{ft.}^2$$

$$L = .645\ \text{ft.} = 7.74\ \text{inches.}$$

The weight of this simple radiation system would be approximately 14.2 lbs. Optimization could probably decrease this to 10 lbs.

Diode arrays might be operated at lower temperatures than 20 °C. We have considered the effect of such lower temperature operation on the radiation cooler using the methods of this section.

The relative radiation area requirements for 100 watts dissipation as a function of temperature are shown in Figure 6-8. The lower curve, Curve 1, is based on the condition that the total radiating area is operating at the same temperature, the base input temperature. This situation would be considered 100% fin efficiency since the whole fin is at the maximum possible temperature. This is, of course, not obtainable in any real situation, since to have no temperature drop outward from the input flux point would require a fin of infinite thickness or a material of infinite conduction. Curve 2 represents what could reasonably be expected in an actual system with radiative fins constructed of a good metallic conductor such as aluminum and with minimum weight as a criteria.

It can be seen from the curves that there are very positive size (and weight) advantages for a device that can be operated at some reasonably high temperature, preferably above 0 °F. This curve can be roughly converted to radiation cooler weight by assuming 1/8"aluminum for the fins which weighs 1.75 lbs/ft.^{2}

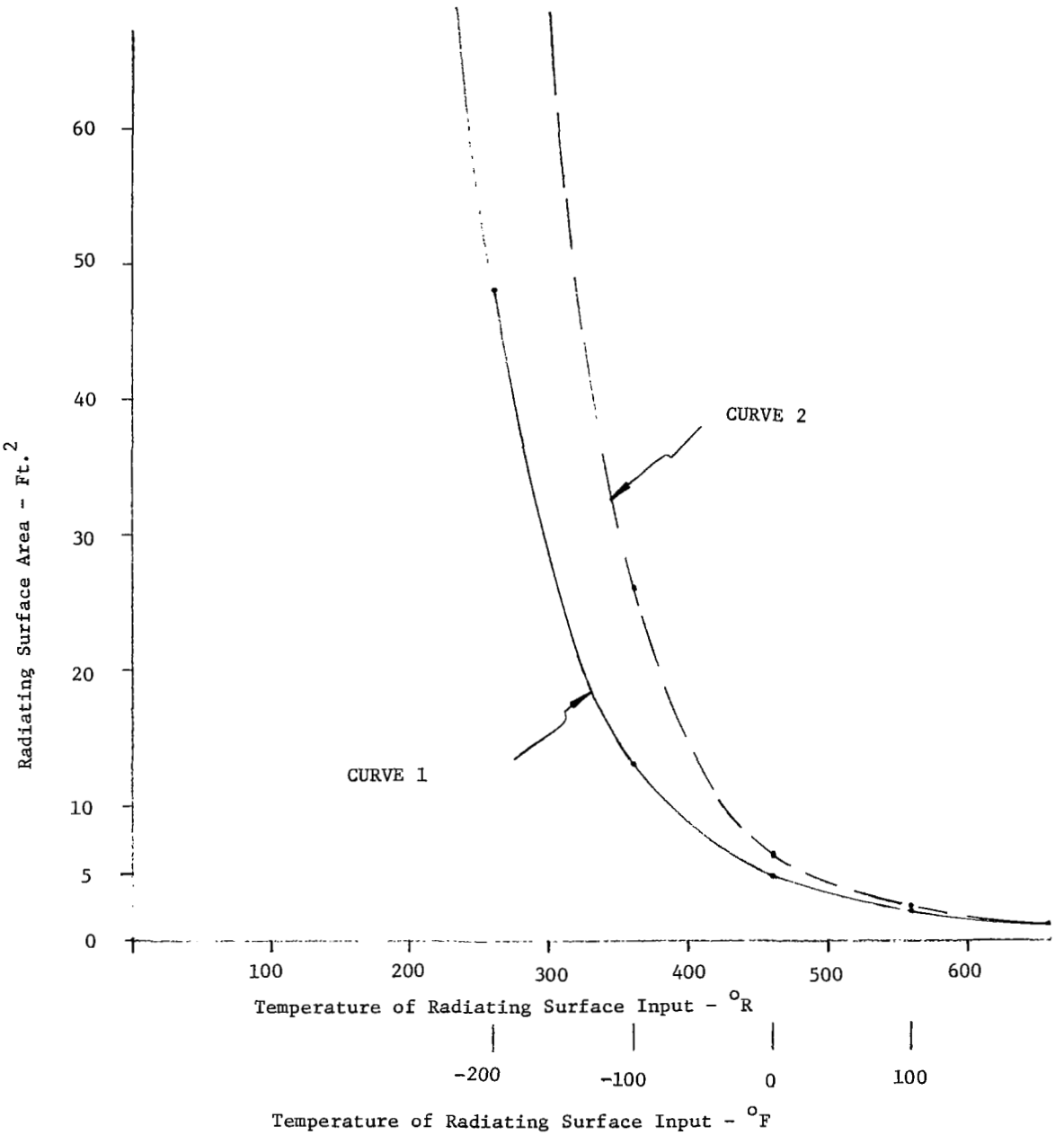

Figure 6-8 Radiating Surface Area Required to Dissipate 100 Watts as a Function of Temperature. Curve 1 - 100 Watts Dissipation - Minimum Required Surface Area Needed Assuming All Of Radiative Surface is at Base Temperature. Curve 2 - 100 Watts Dissipation - Anticipated Actual Required Area. Less Than 100% Fin Efficiency Due to Conduction Losses From Input to Outer Fin Surfaces.

Section 7

MODE LOCKING OF THE SPACE QUALIFIED ND:YAG LASER

As pointed out before, the space qualified Nd:YAG laser will be a low gain device. The requirement for getting efficient operation is to have minimum optical loss in the laser cavity. Typical techniques for mode locking Nd:YAG lasers utilize intracavity modulators which introduce as much as two or three percent single pass loss. In Figs. 3-13 and 4-9 we showed the bad effect of loss on laser efficiency. In particular, modulators that utilize electro-optic crystals like $LiNbO_3$ are bad. These modulators may show less than one percent loss external to the laser, but typically show more than two percent loss intracavity with laser power circulating through them.

Therefore, different low loss techniques must be utilized for mode locking the space qualified Nd:YAG laser. We will consider three candidates below.

1) Laser Optical Length Variation - Targ and Massey[46], and, independently, Henneberger and Schulte[47] have succeeded in mode-locking HeNe lasers by vibrating one of the end mirrors at the mode-separation frequency, $\nu = c/2L$. The physical explanation involves light being Doppler shifted out of the bandpass of the laser oscillator (the region with gain) unless it strikes the mirror at the zero velocity position.[47,48] Therefore the photons are bunched, and mode locked pulses result.

Smith[49] succeeded in mode-locking a HeNe laser by slow (∿10 cm) translation of one end mirror, but this phenomenon seems basically a result of the HeNe laser's tendency to self-lock.

With particular reference to the Nd:YAG laser, it seems both of these schemes are inappropriate: the mirror translation scheme is inapplicable since the YAG laser has little tendency to self-lock; the vibrating mirror fails because the mode-separation is typically from 400 MHz to 900 MHz and the mirror excursion required is far larger than the 1.4Å obtained by Hennenberger and Schulte[47] at 59.4 MHz. According to McDuff and Pardue[48], a peak excursion of 170Å would be needed at 1.06μ for reliable mode locking. Since mirrors cannot be moved that far that fast, the vibrating mirror scheme is inapplicable.

2) Internal Loss Modulation - High quality fused quartz is available and it can be polished with extremely high quality optical surfaces. Quartz resonant acousto-optic loss modulators can be constructed with very low loss, typically as low as 0.2 percent single pass. The first mode locking was achieved with such a modulator in a HeNe laser[50], and Nd:YAG was first mode-locked with such a modulator[4].

Fig. 7-1 shows an acousto-optic loss mode locked Nd:YAG laser. The loss modulator is oriented at Brewster's angle to produce loss for the polarization perpendicular to that of the laser and to achieve low loss for the laser polarization at the modulator surfaces. The modulator is resonant at 1/2 (c/2L) frequency and must be well temperature controlled because of the temperature sensitivity of the acoustic resonance. The laser

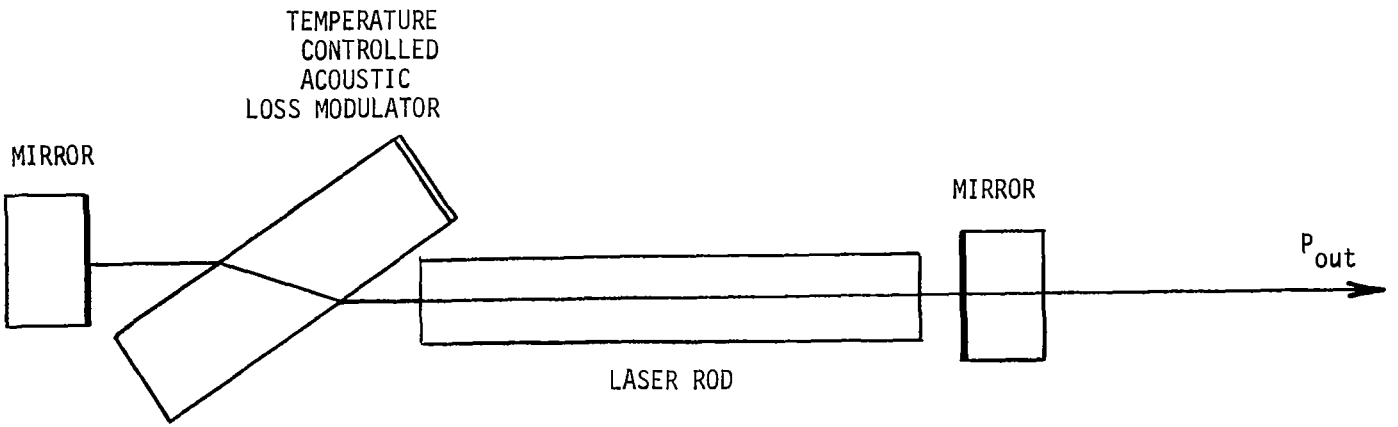

Figure 7-1. Acoustic Loss Modelocking

is mode locked at c/2L frequency since twice per cycle the modulator shows zero birefringence in the optical cavity. Optical pulses can get through these gates in time without suffering loss due to birefringent shift to the polarization with loss at the Brewster's angle surfaces.

Temperature control of the modulator significantly complicates design of a space qualified mode locked laser. For this reason we do not recommend this as the best choice but prefer the scheme discussed next.

3) Injection Locking - Injection locking consists of injecting a signal from one oscillator into another, with the result that the second oscillator locks on to the injected signal. It was first proposed by Adler[51] and theoretically applied to lasers by Tang and Statz[52] and Siegman[53]. Experimentally, Stover and Stein[54] completely verified the theory for single frequency oscillators.

With regard to multi-frequency oscillators, such as Nd:YAG laser having many longitudinal modes, the work of Foster, Ewy and Crumly[55] is particularly important. They succeeded in mode-locking the HeNe laser by re-injecting its own light after frequency shifting it by c/2L in an external cavity. Fig. 7-2 shows their set-up for Nd:YAG.

The Bragg acoustic modulator is driven at 1/2 (c/2L) frequency. A portion of the light incident upon the modulator is diffracted by the travelling acoustic wave and shifted in frequency by 1/2 (c/2L). A mirror sends this light back through the modulator where a portion is again

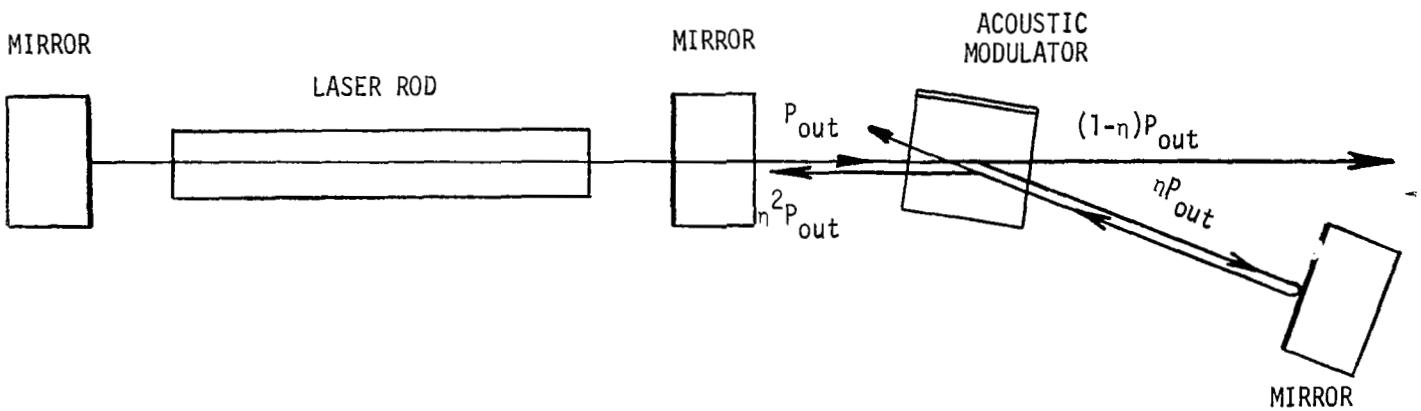

Figure 7-2 Injection Modelocking

diffracted and shifted in frequency. The light has now been shifted by c/2L and each laser mode has shifted to that of its nearest neighbor. Some of this light is transmitted through the mirror back into the laser. The result is phase locking of the optical modes and a mode locked output pulse train. The output from the injection locked laser is the light transmitted by the acoustic modulator cell.

We will analyze this technique in some detail in order to understand its application to the space qualified Nd:YAG laser.

Assume an injected field E_2 enters the laser cavity through a transmitting mirror as shown in Fig. 7-3. We assume that the original field cavity is E_1:

$$\text{Main Cavity Wave} \begin{cases} (E_1)\ \text{inc} = E_1 e^{j(\phi_1+\alpha_1)} \\ (E_1)\ \text{ref} = E_1 r e^{j(\phi_1+\beta_1)} \end{cases}$$

$$\text{Injected Signal} \begin{cases} (E_2)\ \text{inc} = E_2 e^{j(\phi_2+\alpha_2)} \\ (E_2)\ \text{trans} = E_2 \tau e^{j(\phi_2+\beta_2)} \end{cases}$$

where T = the power transmission

$= (1-R) = \tau^2$

R = the mirror power reflection coefficient

τ = the field transmission coefficient

r = the field reflection coefficient

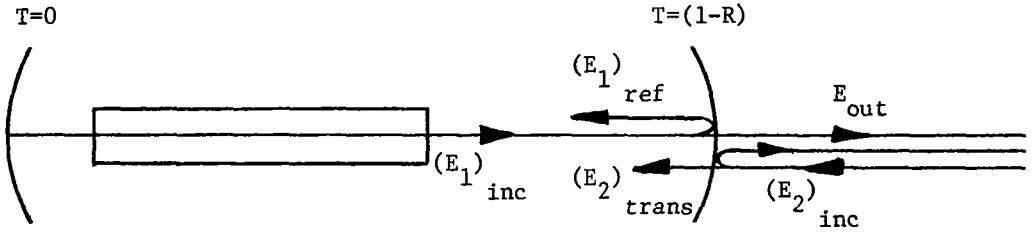

Figure 7-3. Injection Locking

α, β fixed phase shifts

ϕ varies with time as $2\pi\nu t$ approximately

The total field leaving the mirror is:

$$E_t = (E_1)\ \text{ref} + (E_2)\ \text{trans}$$

$$= E_1 r e^{j(\theta_1+\beta_1)} + E_2 \tau e^{j(\theta_2+\beta_2)}$$

or

$$\frac{E_t}{(E_1)\text{ref}} = 1 + \frac{E_2\tau}{E_1 r}\, e^{j(\theta_2-\theta_1+\beta_2-\beta_1)}$$

$$= 1 + \frac{E_2\tau}{E_1 r}\cos(\theta_1-\theta_2+\beta_1-\beta_2)$$

$$- j\,\frac{E_2\tau}{E_1 r}\sin(\theta_1-\theta_2+\beta_1-\beta_2)$$

Thus we have an in-phase amplitude change caused by the cosine term and a quadrature-phase phase shift from the sine term. The laser gain is saturated in the steady state; thus gain will change to make the wave amplitude stable near its original value. We neglect the phase shift $\Delta f_G = \left(\frac{\partial\theta}{\partial G}\right)_{\text{lasers}} \times \Delta G$ from this gain change ΔG, assuming that the mode is near line center and that the line is nearly symmetrical. Thus, the effect of

the injected signal is to produce a single-pass phase shift of the amount

$$\Delta\phi_1 \approx \frac{E_2\tau}{E_1 r} \sin(\theta_1-\theta_2 + \beta_2-\beta_1)$$

Now in the quasistatic approximation the frequency $\frac{1}{2\pi}\frac{d\theta_1}{dt}$ changes with round trip cavity phase shift by the factor $\frac{1}{2\pi}\frac{\partial\omega_1}{\partial t}$; hence

$$\frac{d\theta_1}{dt} = \frac{\partial\omega_1}{\partial\phi} d\phi_1 + 2\pi\nu_{10}$$

where ν_{10} is the unperturbed resonance frequency of the mode and

$$\frac{\partial\omega_1}{\partial\phi} = -\frac{c}{2L} \qquad \begin{cases} L = \text{cavity length} \\ c = \text{velocity of light} \end{cases}$$

Thus

$$\frac{d\theta_1}{dt} = \left(\frac{c}{2L}\right)\left(\frac{E_2\tau}{E_1 r}\right) \sin(\theta_1-\theta_2 + \beta_1-\beta_2)$$

$$+ 2\pi\nu_{10}$$

Let $\theta_b = \theta_1-\theta_2 =$ beat phase

$$\frac{d\theta_b}{dt} = \frac{d\theta_1}{dt} - \frac{d\theta_2}{dt} = \frac{d\theta_1}{dt} - 2\pi\nu_2$$

Therefore,

$$\frac{d\theta_b}{dt} = \left(\frac{c}{2L}\right)\left(\frac{E_2\tau}{E_1 r}\right) \sin(\theta_b + \beta_1-\beta_2) + 2\,(\nu_{10}-\nu_2)$$

Let $2\pi(\nu_{10}-\nu_2) = \omega_d$, the detuning angular frequency,

or $\nu_{10}-\nu_2 = \nu_d$

Therefore,

$$\frac{d\theta_b}{dt} = \left(\frac{c}{2L}\right)\left(\frac{E_2\tau}{E_1 r}\right) \sin(\theta_b + \beta_1-\beta_2) + \omega_d \qquad (7\text{-}1)$$

This is Adler's[51] differential equation for phase-coupled oscillators.

There is a phase-locked solution for

$$\frac{d\theta_b}{dt} = 0$$

when

$$\omega_d < \left(\frac{c}{2L}\right)\left(\frac{E_2\tau}{E_1 r}\right)$$

Thus, the restriction on locking is

$$\left(\frac{E_2}{E_1}\right) > \left(\frac{r}{\tau}\right)\frac{\omega_d}{(c/2L)}$$

or

$$\frac{P_2}{P_1} > \frac{R\ 4\pi^2\ f_d^{\,2}}{T\ (c/2L)^2} \qquad (7\text{-}2)$$

Consider the injection locking arrangement in Figure 7-2. In terms of our analysis,

$$P_{out} = T P_1$$

$$\eta^2 P_{out} = P_2$$

where η = the acoustic modulator power diffraction coefficient.

Substituting into equation (7-2)

$$\eta^2 > \frac{R}{T^2} \frac{4\pi^2 f_d^2}{(c/2L)^2}$$

$$\eta > \frac{2\pi\sqrt{R}}{T} \frac{f_d}{(c/2L)} \qquad (7\text{-}3)$$

Now f_d, the detuning frequency, refers to the amount by which twice the acoustic modulator frequency misses the spacing between adjacent longitudinal modes in the laser. Various frequency pulling effects cause the spacing between various near neighbor modes to be different, depending upon their location under the laser fluorescence line. The half width of the c/2L beat frequency from the free running Nd:YAG laser gives some indication of the value of f_d we should use. Typically, the half width is 300 kHz. Actually, the widest part of the beat note may be caused by a small number of outside modes and the average, f_d, may be much less than this. We estimate it may be as small as 50 kHz.

We have considered a one watt Nd:YAG laser with a 5% single pass unsaturated gain with optimum output coupling T = 2.2 percent. The acoustic diffraction coefficient η required for injection mode locking has been plotted in Figure 7-4 for various choices of f_d as a function of mode locking frequency c/2L. It should be noted that the higher the frequency, the easier it is to injection mode lock. Typically, Nd:YAG lasers are built with cavity lengths of about 12 inches and have c/2L frequencies near 500 MHz. From the Figure, we estimate that only 2% to 20% of the output laser power needs to be diffracted to injection lock the Nd:YAG laser. At higher frequencies, even smaller acoustic diffraction is required. At low frequencies or long cavity length lasers, a large amount of the laser output must be diffracted. At 100 MHz from 16% to 100% is required.

We should also mention that the low gain of the Nd:YAG laser necessitates that lasers with low c/2L frequencies cannot be folded using delay line techniques. Multiple reflections over a short path during each light round trip in the laser greatly increase the single pass laser loss and as we have shown, the space qualified Nd:YAG laser will not tolerate loss.

We conclude, then, that injection locking can be used to mode lock the space qualified Nd:YAG laser. High modulation frequencies in the 300 MHz to GHz range must be employed, however. The space qualified Nd:YAG laser should therefore be considered primarily for wide bandwidth systems.

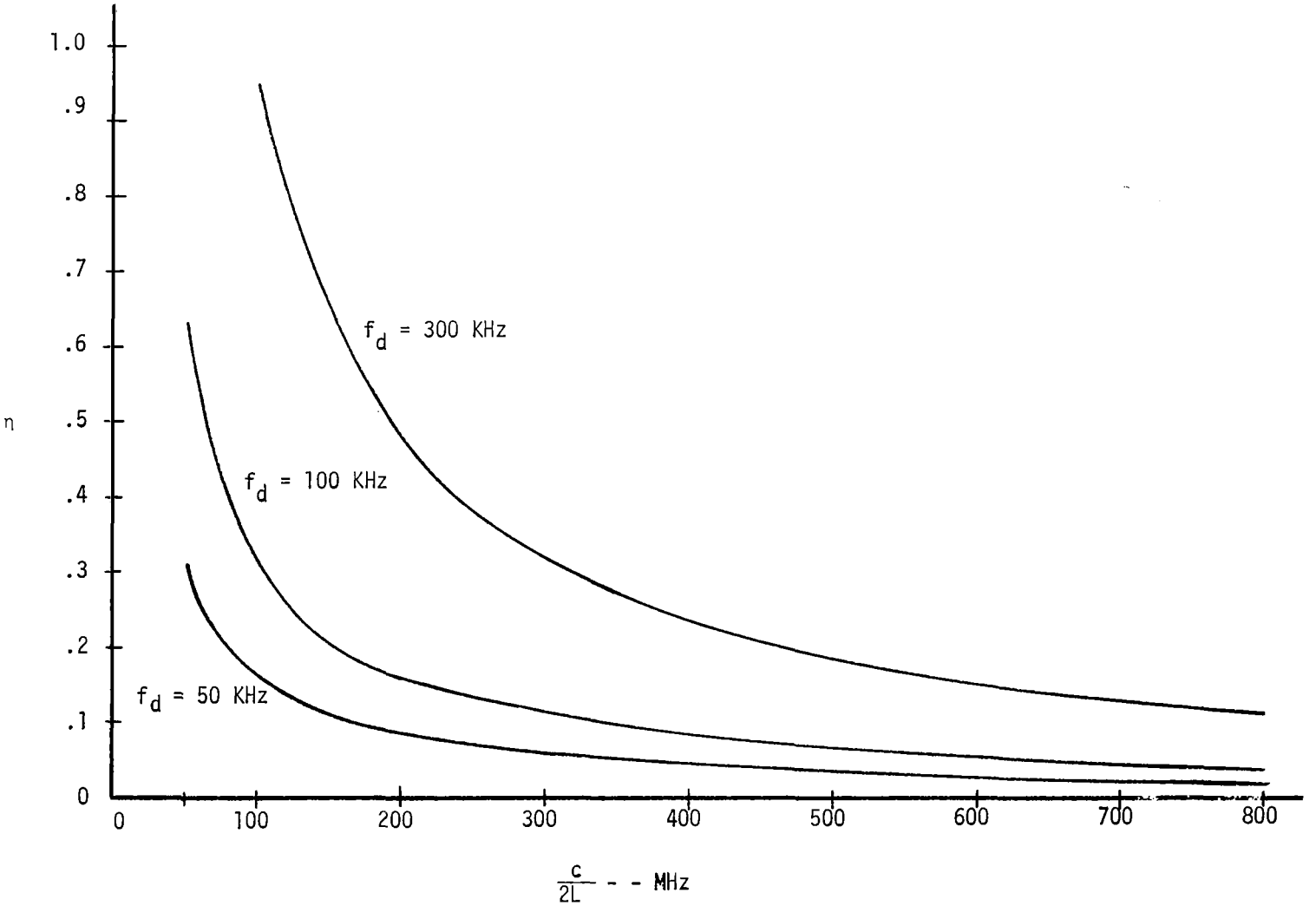

FIGURE 7-4. EFFECT OF MODELOCKING FREQUENCY AND DETUNING ON INJECTION MODELOCKING

SECTION 8

PRELIMINARY DESIGN OF THE SPACE QUALIFIED Nd:YAG LASER

The design study that has been presented in the preceding sections provides us with an understanding of the basic principles involved in designing a space qualified Nd:YAG laser. Utilizing the results of the design study, we can make a prototype design for the space qualified Nd:YAG laser.

We have shown that operation at 77°K is not feasible. We must, therefore, conclude that the present "state-of-the-art" in incoherent semiconductor diode pumped Nd:YAG is not sufficiently developed for consideration as a pump source in a prototype. We choose, then, the potassium arc lamp as the pump source for our prototype design. We do recognize the potential of room temperature diode pump sources. Proper research and development effort should result in diode pump sources within a few years. We, therefore, require that the technology of our lamp pumped space qualified laser design be applicable to future diode pump requirements, also. The rod cooling technology, compatibility with sun pumping, etc., will work with diode pumping as well as with lamp pumping.

In this section we will present our prototype design of a potassium arc pumped space qualified Nd:YAG laser. This design is only on paper. It has been beyond the scope of this program to do the development work on the design, to build it, and to check it to environmental specifications. The original plan was for these steps to be accomplished during the next phase of the program. The closing of the NASA Electronics Research Center has

greatly clouded the future of the program, however. We do report at the end of this section on some preliminary experiments which were performed with a breadboard conductively-cooled laser design. This design has many of the characteristics of the prototype design without some of the technologically-difficult vacuum seals, etc.

8.1 Laser Design

8.1.1 Design Requirements

Based upon the design study we have reported previously, we compiled the following list of design requirements on which to base our preliminary space qualified Nd:YAG laser design.

1. Vacuum insulate the Potassium Arc
2. Small Weight and Size
3. Conductive Cooling to Heat Pipes and on to Radiation Coolers
4. Laser Rod at ~20°C
5. Lamp Waste Heat Removal from High Temperature Source (~350°C)
6. Operable in Earth Environment for Ground Check-out
7. Compatible with Sun Pumping
8. Ultimately Compatible with Diode Pumping
9. Space for Intracavity Elements in the Laser.

In addition to this list, we, of course, considered the NASA design goals outlined in Section 1.

8.1.2 Pump Cavity Design

The potassium lamp has the characteristic that its luminous arc diameter is only ~1/3 of the inside bore diameter. This characteristic, coupled with conductive cooling which requires the laser rod to be bonded to a heat sink, makes pump cavity design very difficult. Liberman, et al.[7] used a large 10-inch diameter spherical pump cavity and water cooling in their experiment which is the most efficient low power laser that has been reported. The spherical cavity is large and heavy, qualities that are unattractive for the space qualified laser. Conductive cooling also disrupts the pumping arrangement of the spherical cavity, reducing its efficiency.

An exfocal elliptical cylinder pump cavity[57] with the rod mounted on a heat sink at the end of the ellipse is a possibility. The small luminous arc of the potassium lamp must be mounted at the opposite end of the ellipse, however. The elliptical cylinder and the lamp jacket intersect unless a cylinder is removed at the ellipse end to accommodate the lamp. Such a cylinder traps much of the light and reduces the efficiency of the exfocal ellipse.

After considering the above and other possibilities, we chose the simple close-coupling plus a condensing wedge approach shown in the layout drawing of Figure 8-1. Ray trajectories in this cavity leave the small luminous arc and after a few reflections end up in the laser rod. The ratio of laser rod to pump cavity volume has been kept as high as possible to maximize the probability of reaching the rod.

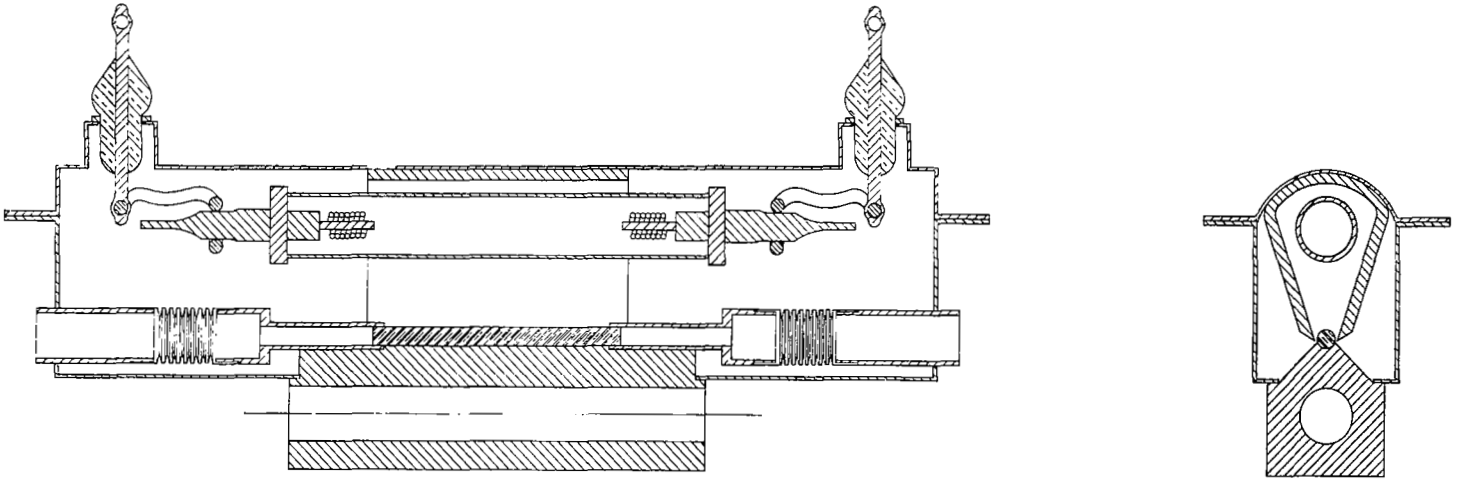

Figure 8-1 Space Qualified Nd:YAG Laser Layout Drawing

8.1.3 Prototype Lamp Pumped Laser Design

Figure 8-1 also shows other fundamental features of the final design. A vacuum is maintained in the pump cavity. The ends of the laser rods are outside the vacuum with the vacuum seal at the rod ends. The rod mounts onto a niobium heat sink. The niobium in turn is brazed to a thin walled stainless steel vacuum jacket which supports the pump cavity and the lamp. The pump cavity reflectors are maintained at a high temperature (~350°C). The thin walled stainless steel is designed to minimize heat flow (12 watts) from this high temperature source into the niobium heat sink. Heat from the high temperature pump cavity reflectors is transferred through the thin walled stainless steel wall to a heat conducting block at the top (not shown). Heat from the niobium laser rod mounting block is conducted to a cylindrical heat pipe (not shown). Differential thermal expansion between the Nd:YAG laser rod and the stainless steel envelope is accommodated by bellows at each end of the rod seals. A future diode pumped laser would dispense with the vacuum jacket and would use a smaller pump cavity. The rod cooling arrangement is identical to what would be used for diode pumping.

Based upon this layout design, a complete set of design drawings were prepared for the prototype lamp pumped space qualified Nd:YAG laser. The assembly drawing for the laser is shown in Figure 8-2, and the drawing of the pump cavity assembly is shown in Figure 8-3. To insure compatibility with sun pumping, the pump cavity was designed with a cone condenser for end sun pumping attached. This arrangement is similar to that being developed on Air Force Contract F33615-70-C-1255 for Sun Pumping Nd:YAG.

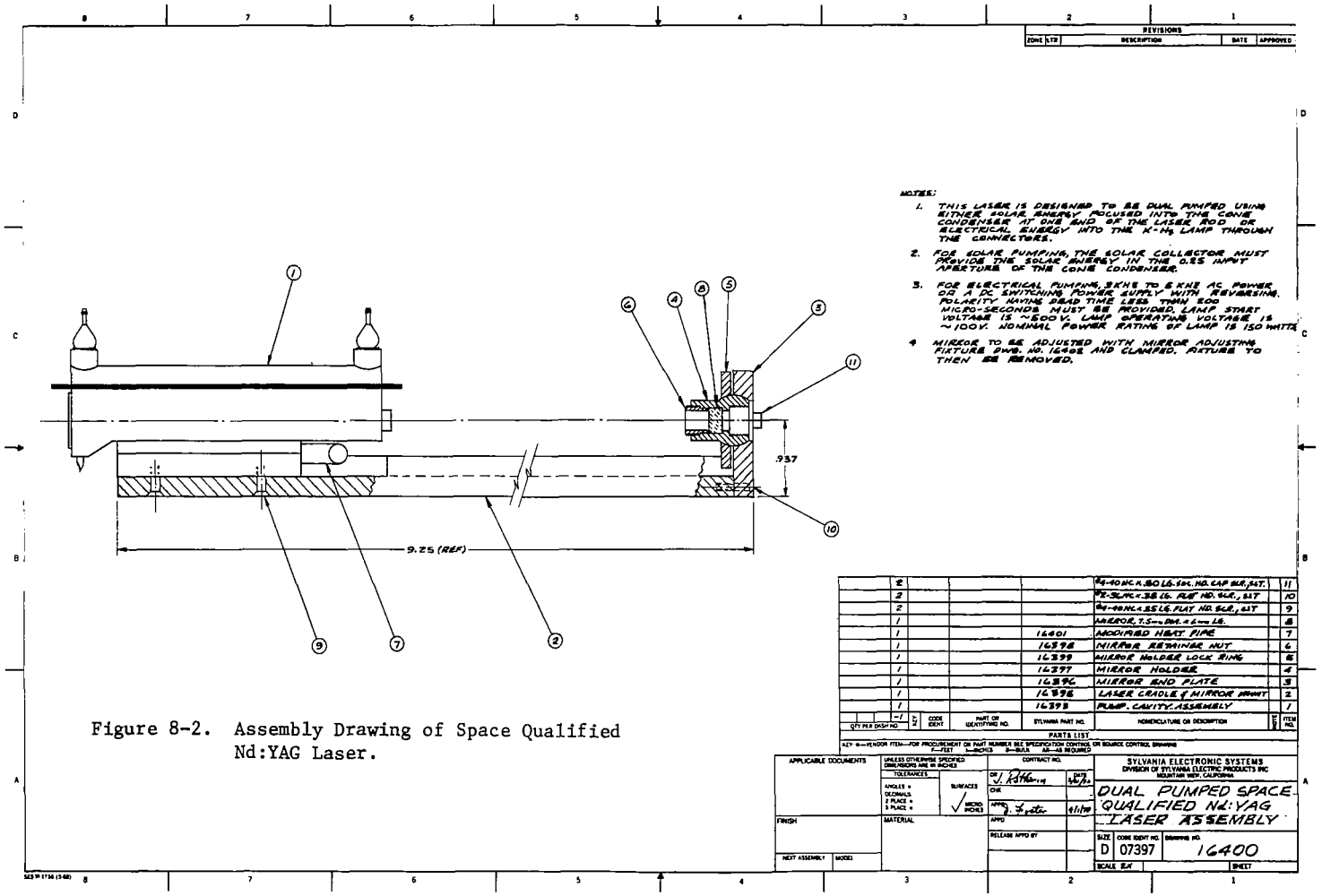

Figure 8-2. Assembly Drawing of Space Qualified Nd:YAG Laser.

Figure 8-3. Pump Cavity Assembly Drawing of Space Qualified Nd:YAG Laser.

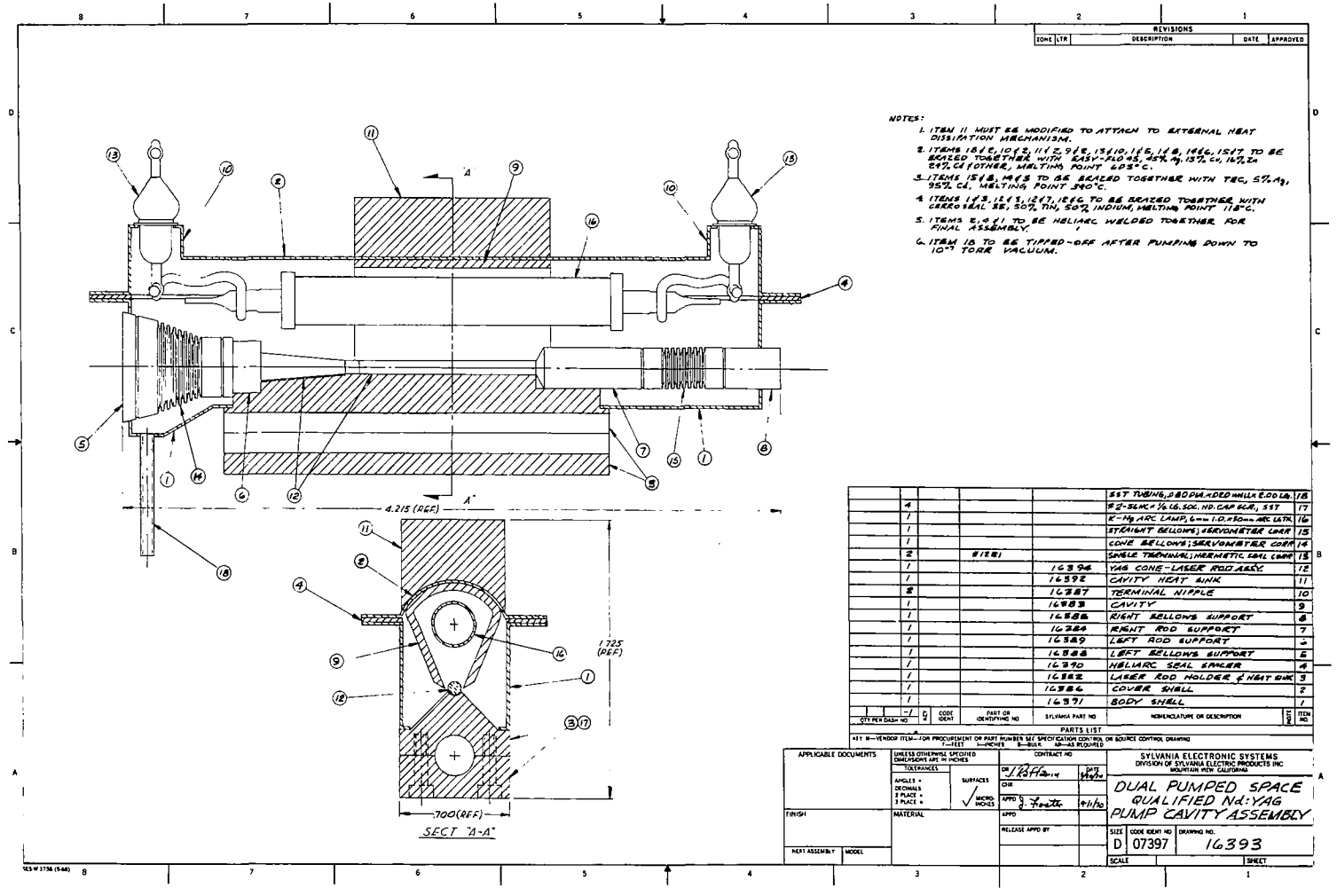

One of the laser mirrors is attached to the end of the cone. For a non-dual pumped laser, the design becomes symmetrical and both ends of the pump cavity and the laser optical cavity are made identical.

This laser has been designed with a 2 mm diameter Nd:YAG rod 30 mm long. The single pass unsaturated laser gain has been chosen at 5% to insure reliability. The design has a potassium-mercury arc lamp with a rated power of 150 watts. Recent success at ILC Corporation with pure potassium which operates with a DC supply changes this lamp choice. The P_o for the lamps will be 23 watts as shown in Figure 3-8.

The theoretical operating characteristics of this laser as a function of dissipative loss, α_o, were shown in Figure 3-13. Without any intracavity devices, the expected dissipative loss is 0.006. The expected laser performance is then ~1 watt at ~0.7 percent efficiency.

The mirrors for the laser are chosen with the long radius cavity configuration. The cavity length of ~25 cm and a limiting aperture of 1.5 mm result in a Fresnel number of ~2 which allows good discrimination for TEM_{oo} mode operation.[58] Operation of the laser in the conductively cooled cartesian temperature gradient arrangement should simplify thermal focusing problems[3] and allow reliable TEM_{oo} mode operation. The linear temperature gradient will produce a prism effect in the laser rod, however.

The laser will, therefore, need to be always operated at the same output power level for fixed mirror adjustments. Electronic mirror adjustments can be provided if variation in laser output power is desired. We have chosen fixed power level operation with locked down mechanical mirror adjustments. The power supply has been chosen to have stepwise variable input powers to the potassium arc lamp. This allows fine adjustment of the laser to the desired operating output power level.

8.1.4 Power Supply Design

Development of the pure potassium arc lamp by ILC has greatly simplified the power supply requirements. A simple current controlled DC supply with some remote control features is all that is required. A block diagram of the supply and its interface with the spacecraft and the laser is shown in Figure 8-4. Telemetry information of power supply current and voltage and laser output power are supplied. Command functions are on-off, current step increase and current step decrease.

The power supply design itself is essentially identical to that of the space qualified CO_2 laser.[59] Instead of a laser tube, the supply is for an arc lamp. It must perform the same functions, except at a lower voltage. The functions required of the power supply are:

1. Automatic starting of the lamp
2. Current regulation
3. Current level set
4. Telemetry outputs for current and voltage.

Table 8-1 lists the power supply specifications required to drive the potassium lamp. The power supply described in the rest of this section uses variable frequency control and variable pulse width with flyback voltage conversion to obtain regulated output and high efficiency over a wide range of output power.

The input-to-output power-conversion efficiency of conventional inverters is typically 70 to 80 percent at full output power, but drops off at less than full output power due to fixed losses in the drive and control circuits. The power supply described here uses less than one percent of its output power in the unloaded condition. The overall efficiency is greater than 80 percent over a wide range of output power.

Table 8-1.

Power Supply Specifications for
Space Qualified Nd:YAG Laser

1.	Input Voltage	28 VDC ± 4 V
2.	Output Voltage Maximum Operating	500V ~50V
3.	Output Current	~3 amps
4.	Current Regulation	±5%
5.	Current Adjust	Step adjustment from 2 amps to 4 amps in 0.2 amp steps
6.	Ripple	Less than .01% rms
7.	Telemetry Output (voltage and current)	0-5 VDC
8.	Starting	Overvoltage capability to be provided until lamp draws current.

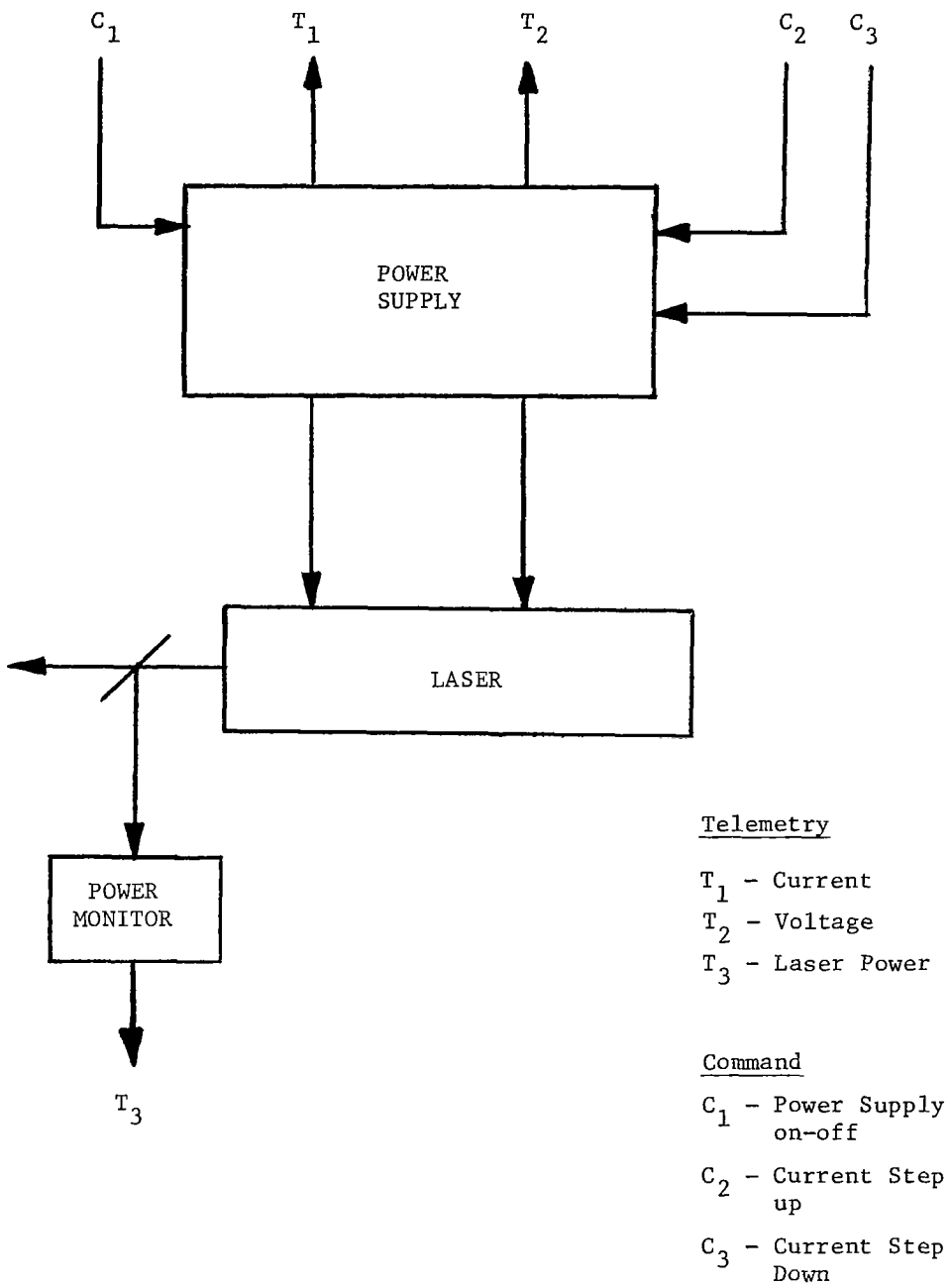

Figure 8-4. Block Diagram Space Qualified Nd:YAG Laser Power Supply and Space Craft Interface.

Circuit Description

Figure 8-5 shows a block diagram of the power supply, and Figure 8-6 shows a simplified circuit for the control circuitry of the power supply. A sample of the output voltage (or current) is applied to the reference amplifier input. This sample is compared to a constant reference voltage from a Zener diode. The difference output from the reference amplifier is used to control the frequency of the voltage controlled oscillator. For example, if the output voltage from the reference amplifier is high, the frequency of the oscillator is lowered. The output of the oscillator is used to trigger a one-shot multivibrator which provides a constant output pulse width and voltage level. Variations in the input voltage are used to vary the pulse width of the one shot. With a constant output voltage, an increase in the supply voltage causes a decrease in pulse width. Therefore, under constant load conditions, the energy in the output pulse is constant.

The output pulse is used to drive the input to the voltage converter, Figure 8-7. The sharply rising V_{be} pulse saturates Q_1, bringing the collector voltage to nearly ground potential as shown in Figure 8-7c. While the collector is near ground, the unregulated input voltage appears across the primary of the output transformer.

At the end of the V_{be} pulse, Q_1 begins to turn off, causing the polarity of the transformer primary to reverse. This flyback effect increases the collector voltage to a value greater than the input supply voltage as shown in Figure 8-7. The energy stored in the field of the

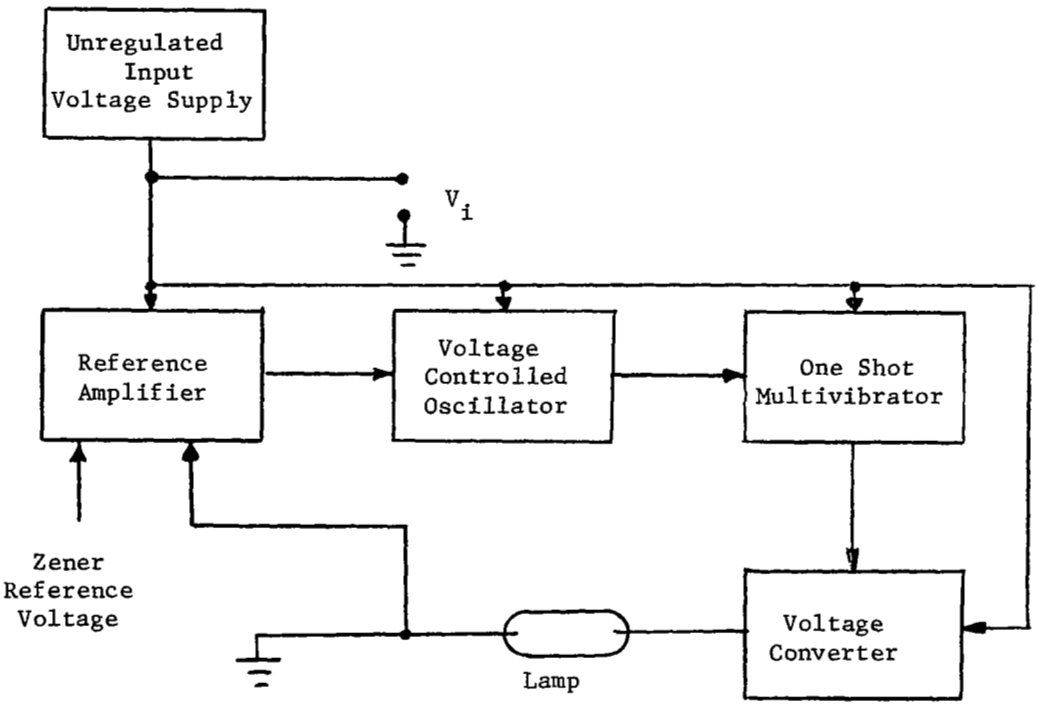

Figure 8-5. Power Supply System Block Diagram.

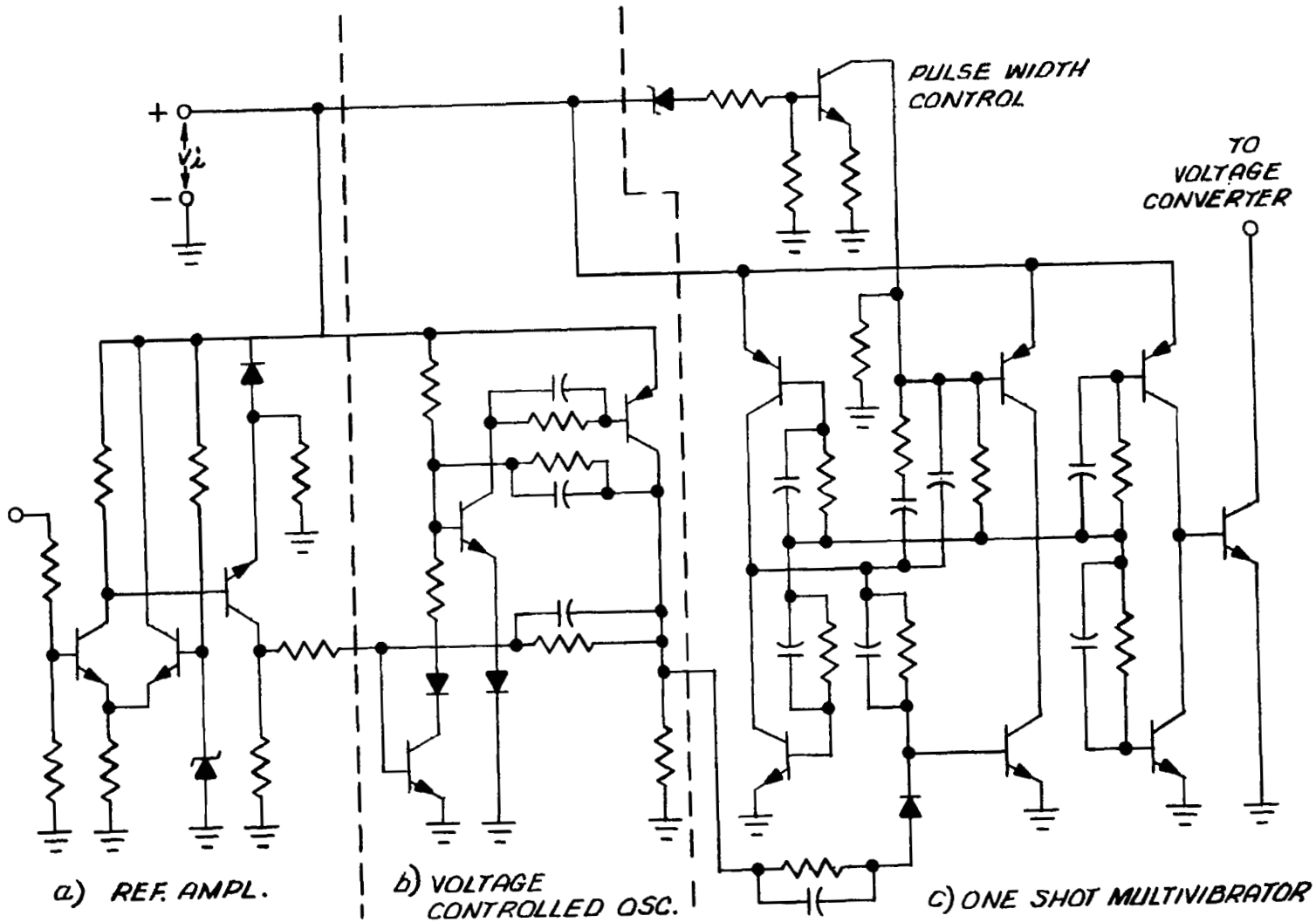

Figure 8-6. Typical Simplified Circuit

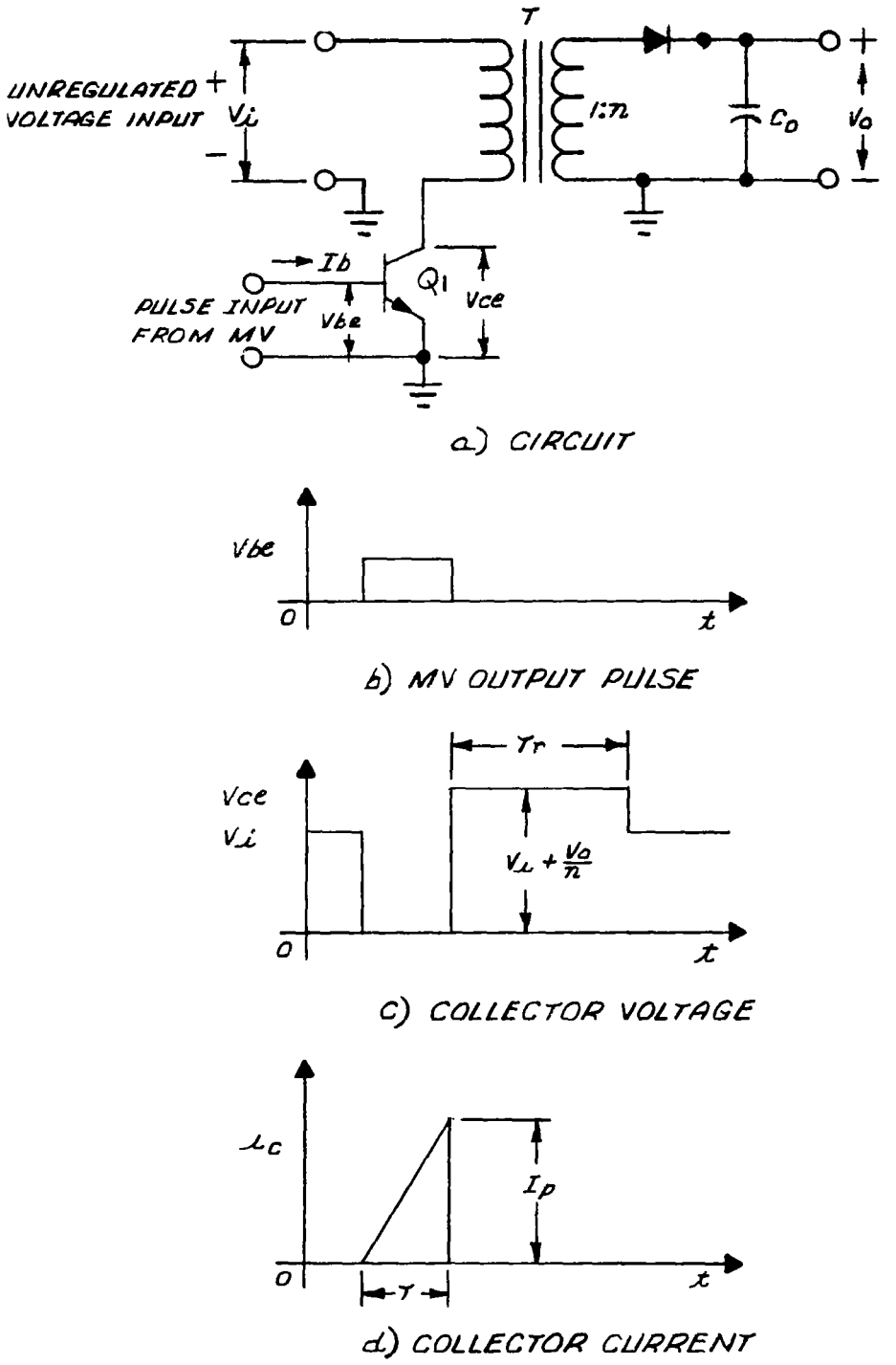

Figure 8-7. Voltage Converter and Waveforms.

transformer is transferred to the output capacitor, C_o, because a decreasing current in the primary induces a voltage in the secondary in the correct direction for current to flow through the diode. This flyback technique, that is opening an inductive circuit to obtain an energy transfer, provides a lossless energy transfer if all components are ideal, and low-loss transfer even with non-ideal components. This same technique has been used at Sylvania in switching regulators with very good efficiency.

Starting Circuit

Whenever power is applied, the power supply will supply 500V pulses until the lamp fires. When the laser fires, the supply will regulate at the programmed current level at approximately 50 volts.

Command Circuit

Ten current levels may be programmed externally. Magnetic latching relays and diode "OR" gates provide a memory for the last command. A +28 volt pulse, 10 milliseconds long, is required to set the relays for the proper command. The diode "OR" gate will only accept one command at a time. In the event that two commands are given at the same time, the relays will oscillate for the duration of the command with the final resting state indeterminate.

Monitor Outputs

Two monitor outputs are provided, an output voltage and output current monitor with the following characteristics:

Output Level = 0 V to +5 VDC

Output Impedance = 10K Minimum.

Packaging

Extensive use of thick film techniques will allow most of the discrete components to be replaced by a 1" x 2" thick film circuit. The power transformer, power transistor, relays and filter capacitors will be mounted to the chassis. The following specifications apply to the power supply:

Estimated Size = 2" x 2" x 9", 36 $in.^3$

Estimated Weight = 2.1 lbs.

Estimated Efficiency = 80 percent

Voltage Output = 25 V to 500 VDC

Current Output = 2A to 4A

Ripple $\leq$.01 percent rms.

The overall package will be RFI tight, with filtering on all leads entering or leaving the package. Two such packages are required for the laser tube, making the total estimated power supply weight 4.2 lbs.

8.2 Laser Conductive Cooling Experiments

The pump cavity configuration and the conductive cooling technique used in the prototype space qualified Nd:YAG laser are quite different from conventional practice. Some experiments were, therefore, designed to test these parts of the design.

Figure 8-8 shows the first experimental conductively cooled Nd:YAG laser contrasted with a commercial Sylvania Model 610 Nd:YAG laser. This laser was constructed early in the program. It utilized a copper heat sink

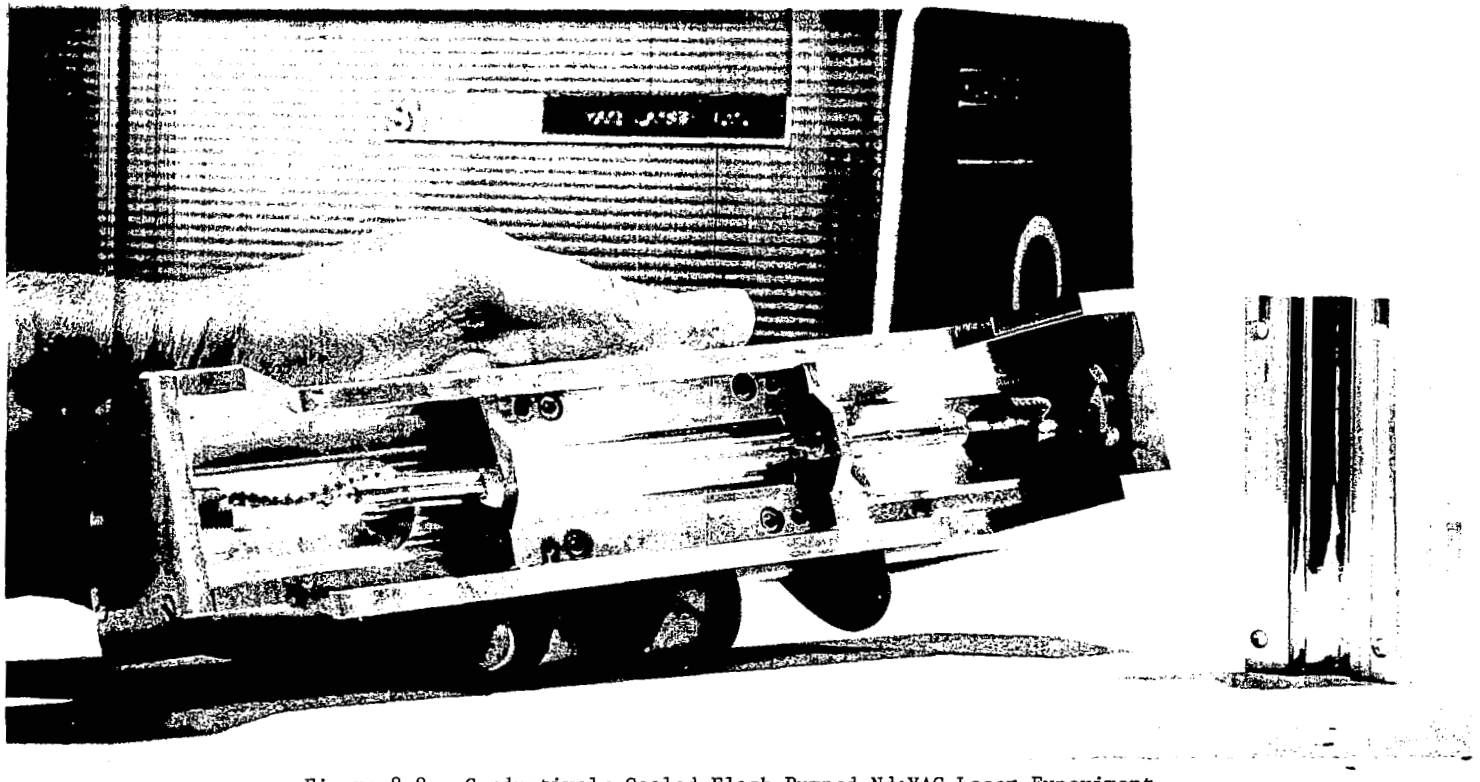

Figure 8-8. Conductively Cooled Flash Pumped Nd:YAG Laser Experiment.

onto which a 3 mm x 50 mm Nd:YAG laser rod was bonded with silver loaded epoxy. A krypton arc flash lamp was used to pump the rod. The laser was operated in a flash pumped mode at 10 Hz 1.5 msec long pulses with an average input power of 105 watts. The average output power from the laser was 0.450 watts. The laser rod temperature was around 120°F with the conductively cooled laser operating stably. Heat pipes were not employed in this experiment. Air convection at the outside of the laser structure was used as the ultimate heat sink. The differential thermal expansion between YAG and copper badly strained the laser rod in this experiment. Experiments were conducted to determine the effect of temperature on the threshold of the laser. Little effect was found up to temperatures of 70°C and the threshold was only up by 20% at 100°C. This does not at all agree with the threshold data presented in Figure 4-1. We attribute this inconsistency to a relaxation of the stress as the rod and copper base are heated, but further experiments should be conducted to further check this important temperature effect.

After design of the engineering prototype described in Section 8.1, it was decided that an experiment should be conducted to test some of the more important features of this design. An experimental laser that tested the conductive cooling and the pump cavity configuration of the prototype design without the complicated vacuum jacket was designed. The layout drawing of this laser is shown in Figure 8-9. The laser utilizes a water cooled Kr arc as a pump lamp in the pump cavity configuration of the prototype. Photographs of the experimental laser are shown in Figures 8-10 through 8-14.

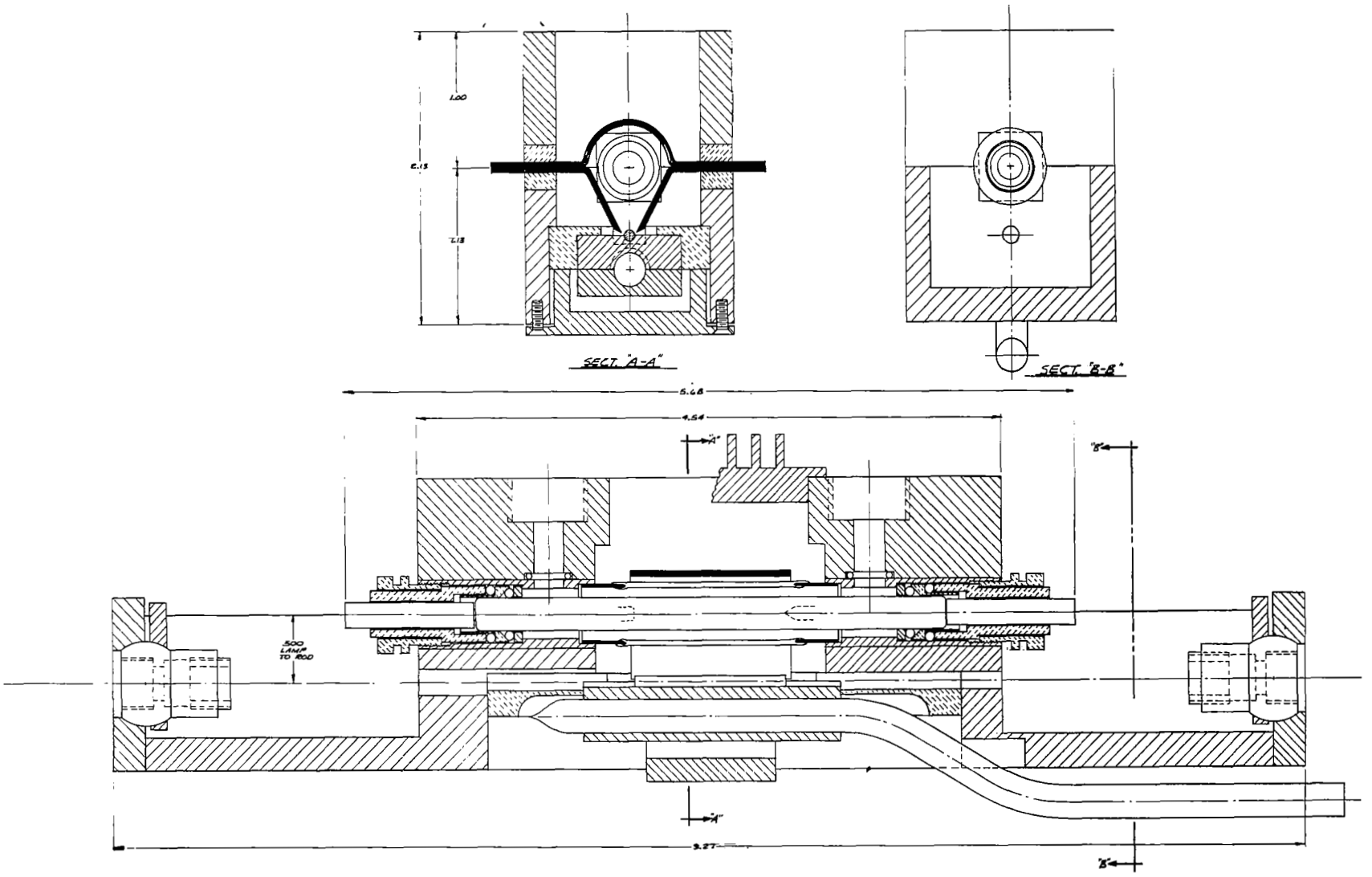

Figure 8-9 Assembly Drawing of Krypton Arc Pumped Conductively Cooled Nd:YAG Laser.

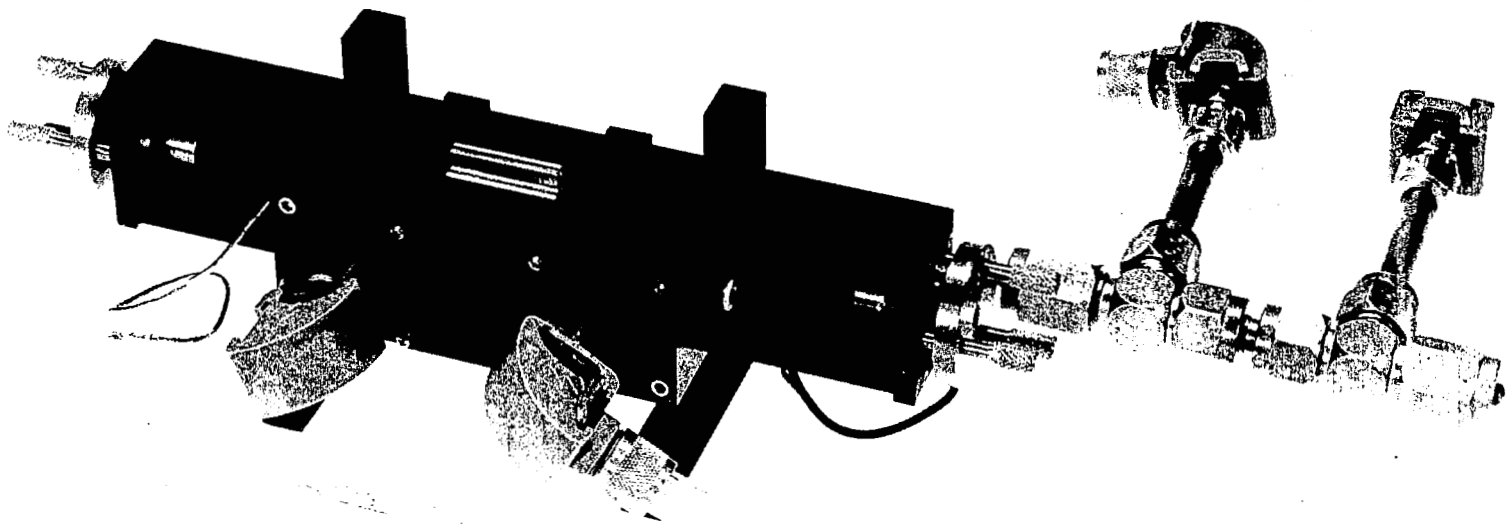

Figure 8-10 Krypton Arc Pumped Conductively Cooled Nd:YAG Laser.

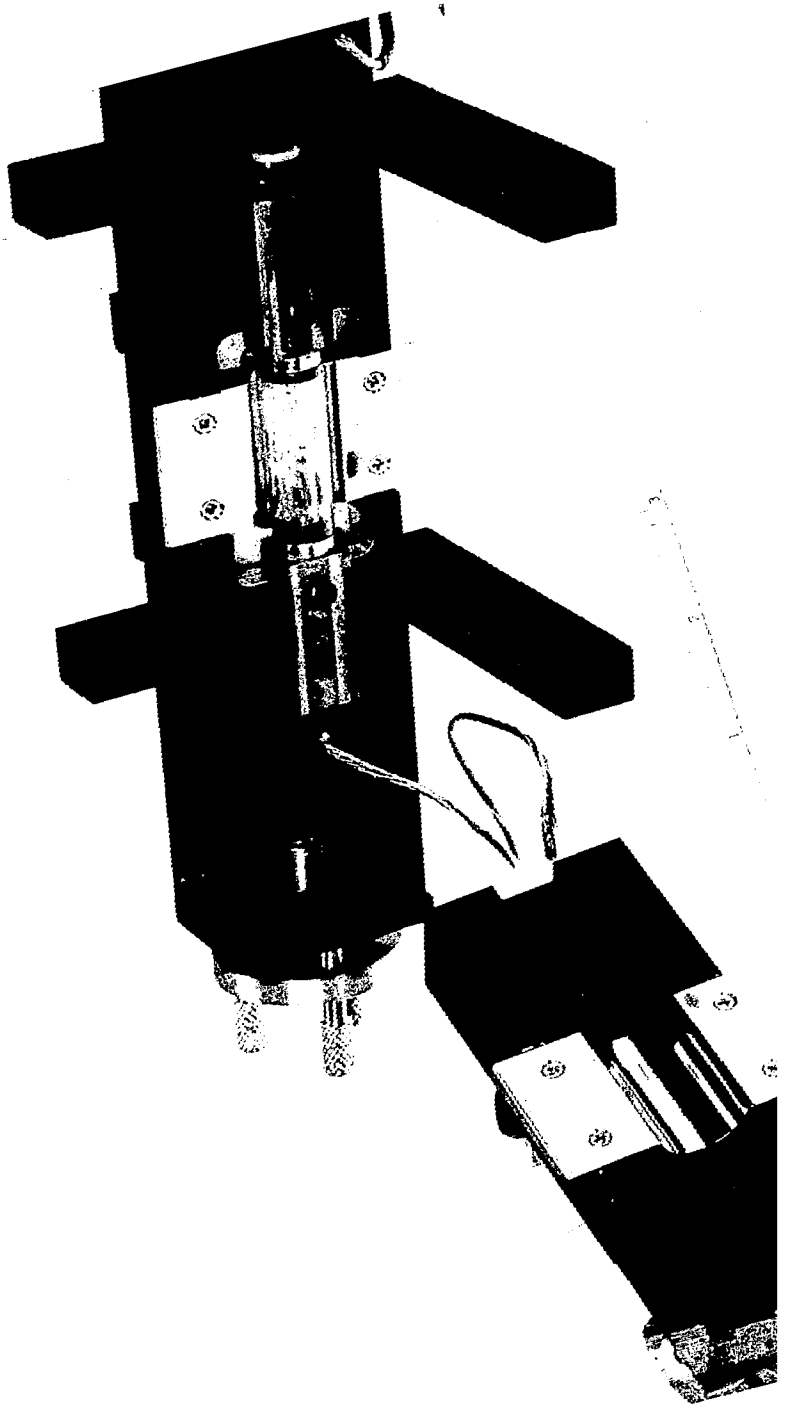

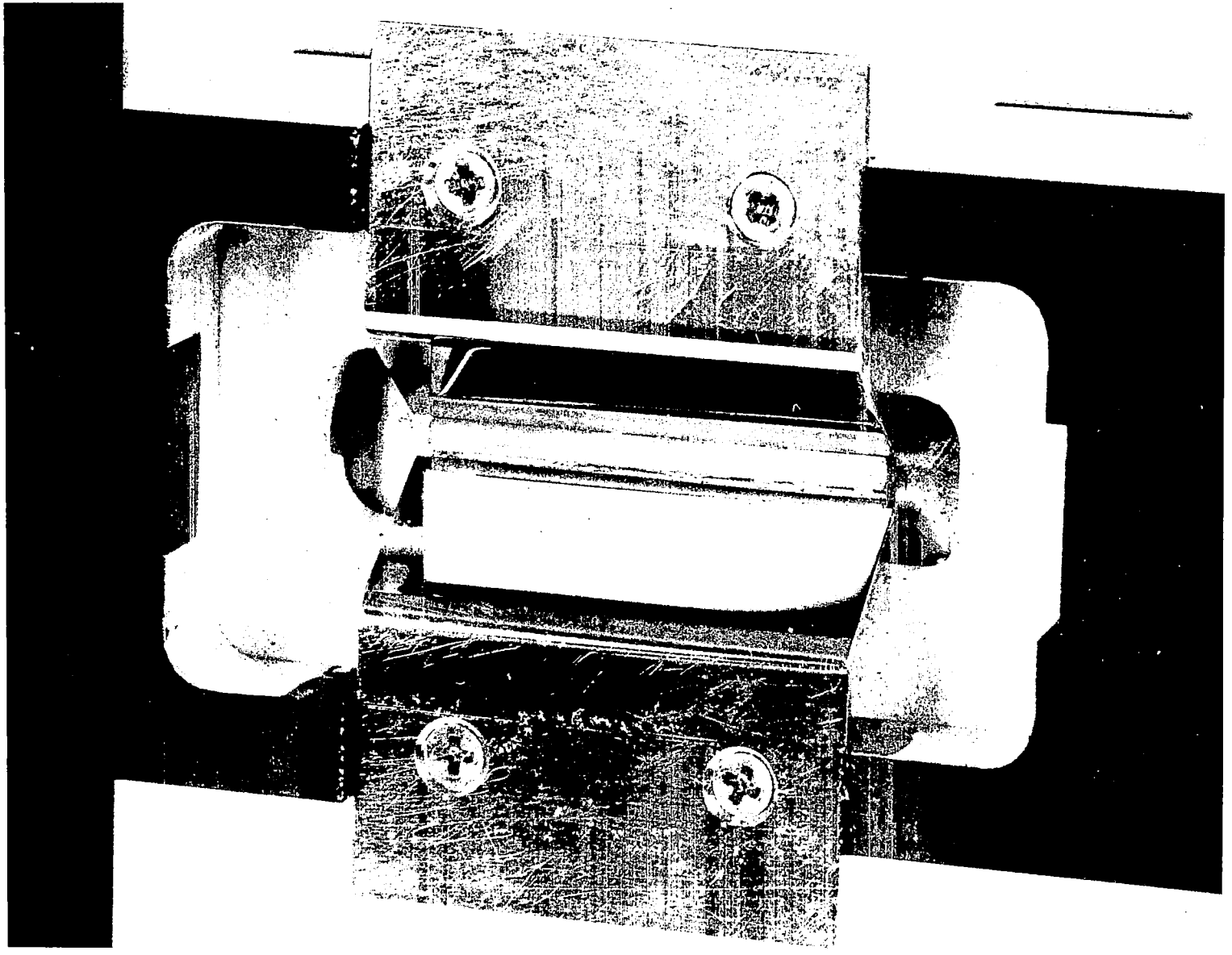

Figure 8-12. Pump Cavity of Conductively Cooled Nd:YAG Laser.

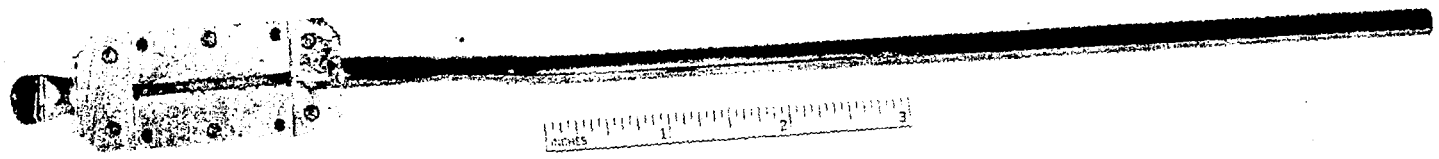

Figure 8-13. Conductively Cooled Nd:YAG Rod Mounting and Heat Pipe.

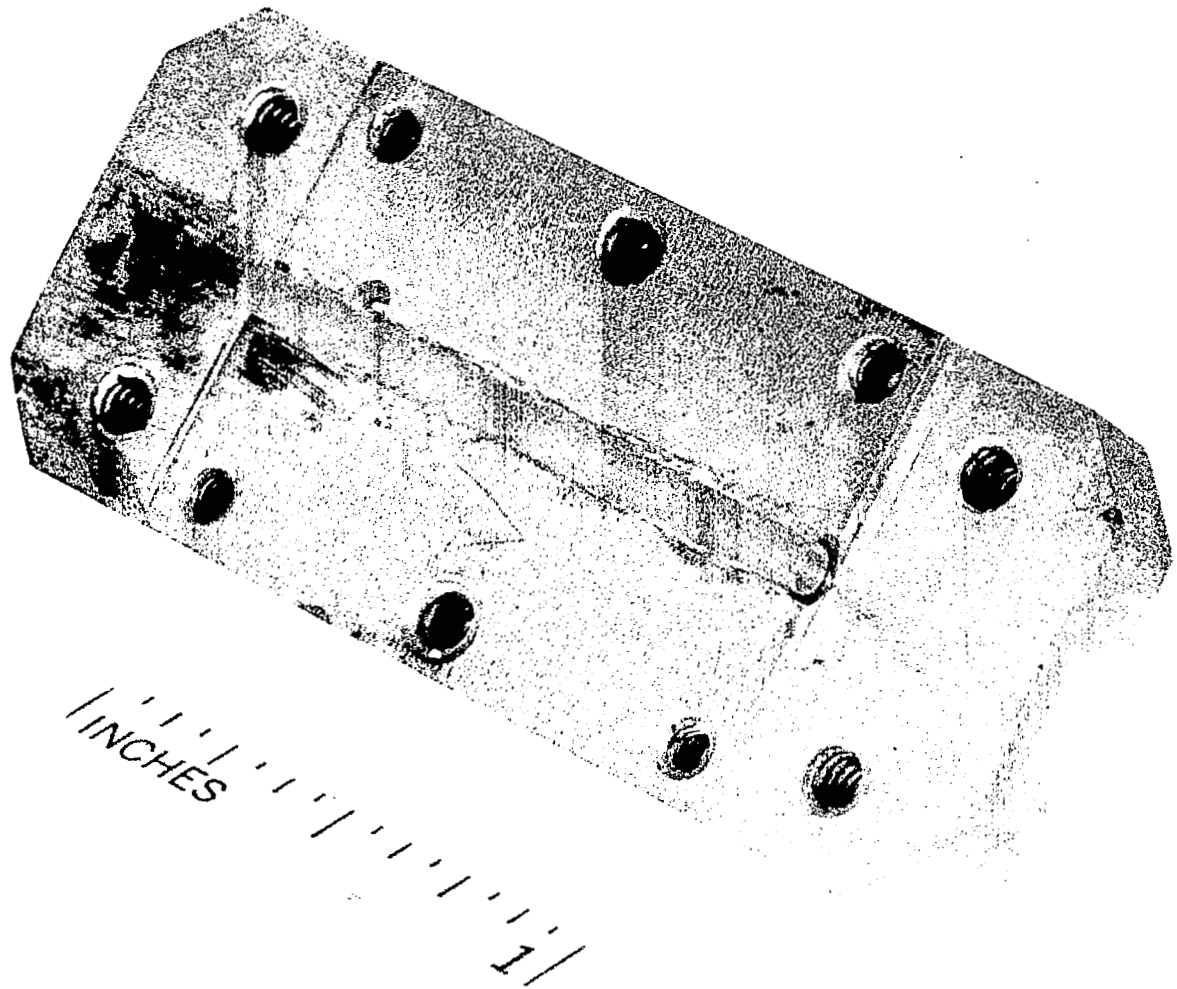

Figure 8-14 Conductively Cooled Nd:YAG Laser Rod Mounting.

This experimental laser was built late in the program after the design study was complete and the prototype design was complete. It really represents work beyond the scope of the program but was attempted anyway. A Sylvania-owned Nd:YAG rod was sent out for the high reflection coating. Problems were encountered with the coating, however. This gold-on-transparent-oxide coating was made by Liberty Mirror Division of Libby Owens Ford and has been described in Section 6. The gold film seemed to be scavenged by the indium solder in several places, even with a protective nickel layer. This can be seen in Figure 8-14, as the magnified white spots that can be seen through the laser rod.

Operation of the pump lamp resulted in immediate separation of the rod from the rest of the coating. The resulting uncooled rod did not lase. The experimental laser has, therefore, not been successfully operated at the time this report is being written. The laser rod is being recoated, however, and we hope to operate the laser.

The Sylvania Lamp Division gave us a one-inch arc length potassium-mercury lamp with sapphire jacket similar to lamp specified in the prototype laser design. This lamp is shown with a 2 mm Nd:YAG laser rod in Figure 8-15. We have designed an alternate pump cavity for the experimental laser shown in Figures 8-9 through 8-14 that utilizes this lamp. A layout drawing of the laser with this pump cavity in place is shown in Figure 8-16.

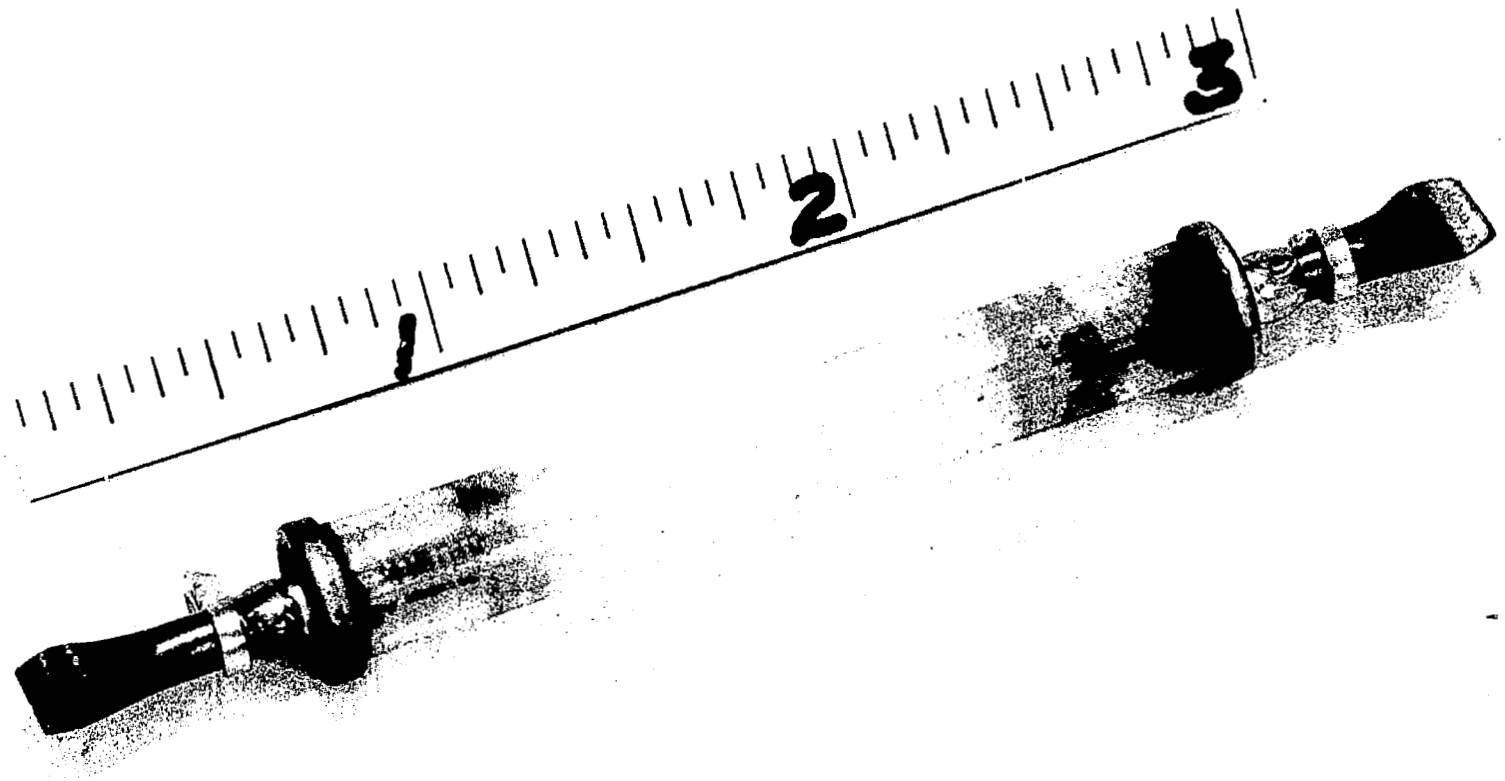

Figure 8-15 . Potassium-Mercury Arc Lamp and 2mm Nd:YAG Laser Rod.

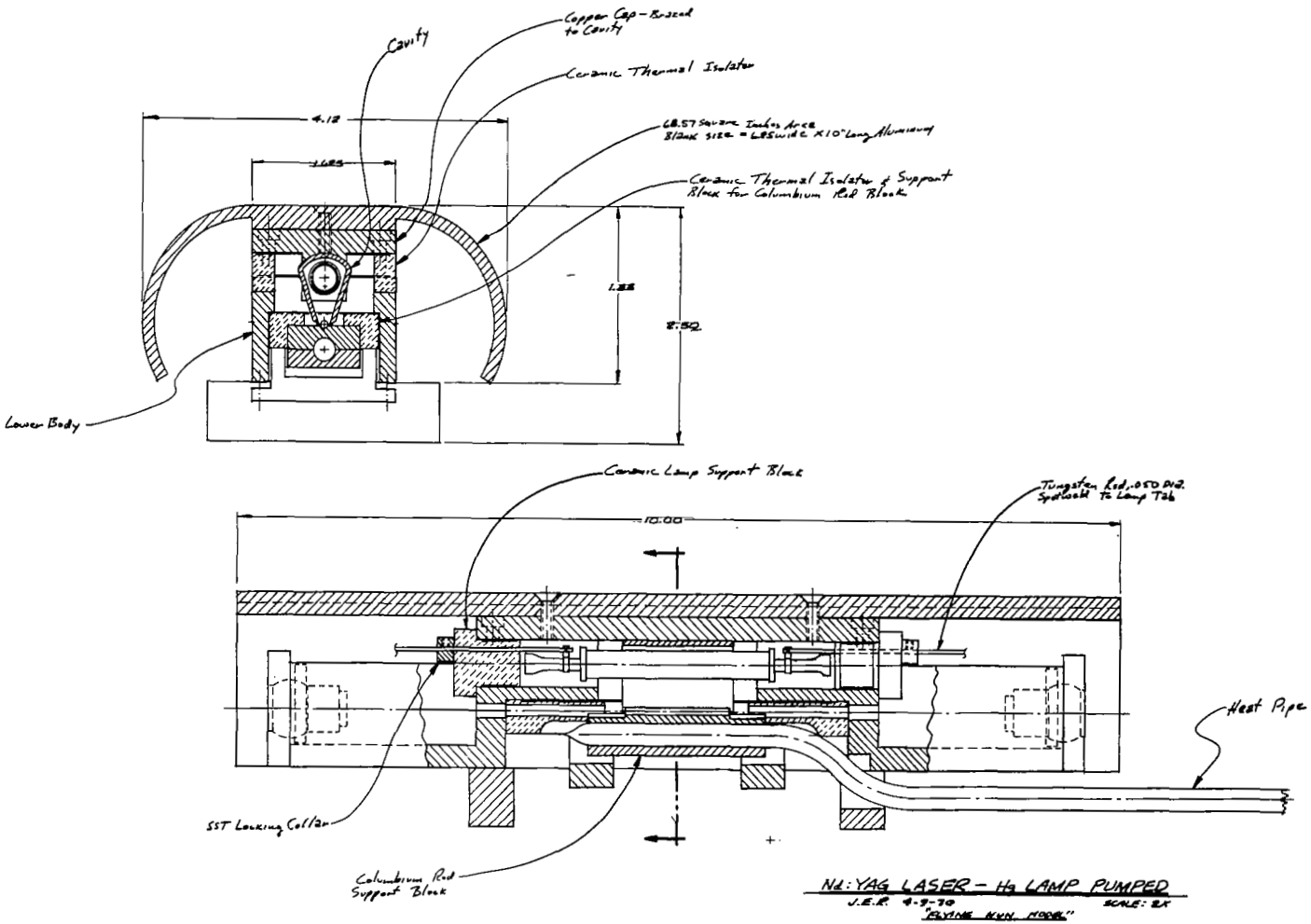

Figure 8-16. Assembly Drawing of Potassium Arc Pumped Conductively Cooled Nd:YAG Laser.

The rationale is to operate the laser with the krypton arc pump lamp and optimize its alignment. The potassium lamp will then replace the krypton and the complete prealigned laser will be inserted into a vacuum. The laser will then be operated in a vacuum with no further adjustments. The parts for this experiment have been completed, but the experiment has not been conducted because of the laser and bonding problems.

ILC Corporation[17] has recently made some pure potassium lamps of the size that fits this laser. We hope to operate the laser with these lamps as well as with the Sylvania K-Hg lamps.

SECTION 9

CONCLUSIONS AND RECOMMENDATIONS

9.1 Conclusions

The design study reported here has developed a theoretical model of the Nd:YAG that allows evaluation of the effect of various parameters on laser performance. This model has been found to agree well with experimental data on Nd:YAG lasers with various pump lamps.

A low power (1 watt) output space qualified Nd:YAG laser will be a low gain device. The efficiency of the laser will be very much affected by internal dissipative loss in the laser cavity. Good performance can, therefore, not be expected with high loss intracavity elements such as non-linear second harmonic generation crystals or electro-optic modulator crystals. The laser must be operated with no intracavity elements and with lowest loss mirrors, laser rod and optical coatings for best performance.

Heat loss from optical pump lamps greatly influences their efficiency in pumping laser materials. Maximum efficiency is obtained when heat loss is a minimum and the only cooling mechanism is radiation. Sapphire jackets are required to withstand the thermal environment of radiation cooled lamps. These jackets must be transparent and not scatter the radiation, thereby reducing lamp brightness. Potassium in a high pressure broadened and reversed emission characteristic is the best pump lamp presently available for pumping Nd:YAG. With this lamp

good laser performance can be obtained at power inputs of 150 watts and above. Lifetimes of 10,000 hours appear possible with such lasers.

Radiation cooling area and weight requirements make cryogenic (77°C) operation of Nd:YAG lasers in space impractical. Operation at 0°C or above is required for reasonable cooler size.

Incoherent semiconductor diodes show great promise for pumping Nd:YAG lasers. Room temperature devices can probably be made but have not as yet. The lifetime of these devices can probably be extended to 100,000 hours. Approximately 90 diodes of GaAlAs in an array should produce one watt output at one percent efficiency at 20°C.

Sun pumping, especially in a dual pumping arrangement with optical lamp pumping, appears to be a feasible, very long-life approach for space qualified Nd:YAG.

Conductive cooling of the Nd:YAG laser rod and use of heat pipes to move the heat to a radiation cooler is the preferred technique for a space qualified laser design. Some problems are involved in achieving good thermal transfer and high optical reflection at laser rod conduction cooling interface.

Low mode locking of the Nd:YAG laser can be accomplished with injection locking at high frequencies like 500 MHz. Operation at low frequencies (50 - 100 MHz) is not practical with this technique. Loss

modulation with an intracavity fused quartz resonant acousto-optic modulator is the best mode locking technique for the lower frequencies. Little modulator loss is required for acceptable efficiency.

A prototype space qualified Nd:YAG laser design can not presently be made with room temperature electroluminescent diodes because such diode laser pumps have not yet been developed. We have presented a prototype design of a potassium lamp pumped space qualified Nd:YAG laser. We have tested some of the design features of this experimentally and have built an experimental laser capable of testing the design concept in full. Technological problems with the high reflectivity heat conduction bond to the Nd:YAG rod have prevented us from completing these tests on this program.

9.2 Recommendations

We believe the results of this engineering design study and our prototype space qualified Nd:YAG laser design are encouraging. Nd:YAG, it appears, can be made into a long life, reliable, high efficiency optical source for use in space. Based upon these conclusions, we recommend the following:

A. Construction of a prototype space qualified Nd:YAG laser.

   1. Basic design should be compatible with either lamp or diode pumping.

   2. Lamp pumping should be used in the prototype.

B. Room-temperature (or higher) diodes should be developed. Little effort should be expended in making lasers with low temperature diodes.

C. Long life lamp development should be initiated after prototype demonstration.

D. Work should be started on modulation of the Nd:YAG laser output for direct detection communications.

SECTION 10

REFERENCES

1. J. E. Geusic, H. M. Marcos, and L. G. VanUitert, "Laser Oscillation in Nd-Doped Yttrium Aluminum, Yttrium Gallium and Gadolinium Garnets," Appl. Phys. Lett. 4, 182 (15 May 1964).

2. C. H. Church and I. Liberman, "The Spherical Reflector for use in the Optical Pumping of Lasers," Appl. Optics 6, 1966 (Nov. 1967).

3. J. D. Foster and L. M. Osterink, "Thermal Effects in a Nd:YAG Laser," to be published, J. Appl. Phys 41 (Aug. 1970).

4. M. DiDomenico, Jr., J. E. Geusic, H. M. Marcos, and R. G. Smith, "Generation of Ultrashort Optical Pulses by Mode Locking the YAlG:Nd Laser," Appl. Phys. Lett. 8, 180 (1 April 1966).

5. L. M. Osterink and J. D. Foster, "A Mode-Locked Nd:YAG Laser," J. Appl. Phys. 39, 4163 (Aug. 1968).

6. J. E. Geusic, H. J. Levinstein, S. Singh, R. G. Smith, and L. G. VanUitert, "Continuous 0.532 Micron Solid-State Source Using $Ba_2NaNb_5O_{15}$," Appl. Phys. Lett. 12, 306 (1968).

7. I. Liberman, D. A. Larson, and C. H. Church, "Efficient Nd:YAG CW Lasers Using Alkali Additive Lamps," IEEE J. Quant. Elec., QE-5, 238 (May 1969).

8. R. B. Allen and S. J. Scalise, "Continuous Operation of a YAlG:Nd Laser by Injection Luminescence Pumping," Appl. Phys. Lett. 14, 188 (15 March 1969).

9. W. W. Rigrod, "Gain Saturation and Output Power of Optical Masers," J. Appl. Phys. 34, 2602 (Sept. 1963).

10. W. Elenbaas, "The High Pressure Mercury Vapor Discharge," (Interscience Publishers Inc., New York, 1951), pp. 18-31.

11. T. B. Read, "The CW Pumping of YAG:Nd by Water-Cooled Krypton Arcs," Appl. Phys. Lett. 9, 32 (1 Nov. 1966).

12. I. Liberman and R. L. Grassel, "A Comparison of Lamps for Use in High Continuous Power Nd:YAG Lasers," Appl. Opt. 8, 1875 (Sept. 1969).

13. General Electric "Lucalox" lamp data sheet.

14. J. F. Waymouth, W. C. Gungle, J. M. Harris, and F. Koury, "A New Metal Halide Arc Lamp," Illum. Engr., 85 (Feb. 1965).

15. W. Elenbaas, "The High Pressure Mercury Vapor Discharge," (Interscience Publishers Inc., New York, 1951), pp. 11-18.

16. I. Liberman, D. A. Larson, R. G. Young, L. Armstrong, Jr., R. Liebermann, and C. H. Church, "Optical Pumps for Lasers -- Phase II," Final R & D Report ECOM-02097-F, Contract No. DA-28-043-AMC-02097(E), U. S. Army Electronics Command, Fort Monmouth, N. J. (October 1968).

17. L. Nobel, ILC Corporation, private communication.

18. A. A. Kaminskii, "Stimulated Radiation from $Y_3AL_5O_{12}$-Nd^{3+} Crystals," Soviet Physics JETP 24, pp. 33-39 (Jan. 1967).

19. R. B. Allen, S. J. Scalise, and R. E. DeKinder, Jr., "Efficiency CW Operation of a Diode-Pumped YAlG:Nd Laser," Paper 12.5, Conference on Laser Engineering and Applications, Washington, D.C., May 26-28, 1969.

20. W. W. Holloway, M. Kesigian, F. F. Y. Wang, and G. F. Sullivan, "Temperature-Dependent Nd Fluorescence Parameters and Laser Thresholds," J. Opt. Soc. Am., 56, pp. 1409-1410 (Oct. 1966).

21. F. W. Ostermayer and J. E. Geusic, Bell Telephone Laboratories, private communication.

22. A. H. Herzog, W. O. Graves, and M. G. Craford, "Electroluminescence of Diffused $GaAs_{1-x}P_x$ Diodes with Low Donor Concentrations," J. Appl. Phys. 40, pp. 1830-1838 (March 1969).

23. H. Rupprecht, J. M. Woodall, and G. D. Pettit, "Efficiency Visible Electroluminescence at 300°K from $Ga_{1-x}Al_xAs$ p-n Junctions Grown by Liquid-Phase Epitaxy," Appl. Phys. Lett. 11, pp. 81-83 (1 Aug. 1967).

24. H. Kressel, F. Z. Hawrylo, and N. Almeleh, "Properties of Efficiency Silicon-Compensated $Al_xGa_{1-x}As$ as Electroluminescent Diodes," J. Appl. Phys. 40, pp. 2248-2253 (April 1969).

25. H. F. Quinn and W. O. Marton, "Gallium Aluminum Arsenide Electroluminescent Diodes and Injection Lasers--Properties and Applications," preprint supplied by H. F. Quinn, IBM Federal Systems Div., Yorktown Heights, N.Y.

26. R. H. Saul, J. Armstrong, and W. H. Hackett, Jr., "GaP Red Electroluminescent Diodes with an External Quantum Efficiency of 7%," Appl. Phys. Lett. 15, pp. 229-231 (1 Oct. 1969).

27. H. F. Quinn, private communication.

28. C. Lanza, K. L. Konnerth, and C. E. Kelly, Solid-State Electron 10, 21 (1967).

29. K. L. Konnerth, J. C. Marinace and J. C. Topalian, "Zinc-Diffused GaAs Electroluminescent Diodes with Long Operating Life," J. Appl. Phys. 41, 2060 (April 1970).

30. American Optical Co. Staff, "Investigation and Development of a Sun-Powered Laser Transmitter," prepared under Contract AF33(616)8025. Report designation ASD-TDR-62-447.

31. C. R. Simpson, "Experimental Verification of Sun-Powered Laser Transmitter," prepared under Contract AF33(657)8619. Report designation ASD-TDR-63-727, AD 420 983.

32. G. R. Simpson, "Continuous Sun-Pumped Room Temperature Glass Laser Operation," Appl. Optics 3, 783-784 (June 1964).

33. J. Bordogng, W. Hannan, C. Reno, and R. Tarzaiski, Final Report on "Solar-Pumped Laser," prepared under Contract NAS9-3671. Report designation N66-19516.

34. C. G. Young, "Sun-Pumped Laser," prepared under Contract AF33(615)1899. Report designation AFAL-TR-66-41, AD 481 927.

35. C. G. Young, "A Sun-Pumped cw One-Watt Laser," Appl. Optics 5 (6), 993-997 (June 1966).

36. N. A. Kozlov, A. A. Mak, and B. M. Sedov, "Solid-State, Sun Pumped Laser," Soviet J. of Opt. Tech. 33, 549-553 (Feb. 1966).

37. L. Rothrock, Union Carbide Corp., private communication.

38. R. J. Pressley, et al., "Solid State Laser Explorations," Tech. Rpt. AFAL-TR-66-129, Contracts No. AF33(615)2645 and BPS No. 5-674156-415608, Air Force Avionics Lab., Wright-Patterson AFB, Ohio (June 1966).

39. D. F. Nelson and W. S. Boyle, "A Continuously-Operating Ruby Optical Maser," Appl. Optics 1, 181-183 (March 1962).

40. J. D. Foster and L. M. Osterink, "Index of Refraction and Expansion Thermal Coefficients of Nd:YAG," Appl. Optics 7, No. 12 (Dec. 1968).

41. H. H. Manko, "Solders and Soldering," McGraw-Hill Book Co., 1964.

42. Thomas D. Sheppard, "Heat Pipes and Their Application to Thermal Control in Electronic Equipment," Presented at NEPCON-West, 1969.

43. Allan D. Kraus, "Cooling Electronic Equipment," Prentice-Hall, 1965.

44. Allen B. Chertoff and James J. Foti, "Problems of Heat Removal Chill Progress in IC's," Electronics, 1967.

45. A. D. Kraus, "Extended Surfaces," Baltimore, Md., Spartan Books, 1963.

46. R. Targ, private communication.

47. W. C. Henneberger and H. J. Schulte, "Optical Pulses Produced by Laser Length Variation," J. Appl. Phys. 39 (5), 2189 (April 1966).

48. O. P. McDuff and A. L. Pardue, Jr., "Theory of Mode Coupling in the Length-Modulated Laser," IEEE J. Quant. Elec. QE-4 (3), 99-100 (March 1968).

49. P. W. Smith, "Phase Locking of Laser Modes by Continuous Cavity Length Variation," Appl. Phys. Lett. 10 (2), 51-53 (15 Jan. 1967).

50. L. E. Hargrove, R. L. Fork, and M. A. Pollack, "Locking of He-Ne Laser Modes by Synchronous Intracavity Modulation," Appl. Phys. Lett 5 (1), 4-6 (Jan. 1964).

51. R. Adler, Proc. IRE 34, 351-357 (1946).

52. C. L. Tang and H. Statz, "Phase-Locking of Laser Oscillators by Injected Signal," J. Appl. Phys. 38 (1), 323-324 (Jan. 1967).

53. M. W. Sasnett, R. S. Reynolds, and A. E. Siegman, "10.6μ Single Mode Frequency Control," AFAL-TR-69-337, (31 Oct. 1969).

54. H. L. Stover and W. H. Steier, "Locking of Laser Oscillators by Light Injection," Appl. Phys. Lett 8 (4), 91-93 (15 Feb. 1966).

55. L. Curtis Foster, M. D. Ewy, and C. Burton Crumly, "Laser Mode Locking by an External Doppler Cell," Appl. Phys. Lett 6 (1), 6-8 (1 Jan. 1965).

56. D. Roess, "Exfocal Pumping of Optical Masers in Elliptical Mirrors," Appl. Optics 3 (2), 259-265 (Feb. 1964).

57. T. Li, "Diffraction Loss and Selection of Modes in Maser Resonators with Circular Mirrors," Bell Systems Tech. J. 45, 917 (May 1965).

58. R. S. Reynolds, "Space Qualified CO_2 Laser," Final Report, Contract NAS12-2021 (Dec. 1969).

NASA-Langley, 1971 — 16 CR-177